Advanced Drug Delivery Reviews 175 (2021) 113831

Contents lists available at ScienceDirect

Advanced Drug Delivery Reviews

journal homepage: www.elsevier.com/locate/adr

Therapeutic and diagnostic targeting of fibrosis in metabolic, proliferative and viral disorders

Alexandros Marios Sofias [a,b,c,1,*], Federica De Lorenzi [a,1], Quim Peña [a], Armin Azadkhah Shalmani [a], Mihael Vucur [d], Jiong-Wei Wang [e,f,g,h], Fabian Kiessling [a], Yang Shi [a], Lorena Consolino [a,*], Gert Storm [e,h,i,j,*], Twan Lammers [a,i,j,*]

[a] Department of Nanomedicine and Theranostics, Institute for Experimental Molecular Imaging, Faculty of Medicine, RWTH Aachen University, Aachen, Germany
[b] Mildred Scheel School of Oncology (MSSO), Center for Integrated Oncology Aachen Bonn Cologne Duesseldorf (CIO^{ABCD}), University Hospital Aachen, Aachen, Germany
[c] Department of Circulation and Medical Imaging, Faculty of Medicine and Health Sciences, Norwegian University of Science and Technology (NTNU), Trondheim, Norway
[d] Department of Gastroenterology, Hepatology and Infectious Diseases, University Hospital Duesseldorf, Medical Faculty at Heinrich-Heine-University, Duesseldorf, Germany
[e] Department of Surgery, Yong Loo Lin School of Medicine, National University of Singapore, Singapore, Singapore
[f] Cardiovascular Research Institute, National University Heart Centre Singapore, Singapore, Singapore
[g] Department of Physiology, Yong Loo Lin School of Medicine, National University of Singapore, Singapore, Singapore
[h] Nanomedicine Translational Research Programme, Centre for NanoMedicine, Yong Loo Lin School of Medicine, National University of Singapore, Singapore, Singapore
[i] Department of Pharmaceutics, Utrecht Institute for Pharmaceutical Sciences, Utrecht University, Utrecht, the Netherlands
[j] Department of Targeted Therapeutics, University of Twente, Enschede, the Netherlands

ARTICLE INFO

Article history:
Received 17 March 2021
Revised 30 May 2021
Accepted 10 June 2021
Available online 15 June 2021

Keywords:
Fibrosis
Drug targeting
Nanomedicine
Imaging
Atherosclerosis
Cardiovascular disease
Cancer
Diabetes
Liver
Viral infection

ABSTRACT

Fibrosis is a common denominator in many pathologies and crucially affects disease progression, drug delivery efficiency and therapy outcome. We here summarize therapeutic and diagnostic strategies for fibrosis targeting in atherosclerosis and cardiac disease, cancer, diabetes, liver diseases and viral infections. We address various anti-fibrotic targets, ranging from cells and genes to metabolites and proteins, primarily focusing on fibrosis-promoting features that are conserved among the different diseases. We discuss how anti-fibrotic therapies have progressed over the years, and how nanomedicine formulations can potentiate anti-fibrotic treatment efficacy. From a diagnostic point of view, we discuss how medical imaging can be employed to facilitate the diagnosis, staging and treatment monitoring of fibrotic disorders. Altogether, this comprehensive overview serves as a basis for developing individualized and improved treatment strategies for patients suffering from fibrosis-associated pathologies.

Contents

1. Introduction . . . 2
2. Identifying targets for therapeutic modulation of fibrosis . . . 2
   2.1. Fibrogenic cells as anti-fibrotic targets . . . 3
   2.2. Immune cells as anti-fibrotic targets . . . 6
   2.3. Genes as anti-fibrotic targets . . . 11
   2.4. Messenger RNA nucleotides as anti-fibrotic targets . . . 11
   2.5. miRNA, lncRNA, and sscRNA nucleotides as anti-fibrotic targets . . . 12
   2.6. TGF-β, NF-κB, Wnt/β-catenin, and p38 MAPK pathway proteins as anti-fibrotic targets . . . 12
   2.7. Other proteins as anti-fibrotic targets . . . 13

* Corresponding authors.
E-mail addresses: asofias@ukaachen.de (A.M. Sofias), lconsolino@ukaachen.de (L. Consolino), g.storm@uu.nl (G. Storm), tlammers@ukaachen.de (T. Lammers).
[1] Authors contributed equally: A.M. Sofias; F. De Lorenzi.

https://doi.org/10.1016/j.addr.2021.113831
0169-409X/

2.8. Metabolites as anti-fibrotic targets . . . 14
3. Therapeutic outlook: Clinical status, drug repurposing and drug delivery . . . 14
3.1. Approved anti-fibrotic agents, clinical trials and drug repurposing . . . 14
3.2. Integrating nanomedicine for targeting fibrosis . . . 15
4. Imaging modalities for diagnostic assessment of fibrosis . . . 16
4.1. Imaging fibrosis in atherosclerosis and cardiac diseases . . . 16
4.2. Imaging fibrosis in cancer . . . 19
4.3. Imaging fibrosis in diabetes . . . 22
4.4. Imaging fibrosis in liver diseases . . . 22
4.5. Imaging fibrosis in viral disorders . . . 24
5. Diagnostic outlook: Multimodality and molecular probes for imaging fibrosis . . . 25
6. Concluding remarks . . . 26
Declaration of Competing Interest . . . 26
Acknowledgements . . . 26
References . . . 26

1. Introduction

Pathological fibrosis is the dysregulated deposition of scar tissue in response to chronic injury and inflammation. This manifestation occurs in many different pathologies, including idiopathic pulmonary fibrosis (IPF), atherosclerosis, cardiac disease, cancer, diabetic nephropathy and cardiomyopathy, non-alcoholic steatohepatitis, non-alcoholic fatty liver disease, viral pneumonia, viral hepatitis, and certain autoimmune diseases (Fig. 1a) [1-10].

The formation of pathological fibrosis in these disorders is typically characterized by an insidious onset. Due to the lack of early diagnosis, fibrosis progresses unnoticed for years and fibrotic tissue replaces organs' functional units (e.g., nephrons in the kidneys) leading to irreversible damage and organ failure. In addition, the excessive accumulation of extracellular matrix (ECM) components (e.g., collagen and fibronectin) contributes to an increase in tissue stiffness [11,12] that forms an inaccessible microenvironment which hampers drug accumulation, distribution and efficacy.

The fibrotic cascade involves dynamic cross-talk between multiple pro-inflammatory cell populations. Inflammatory immune cells (e.g., macrophages (MΦ), neutrophils, T cells) are recruited to the diseased site and secrete a wide array of cytokines, chemokines and growth factors responsible for amplifying inflammation. Eventually, these factors activate quiescent fibroblasts, epithelial and endothelial cells, and promote their differentiation towards myofibroblasts; a process known as epithelial/endothelial-to-mesenchymal transition (EMT or EndMT, respectively) [13,14]. A key molecule in fibrosis development is transforming growth factor beta (TGF-β), which is an extracellular pro-fibrotic cytokine produced majorly by infiltrating pro-inflammatory MΦs [15-17]. TGF-β induces EMT and EndMT, and activates resident fibroblasts via modulation of Smad-2/3, several protein kinase families (MAPK, PI3K), and the Wnt/β-catenin signaling pathway (Fig. 1b) [15,18-20]. In addition, TGF-β preserves the fibrotic ECM by regulating metalloproteinase expression and upregulating collagen I production. Moreover, various factors connected to TGF-β (e.g., angiotensin II (AngII) [21,22], IL-13 [23,24], IL-3, IL-4 [25], IL-1β, and the tumor necrosis factor alpha (TNF-α) [26-28]), have been demonstrated to stimulate the recruitment of pro-inflammatory immune cells, induce proliferation and activation of fibroblasts, and enhance the production of ECM components.

Considering the multiple driving factors and their complex role in fibrosis generation [29-31], and taking into account that fibrosis-related diseases account for 45% of deaths in the United States [32], it is crucial to develop effective means for diagnosing and treating fibrosis. To contribute to these efforts, this review aims to examine the most recent therapeutic and diagnostic strategies against fibrosis in atherosclerosis and cardiac disease, cancer, diabetes, liver diseases, and viral disorders. With respect to therapeutic modulation of fibrosis, we summarize key anti-fibrotic targets at different levels of transcription and translation, whose regulation can help to inhibit fibrosis progression. In this regard, we present currently approved as well as clinically evaluated anti-fibrotic strategies, and discuss how nanomedicine can potentiate the efficacy of anti-fibrotic therapies. With respect to fibrosis diagnosis, we performed a comprehensive analysis of clinical and preclinical imaging techniques used to visualize fibrosis. In this context, we discuss how the complementary use of multiscale and multimodal imaging, in conjunction with targeted molecular imaging agents can improve fibrosis detection, staging and therapy monitoring.

For our review, we performed multiple systematic searches in the Scopus database. We used standardized keywords related to fibrosis, fibrotic targets, and fibrosis imaging, and we requested them to appear in the title, abstract, or keywords of a manuscript. To reveal recent trends, we narrowed our search down to the last three years (2018–2020), and also included articles in press in 2021. This process was repeated five times, once for each disease (atherosclerosis and cardiac disease, cancer, diabetes, liver diseases, viral disorders). This comprehensive manuscript consequently serves as a go-to manual for up-to-date information on the development of individualized and improved diagnostic and therapeutic strategies for patients suffering from fibrosis-associated pathologies.

2. Identifying targets for therapeutic modulation of fibrosis

Anti-fibrotic strategies generally rely on inhibition of pro-fibrotic cell populations or components of transcription, translation and/or metabolic processes. In this regard, various pro-fibrotic cells, genes, mRNAs, proteins, and metabolites have been modulated using small molecule inhibitors or state-of-the-art therapies, such as RNA interference or gene editing. This section provides an overview of these targets in atherosclerosis and cardiac disease (Fig. 2), cancer (Fig. 3), diabetes (Fig. 4), liver disease (Fig. 5), and viral disorders (Fig. 6), with heart, lungs, heart and kidneys, liver, and liver and lungs to be the most studied organs / tissues per disease, respectively (Table 1).

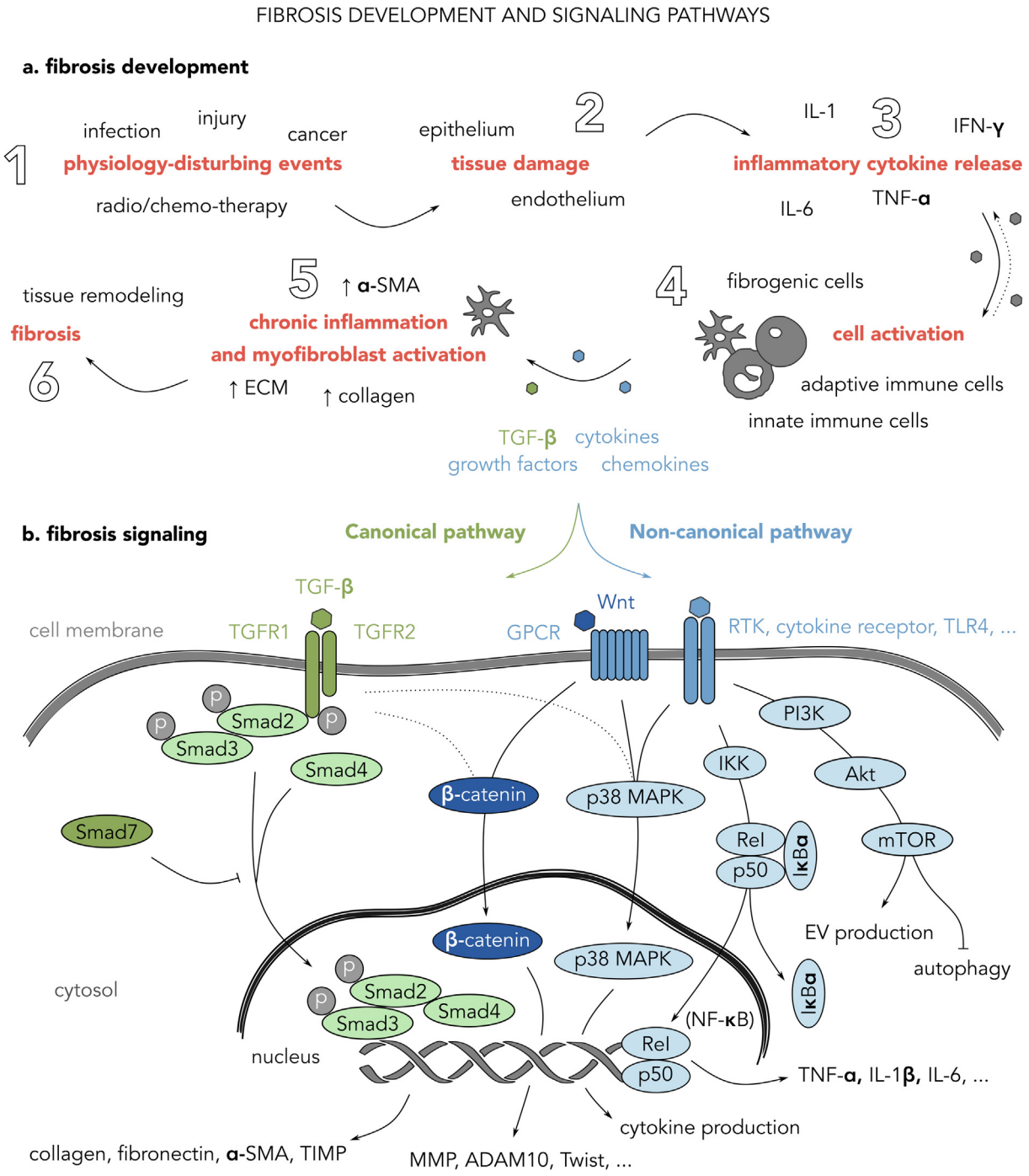

Fig. 1. Fibrosis development and signaling pathways. (a) The development of fibrosis begins with physiology-disturbing events that cause tissue damage. In response to this damage, cells secrete inflammatory cytokines that activate fibrogenic and immune cells. Consequently, fibrogenic and immune cells respond to this cascade by producing cytokines, chemokines, and growth factors aiming to resolve the inflammation. In some cases, the inflammation persists and fibroblasts are continuously activated to myofibroblasts resulting in excessive fibrotic tissue remodeling. (b) The release of specific signaling molecules by fibrogenic and immune cells initiates a cascade of interactions that eventually leads to fibrosis. Several signaling pathways have been incriminated for contribution to fibrosis with the canonical TGF-β/Smad-2/3 pathway to be the most prominent contributor. Non-canonical (i.e., non-Smad-2/3-dependent) pathways, such as the Wnt/β-catenin, the p38 MAPK, the NF-κB, and the PI3K/Akt/mTOR, further enhance fibrosis and inflammation [13,17,19,20].

2.1. Fibrogenic cells as anti-fibrotic targets

Fibrogenic cells (e.g., fibroblasts and stellate cells) have been extensively evaluated as anti-fibrotic targets. For example, myofibroblasts were modulated using icosabutate in atherosclerosis and liver fibrosis. Icosabutate alleviated hepatic fibrosis by reducing myofibroblasts and by limiting the number of infiltrating MΦs in mice [33]. Additionally, the drug enabled downregulation in the metabolic cascade of arachidonic acid; a key lipid mediator in cardiac fibrosis and inflammation [34].

Fibroblasts also play a prominent role in cancer-related fibrosis, where they are involved in the communication between stroma and cancer cells. The use of pirfenidone (approved for (IPF)), inhibited the differentiation of both lung fibroblasts and cancer-associated fibroblasts (CAF) towards the myofibroblast phenotype (i.e., the active differentiated fibroblast population responsible

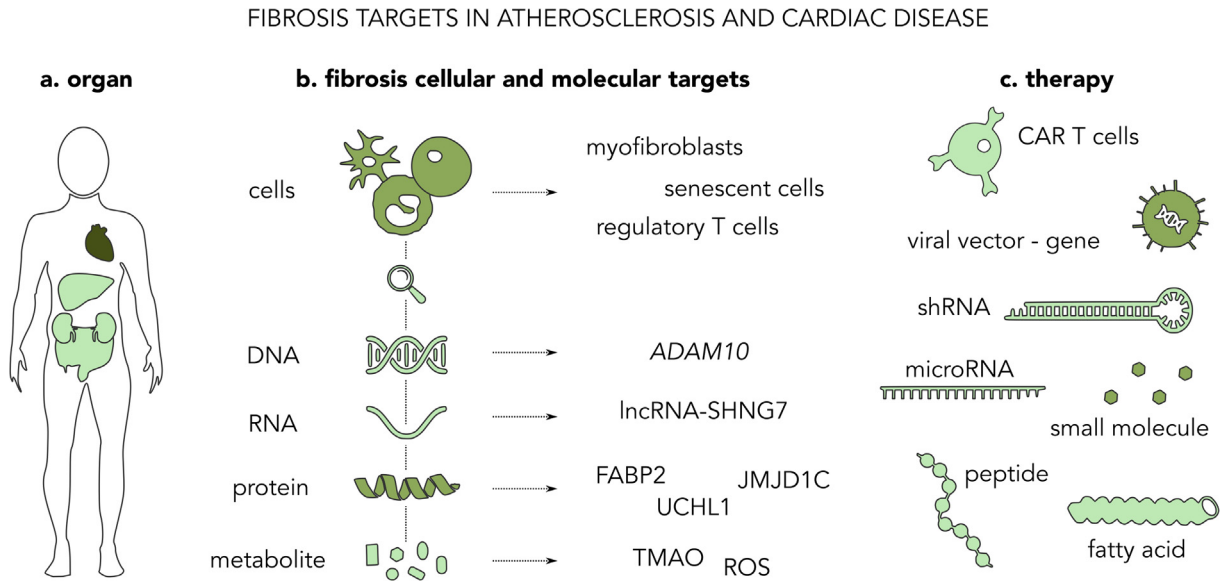

Fig. 2. Fibrosis targets in atherosclerosis and cardiac disease. (a) Investigations on fibrosis development in atherosclerosis and cardiac disease primarily focus on the myocardium and major vessels. The liver and kidneys, as well as intestinal metabolites, have also been examined with the purpose of ameliorating cardiovascular fibrosis. (b) At the macroscopic level, key cell populations in mediating fibrosis are cardiac myofibroblasts, senescent cells, and regulatory T cells. Genetic targets, such as DNA, RNA, proteins and metabolites are also evaluated as anti-fibrotic targets. (c) Various therapeutic entities are explored to inhibit fibrosis, with viral vector-mediated gene delivery and small molecules being the most commonly used ones. Color-coding: the analysis of manuscripts described in section 2 revealed the frequency in which each organ, therapeutic target, and therapeutic intervention are investigated for anti-fibrotic purposes in atherosclerosis and cardiac disease; light green = low frequency; green = medium frequency; dark green = high frequency.

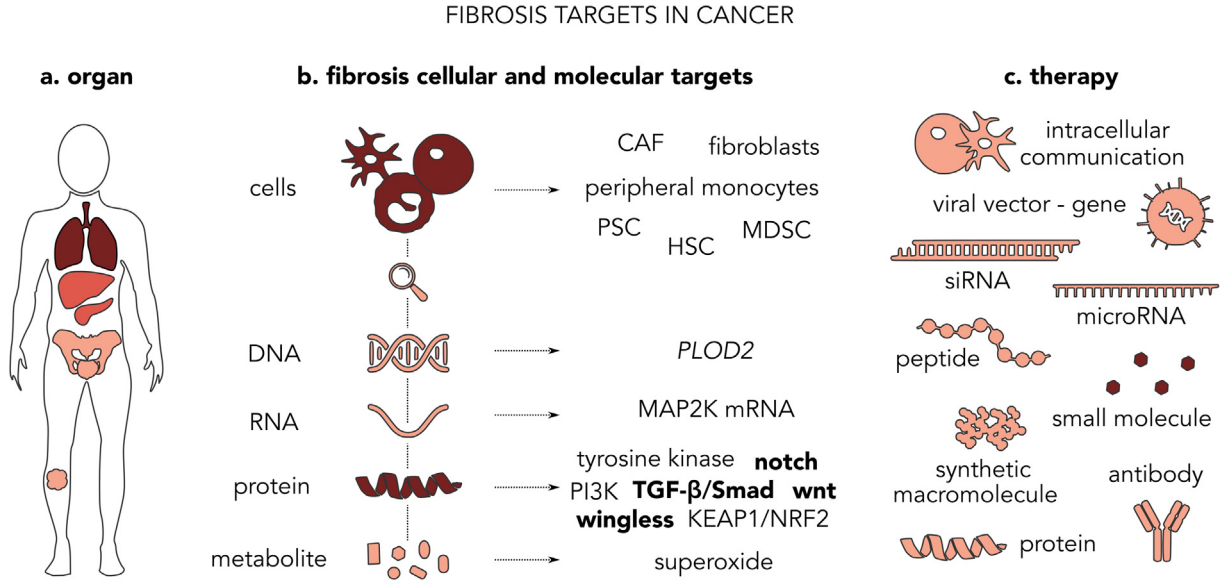

Fig. 3. Fibrosis targets in cancer. (a) Several types of cancer show strong fibrotic manifestation. Non-small cell lung cancer, intrahepatic cholangiocarcinoma and pancreatic cancer are prototypic examples of cancers characterized by excessive fibrotic tissue. (b) Various cells, such as cancer-associated fibroblasts, peripheral monocytes, and pancreatic and hepatic stellate cells, serve as anti-fibrotic targets. In addition, various DNA, RNA, protein and metabolite targets are investigated as potential anti-fibrotic targets; at the protein level, bolding (e.g., TGF-β/Smad) indicates the targeting of multiple protein targets within the highlighted signaling pathway. (c) Majorly small molecules but also nucleotide and aminoacidic therapeutics are used to ameliorate fibrosis in cancer. Color-coding: the analysis of manuscripts described in section 2 revealed the frequency in which each organ, therapeutic target, and therapeutic intervention are investigated for anti-fibrotic purposes in cancer; light red = low frequency; red = medium frequency; dark red = high frequency.

for the vast production of α-SMA and fibronectin [35]) in a non-small cell lung cancer model. Pirfenidone, besides reducing α-SMA expression in TGF-β-activated fibroblasts, also attenuated IL-6 signaling (a major pro-fibrotic and pro-inflammatory cytokine [36]) [37]. In addition to pirfenidone, also nintedanib (approved for IPF) has been evaluated as CAF inhibitor in cancer, in an intrahepatic cholangiocarcinoma model [38]. Nintedanib reduced α-SMA and pro-tumorigenic IL-6 and IL-8 cytokine expression by CAF. This tumor model employed is particularly interesting, because the cross-talk between fibroblasts and intrahepatic cholangiocarcinoma cells results in a very aggressive cancer phenotype [39].

In addition to the pathological formation of fibrosis, radiation treatment has also been incriminated for induction of fibroblast activation and cell senescence. This phenomenon eventually leads to a positive feedback loop with further fibroblast activation. In this situation, adipocytes act in a radio-protective manner, via

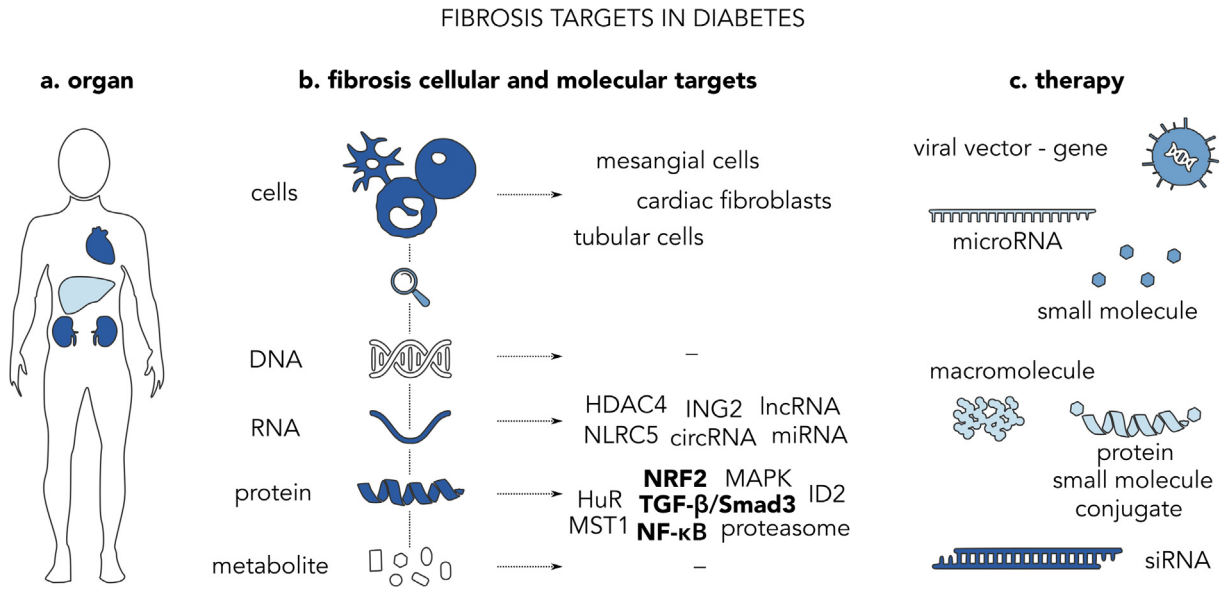

Fig. 4. Fibrosis targets in diabetes. (a) Diabetic cardiomyopathy and diabetic nephropathy are the two major complications of high-glucose conditions. The resulting chronic inflammation leads to severe fibrosis and loss of function in these organs. (b) Cardiac fibroblasts in the heart, as well as mesangial and tubular cells in the kidneys, are the primary targets of anti-fibrotic treatments. At the microscopic level, various RNA variants (i.e., mRNA, lncRNA, circRNA, miRNA), functional proteins in the NRF2, TGF-β/Smad3 and NF-κB pathway, as well as the proteasome, are explored as potential anti-fibrotic targets; at the protein level, bolding (e.g., NRF2) indicates the targeting of multiple protein targets within the highlighted signaling pathway. (c) Given the prominent involvement of RNA analogues in the progression of diabetic fibrosis, RNA interference appears as an appealing therapeutic intervention. Color-coding: the analysis of manuscripts described in section 2 revealed the frequency in which each organ, therapeutic target, and therapeutic intervention are investigated for anti-fibrotic purposes in diabetes; light blue = low frequency; blue = medium frequency; dark blue = high frequency.

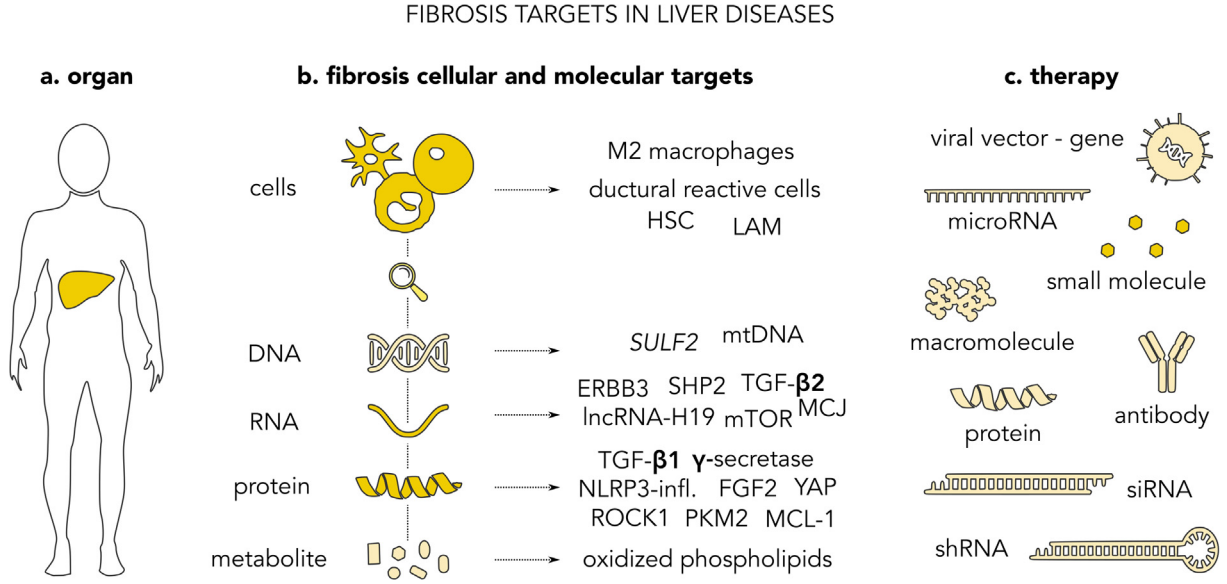

Fig. 5. Fibrosis targets in liver diseases. (a) Fibrotic liver is the major investigated organ in case of the various liver diseases (e.g., NAFLD, NASH). (b) Several cell populations, such as M2-like macrophages, hepatic stellate cells, and lipid-associated macrophages are essential regulators of fibrosis promotion in the liver. Major subcellular targets include various DNA, RNA components (e.g., mitochondrial DNA, TGF-β2 mRNA, mTOR mRNA), proteins (e.g., γ-secretase, the inflammasome, YAP), and metabolites. (c) Given the high number of proteins that are considered anti-fibrotic targets in liver diseases, small molecule inhibitors (e.g., neratinib) appear as the first choice among the various therapeutic interventions. Color-coding: the analysis of manuscripts described in section 2 revealed the frequency in which each organ, therapeutic target, and therapeutic intervention are investigated for anti-fibrotic purposes in liver diseases; light yellow = low frequency; yellow = medium frequency; dark yellow = high frequency.

secretion of adiponectin, which reduces fibroblast activation and cell senescence [40]. A similar result has also been shown in case of liver fibrosis, where the presence of adiponectin inhibited the activation of hepatic stellate cells (HSC) [41]. These examples strongly support the investigation of intercellular cross-talk as a strategy to minimize pathological and treatment-induced fibrosis.

Finally, direct inhibition of HSC and Kupffer cells (NB: immune cells are extensively analyzed in the following section) has also been considered in case of HIV infection. $CD4^+$ T cell depletion is the hallmark of HIV infection [42]. Reduction of the intestinal $CD4^+$ T cells enables the translocation of the intestinal microbiome to the liver portal system resulting in hepatocyte injury. These phenomena induce the production of pathogen-associated molecular patterns (PAMPs) and damage-associated molecular patterns (DAMP), as well as the direct activation of Toll-like receptor 4 (TLR4). This danger signaling, together with ROS generation, result

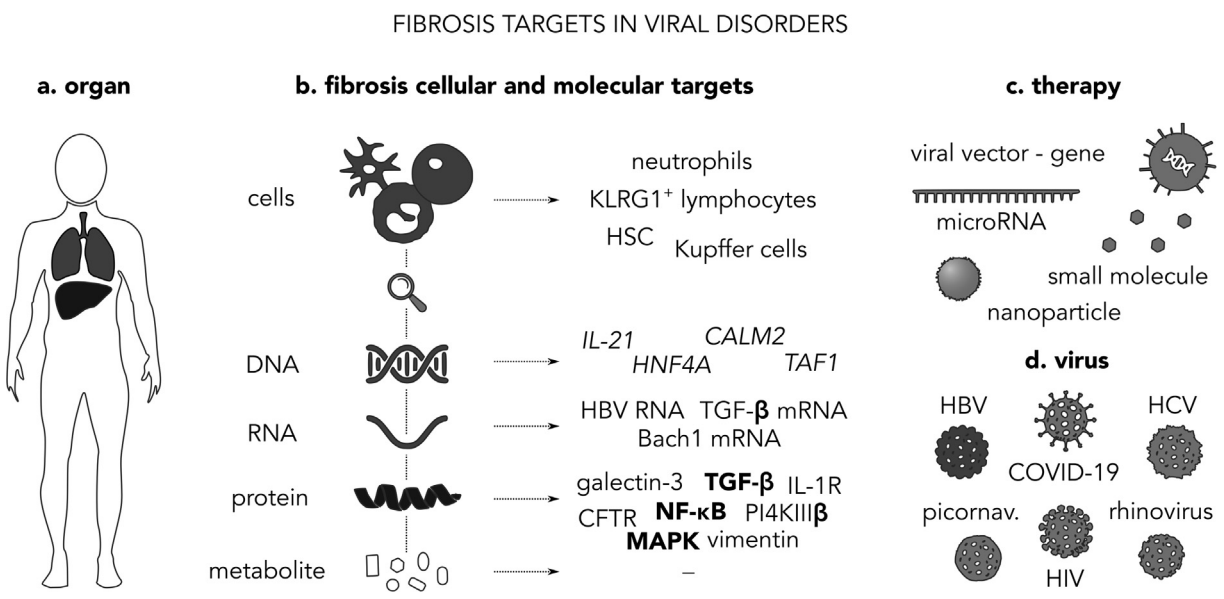

Fig. 6. Fibrosis targets in viral disorders. (a) Liver and lungs are the major recipient organs of virus-associated fibrotic complications. (b) Distinct cell populations, such as neutrophils and hepatic stellate cells, can be targeted to resolve viral fibrosis and inflammation progression. At the sub-cellular level, inhibition of various DNA, RNA, and protein targets (e.g., *IL-21* gene, TGF-β mRNA, and various proteins in the NF-κB, MAPK, and TGF-β signaling pathways) are investigated as fibrotic targets; at the protein level, bolding (e.g., MAPK) indicates the targeting of multiple protein targets within the highlighted signaling pathway. (c) Viral vector-mediated gene delivery, as well as the use of miRNAs and small molecules are prototypic examples of therapeutics used in viral-derived fibrosis. (d) Major types of viruses causing fibrosis are COVID-19 in the lungs, and hepatitis B and C (HBV/HCV) in the liver. Additionally, picornavirus and rhinovirus are critical co-morbidities in patients with cystic fibrosis. Color-coding: the analysis of manuscripts described in section 2 revealed the frequency in which each organ, therapeutic target, and therapeutic intervention are investigated for anti-fibrotic purposes in viral disorders; light gray = low frequency; gray = medium frequency; dark gray = high frequency.

in activation of liver resident macrophages (i.e., Kupffer cells) [43]. Consequently, activated Kupffer cells secrete pro-inflammatory and pro-fibrotic signals (e.g., TGF-β1) that further promote liver fibrosis via activation of HSC [44]. Therefore, inhibition of these cells can be considered as a relevant anti-fibrotic strategy for HIV patients.

2.2. Immune cells as anti-fibrotic targets

In addition to fibrogenic cells, also myeloid and lymphoid immune cells have been investigated as anti-fibrotic targets. CD206$^+$ MΦs (M2 MΦ) have been associated with the activation of fibroblasts and fibrogenesis (apart from their well-known cancer-promoting actions) [45]. The loading of siRNA in nanohydrogel particles decorated with α-mannosyl targeting units enabled the delivery of siRNA to M2 MΦ, making the particles a promising carrier for in vivo RNA interference applications [46]. The same nanoparticle platform was used as a carrier for CSF-1R siRNA delivery into M2 MΦ [47].

A fundamental study on the mechanism of HSC activation links the absence of liver MΦ and infiltrating granulocytes, as well as the presence of mitochondrial DNA, with the progression of hepatic fibrosis. Upon the release of efferocytosis-related factors by hepatocytes, mitochondria respond by releasing mitochondria-derived DAMP (mito-DAMP), with mitochondrial DNA being the prevailing active component. The danger signaling resulted in elevation of TGF-β1 and collagen deposition, while depletion of MΦs and granulocytes further amplified fibrosis. The latter observation suggests that delayed clearance of mito-DAMP causes activation of HSC and fibrosis [48], highlighting the homeostatic importance of clearance-mediating (efferocytotic) phagocytes.

Subsets of MΦ have also emerged as essential regulators in fibrosis promotion [49,50]. In metabolic-associated fatty liver disease (MAFLD), a novel MΦ type present in fibrotic areas was identified. In MAFLD, the resident Kupffer cells are progressively replaced by infiltrating MΦ derived from the bone marrow. It was identified that a specific mononuclear myeloid subtype, namely lipid-associated MΦ (LAM), was characterized by high osteopontin expression and found to be localized in tissue areas with high desmin expression [51] (NB: desmin is typically overexpressed by HSC in fibrotic areas [52]). The fact that LAM were found to express high levels of the cytokine osteopontin indicates their contribution to fibrosis development, since osteopontin has been associated with activation of fibroblasts and HSC, and with promotion of lung and liver fibrosis [53,54]. As such, novel efforts to reprogram hepatic myofibroblasts into hepatocytes [55] should also consider the modulation and polarization of adipose-tissue derived LAM.

Other myeloid cells prominently involved in inflammatory lung diseases [56,57] and fibrosis development [58,59] are neutrophils, which as a unique feature contain neutrophil extracellular traps (NET), composed of DNA fibers and cytoplasmic proteins. NET provide a solid defensive mechanism against pathogens, but they can also cause tissue damage via induction of hyper-inflammatory reactions. NETs have been shown to activate fibroblasts [60] and upregulate fibrotic mediators such as matrix metalloproteinase-2 [61], and have been incriminated for worsening various inflammatory diseases such as cystic fibrosis, systemic lupus erythematosus, and heart disease [62-64]. Post-mortem lung biopsies revealed NET to be present in patients with COVID-19, covering lung airways, contributing to interstitial inflammation, and being part of thrombi in the vascular compartments [65]. This evidence suggests NETosis as a major anti-inflammatory and anti-fibrotic target in the management of COVID-19 repercussions.

A key cell population for the regression of atherosclerosis and heart disease are regulatory T cells, which belong to the lymphoid cell lineage [66,67]. The use of the fatty acid propionate enabled attenuation of fibrosis and other types of cardiovascular damage. Experiments in mice showed that these disease-regression effects were attributable to the regulation of CD25$^+$ Foxp3$^+$ T cells [68,69].

Table 1
Fibrosis targets in atherosclerosis and cardiac disease (green), cancer (red), diabetes (blue), liver diseases (yellow), and viral disorders (gray).

No	Disease category	Investigated tissue	Therapeutic target	Type of target	Treatment	Type of treatment	Nanobiotechnology tools	Outcome	Ref.
1	Atherosclerosis Liver disease	Myofibroblasts		Fibrogenic cells	Icosabutate	Small molecule	n/a	↓ myofibroblasts ↓ macrophage infiltration Downregulation in the metabolic cascade of arachidonic acid	[33]
2	Non-small cell lung cancer	Lungs	Lung fibroblasts Cancer-associated fibroblasts (CAF)	Fibrogenic cells	Pirfenidone	Small molecule	n/a	Inhibited myofibroblast differentiation ↓ α-SMA expression Attenuated IL-6 signaling	[37]
3	Intrahepatic cholangiocarcinoma (ICC)	Liver	CAF	Fibrogenic cells	Nintedanib	Small molecule	Tween-80 surfactant	↓ α-SMA, IL-6, IL-8 expression ↓ cross-talk between CAF and ICC cells	[38]
4	Radiation-derived fibrosis in cancer	Pelvis	Fibroblasts	Fibrogenic cells	Adiponectin (derived by adipocytes)	Intracellular communication	n/a	↓ fibroblast activation ↓ cell senescence	[40]
5	HIV	Liver	Kupffer cells (KC) Hepatic stellate cells (HSC)	Fibrogenic cells	n/a	n/a	n/a	↓ KC- or HSC-mediated pro-inflammatory / pro-fibrotic signaling	[44]
6	Liver disease	$CD206^+$ macrophages (MΦ)		Immune cells	CSF-1R siRNA	RNA interference	α-Mannosyl-functionalized cationic nanohydrogel particles	Cell-specific targeting *CSF-1R* knockdown	[46,47]
7	Liver disease	Liver	Liver MΦ, Infiltrating granulocytes, Mitochondria-derived DAMP (mito-DAMP)	Immune cells mtDNA	n/a	n/a	n/a	↓ MΦ and granulocyte number → delayed clearance of mito-DAMP → HSC activation and ↑ fibrosis	[48]
8	Metabolic-associated fatty liver disease (MAFLD)	Liver	Osteopontin-expressing lipid associated MΦ (LAM)	Immune cells	n/a	n/a	n/a	Modulation and polarization of LAM may alleviate the osteopontin-derived fibrosis promotion	[51]
9	COVID-19	Lungs	Neutrophils (neutrophil extracellular traps – NET)	Immune cells	n/a	n/a	n/a	↓ NET may alleviate interstitial inflammation, thrombi formation, and lung airway blocking	[65]
10	Atherosclerosis Heart Disease	Heart	$CD25^+$ $FoxP3^+$ regulatory T cells	Immune cells	Propionate	Small molecule	n/a	↓ cardiac hypertrophy, fibrosis, vascular dysfunction, hypertension	[68]
11	Hepatitis B	Liver	(Killer cell lectin-like receptor G1) $KLRG1^+$ T cells	Immune cells	n/a	n/a	n/a	Balancing pro-inflammatory $KLRG1^+$ T cells may alleviate liver inflammation and fibrosis	[70]
12	Various (Atherlosclerosis Liver fibrosis Lung adenocarcinoma)	Vessels, Liver, Lung	Senescent cells	Immune cells	uPAR-specific CAR T cells	Immunotherapy	CAR T cells	Senescent cell-specific CAR T cells → ↑ survival and restored homeostasis	[75]
13	Atherosclerosis Heart Disease	Coronary vascular endothelium (CVE)	*ADAM10*	Gene	miR-25-3p agomir	MicroRNA agomir	Exosomes	Uptake of agomir by CVE cells → ↓ several pro-firbotic and pro-inflammatory cytokines, proteins, and lipids	[77]
14	(Various)	Fibroblasts	*PLOD2*	Gene	DNA methyltransferase M.SssI; Krüppel associated box (KRAB)	Protein for epigenetic editing	Zinc finger or CRISPR/dCas9 gene editing technologies	Epigenetic editing → ↓ gene expression → use of TGF-β failed to re-stimulate gene expression	[79]
15	Nonalcoholic fatty liver disease (NAFLD) Steatohepatitis Liver fibrosis	Liver	*SULF2*	Gene	SULF2KO (in vivo) shRNA against sulfatase 2 (in vitro)	Gene knockout RNA interference	n/a	↓ SULF2 → ↓ pro-fibrotic receptors TGF-βR2, PDGFRβ, ↓ collagen I, α-SMA, osteopontin	[80]

(*continued on next page*)

Table 1 (*continued*)

No	Disease category	Investigated tissue	Therapeutic target	Type of target	Treatment	Type of treatment	Nanobiotechnology tools	Outcome	Ref.
16	Hepatitis C	Liver	*HNF4A, TAF1, CALM2*	Gene	n/a	n/a	n/a	Major nodes in the protein–protein interaction network related to liver fibrosis	[81]
17	Hepatitis B	Liver	*IL-21*	Gene	Recombinant HBV loaded with *IL-21*	Epigenetic activation	Recombinant virus	IL-21 induced expression → ↑ viral clearance	[84]
18	Hepatitis B	Liver	TGF-β mRNA, X and S HBV region	mRNA viral RNA	Adeno-associated viral (AAV) particles with DNA encoding shRNA for HBV and TGF-β	Gene delivery RNA interference	AAV particles	shRNA delivery → ↓ TGF-β → ↑ PPAR-γ signaling pathway → further ↓ TGF-β, ↓ NF-κB → oxidative stress, ↓ HSC activation, ↓ ECM	[85]
19	Liver disease	Liver	TGF-β2 mRNA	mRNA	TGF-β2 antisense oligonucleotide	mRNA antisense oligonucleotide	n/a	↓ TGF-β2 → ↓ collagen, α-SMA, ↑ PPAR-γ, ↓ infiltrating inflammatory leukocytes	[87]
20	Diabetic nephropathy	Kidneys	HDAC mRNA	mRNA	miR-29b	MicroRNA	n/a	miR-29b binding to HDAC mRNA → ↓ MΦ-mediated inflammation, fibrosis, TGF-β, collagen IV	[89]
21	Lung (cancer)	Lungs	Lung fibroblasts, MAP2K6 mRNA	Fibrogenic cells, mRNA	miR-375	MicroRNA	n/a	miR-375 → ↓ p38 MAPK pathway, lung fibroblast activation	[91]
22	Diabetic renal fibrosis	Kidneys, tubular cells	Inhibitor of growth 2 (ING2) mRNA	mRNA	siRNA targeting ING2a isoform	RNA interference	n/a	ING2 siRNA → ↓ TGF-β1 mRNA, CTGF mRNA, vimentin, α-SMA	[93]
23	Diabetic cardiomyopathy	Heart	NLRC5 mRNA	mRNA	siRNA targeting NLRC5	RNA interference	n/a	NLRC5 siRNA → ↓ Smad-2/3 phosphorylation, ↓ activation of TGF-β and EndMT, ↓ Snail and Twist	[96]
24	Non-alcoholic steatohepatitis (NASH)	Liver	MCJ mRNA	mRNA	siRNA targeting MCJ	RNA interference	Lipid nanoparticle invivofectamine	↓ MCJ → ↑ hepatocyte capacity to mediate β-oxidation of fatty acids → ↓ lipid accumulation → ↓ steatosis, fibrosis	[101]
25	Alcoholic liver fibrosis	Liver	ERBB3 mRNA	mRNA	miR-148a-3p mimic	MicroRNA	n/a	↓ ERBB3 → ↓ α-SMA, ↓ collagen I, up/down regulated Bax/Bcl2	[105]
26	Hepatitis C	Liver	Bach1 mRNA	mRNA	miR-let-7c	MircoRNA	mRNA-expressing plasmid	↓ Bach1 → ↑ haem-oxygenase-1 (HO-1) expression → ↑ antiviral interferon response → ↓ HCV viral protease activity → ↓ viral replication	[107]
27	Diabetes	Heart, cardiac fibroblasts	miR-150-5p	microRNA	miR-150-5p siRNA	RNA interference	n/a	↓ miR-150-5p → ↓ TGF-β1, pSmad-2/3, α-SMA, collagen I, collagen III, CTGF mRNA, fibronectin mRNA	[112]
28	Diabetic cardiomyopathy	Heart	miR-410-5p	microRNA	miR-410-5p antagomir	RNA interference	n/a	↓ miR-410-5p → ↑ cardiac function, ↓ tissue damage	[113]
29	Cancer	Liver	miR-21-5p, miR-222-3p, miR-221-3p, miR-181b-5p, miR-17-5p	microRNA	n/a	n/a	n/a	miR → ↓ TIMP3 mRNA → inflammatory and fibrotic activity in liver fibrosis and hepatocarcinogenesis	[115]
30	Myocardial infarction	Heart	lncRNA SHNG7, miR-34-5p	lncRNA, microRNA	lncRNA SHNG7 shRNA, miR-34-5p precursor	RNA interference, RNA induction	AAV particles	↓ lncRNA SHNG7 and/or ↑ miR-34-5p → ↓ collagen I, ↓ α-SMA, ↓ matrix deposition, ↑ cardiac function, inhibited fibroblast to myofibroblast transition	[120]
31	Diabetic nephropathy	Kidney, mesangial cells	lncRNA PVT1	lncRNA	PVT1 siRNA	RNA interference	n/a	↓ lncRNA PVT1 → ↓ α-SMA, ↓ fibronectin, ↓ NF-κB pathway	[121]
32	Diabetic cardiomyopathy	Heart	lncRNA MIAT	lncRNA	MIAT siRNA	RNA interference	n/a	↓ lncRNA MIAT → ↓ IL-1β, IL-6, TNF-α, collagen I, collagen III, inability of lncRNA MIAT to attenuate the miR-214-3p-mediated inhibition of pro-inflammatory IL-17	[122]
33	Liver disease	Liver, HSC	lncRNA H19	lncRNA	Gene for lncRNA H19 shRNA	RNA interference	Adenovirus vectors	↓ lncRNA H19 → ↓ HSC activation, ↓ α-SMA, collagen I	[123]
34	Diabetic nephropathy	Kidney, mesangial cells	circ_0123996, miR-149-5p	sscRNA, microRNA	circ_0123996 siRNA, miR-149-5p mimic	RNA interference, RNA induction	n/a	↓ circ_0123996 (sponges miR-149-5p) and/or ↑ miR-149-5p (binds and inactivates Bach1) → ↓ Bach1 mRNA, ↓ fibronectin, collagen	[125]
35	Diabetic nephropathy	Kidney, mesangial cells	circ_0000064	sscRNA	circ_0000064 siRNA	RNA interference	n/a	In presence of miR-143, ↓ circ_0000064 → ↓ collagen I, collagen IV, fibronectin mRNA	[126]

Table 1 (*continued*)

No	Disease category	Investigated tissue	Therapeutic target	Type of target	Treatment	Type of treatment	Nanobiotechnology tools	Outcome	Ref.
36	Diabetic nephropathy	Kidney, tubular cells	circ_WBSCR17	sscRNA	circ_WBSCR17 siRNA	RNA interference	n/a	In presence of miR-185-5p, ↓ circ_WBSCR17 → ↓ cell apoptosis, inflammatory response, fibrosis, ↓ collagen I, collagen IV, fibronectin, TGF-β1	[127]
37	Liver disease	Liver, HSC	TGF- β1, YAP	Proteins	Physalin D	Small molecule	n/a	↓ collagen I, α-SMA, YAP, CTGF, pSmad-2/3	[128]
38	Cardiac disease	Heart	UCHL1	Protein	LDN-57444	Small molecule	n/a	↓ inflammation, fibrosis, remodeling via ↓ TGF-β/Smad-2/3 and NF-κB signaling pathways	[132]
39	Diabetic nephropathy	Kidneys	Proteins in TGF-β/Smad-3 and NF-κB signaling pathways	Proteins	Baicalin-Lysozyme	Small molecule – protein conjugate	Drug-protein conjugate	↑ renal function, ↓ fibrosis, α-SMA, desmin, ↑ E-cadherin; ↓ IL-1β, IL-6, P-p65 (NF-κB pathway) and TGF-β1, P-Smad2/3, Smad4, fibronectin, collagen, SREBP-1 (TGF-β/Smad3 pathway)	[133]
40	Diabetic nephropathy	Kidneys	Inhibitor of differentiation 2 (Id2)	Protein	Oxymatrine	Small molecule	n/a	Oxymatrine → ↑ Id2 → ↓ Twist-mediated renal tubulointerstitial fibrosis, attenuated EMT, ↓ fibronectin, collagen IV, α-SMA, ↑ E-cadherin	[137]
41	Hepatocellular carcinoma	Liver	Proteins in Wnt/β-catenin and Notch signaling pathways	Proteins	Niclosamide	Small molecule	Polymeric micelles	↓ fibrous septa thickness and amount, ↓ Wnt3A mRNA, β-catenin protein, Notch1 mRNA	[138]
42	Cancer	Pancreas, PSC	CBP/β-catenin interaction	Proteins	ICG-001	Small molecule	n/a	ICG-001 → ↓ CBP/β-catenin interaction → ↓ PSC activation, PSC-induced migration of cancer cells, collagen I, α-SMA	[142]
43	Hepatocellular carcinoma	Liver, HSC, MDSC	p38α, p38β	Proteins	SB203580, (Bet762, Anti-PD-L1)	Small molecule, (small molecule, antibody)	n/a	SB203580 → ↓ p38α, p38β → abrogated cross-talk between HSC and MDSC; Bet762, anti-PD-L1 → ↓ MΦ infiltration, ↑ $CD8^+$ T cell infiltration	[144]
44	Liver disease	Liver, HSC	Fibroblast growth factor (FGF) 2	Protein	Neratinib	Small molecule	n/a	↓ FGF2, MAPK signaling, ↓ α-SMA, collagen IA2, collagen IIIA1, TGF-β, PDGFR-β	[145]
45	Non-small cell lung cancer	Lungs	Tyrosine kinase	Protein	Sunitinib, (cRGFfk)	Small molecule, (peptide)	n/a	Inhibited Wnt signaling, ↓ TGF-β-mediated EMT, ↓ Twist	[152]
46	Desmoplastic melanoma		Tyrosine kinase	Protein	Sunitinib, BRAF vaccine	Small molecule, Peptide vaccine	Sunitinib in polymeric micelles, BRAF in lipid calcium-phosphate nanoparticle	Sunitinib → ↓ α-SMA, collagen, BRAF vaccine → ↑ $CD8^+$ T cell infiltration	[153]
47	Liver disease	Liver	γ-secretase	Protein	Dibenzazepine	Small molecule	PLGA nanoparticles	↓ γ-secretase → prevents Notch translocation to the nucleus → ↓ HSC, pro-inflammatory MΦ activation	[156]
48	Liver disease	Liver	NLRP3 inflammasome	Oligomer protein complex	$NLRP3^{-/-}$ transgenic mouse model		n/a	NLRP3 inflammasome absence → ↓ collagen, TPM2β, ↑ GATA4.	[162]
49	Liver disease	Liver, HSC	SHP2, SHP2 mRNA, mTOR, mTOR mRNA, ROCK, REDD1	Protein, mRNA, protein, mRNA, protein, protein	SHP099 SHP2 siRNA, Rapamycin, mTOR siRNA, fasudil, REDD1 gene	Small molecule, RNA interference, small molecule, RNA interference, small molecule, gene induction	Plasmid gene-delivery (REDD1)	SHP2 and PDGF → mTOR activation → pro-fibrotic extracellular vesicle (EV) release → fibrosis, PDGF/mTOR axis → autophagy inhibition → exosome release → fibrosis, mTOR → activate ROCK pathway → EV production → fibrosis, SHP2 → inhibits REDD1 → EV release → fibrosis, Therapeutics → autophagy promotion → EV inhibition → ↓ fibrosis	[165]
50	Diabetic liver, Nonalcoholic steatohepatitis (NASH)	Liver	NFR2	Protein	NRF2 gene	Protein induction	AAV particles	↑ NRF2 → ↑ AGER1 transcription → ↑ AGEs clearance → ↓ fibrosis	[167]
51	Diabetic cardiomyopathy	Heart	NRF2	Protein	Isoliquiritigenin	Small molecule	n/a	↑ NRF2 signaling pathway, ↓ MAPK, inflammation, oxidative stress, cardiac hypertrophy	[169]
52	Diabetic nephropathy	Kidneys	MST1	Protein	Lentiviral particles expressing MST1	Protein induction	Lentiviral particles	↑ MST1 → ↓ diabetic nephropathy, renal fibrosis	[172]
53	Diabetic cardiomyopathy	Heart	PI3K(p110α)	Protein	rAAV6-caPI3K	Protein induction	AAV particles	↑ PI3K → ↓ cardiac remodeling, fibrosis, interstitial and perivascular collagen, CTGF, TGF-β1 mRNA	[173]

(*continued on next page*)

Table 1 (*continued*)

No	Disease category	Investigated tissue	Therapeutic target	Type of target	Treatment	Type of treatment	Nanobiotechnology tools	Outcome	Ref.
54	Cardiac disease	Heart	JMJD1C	Protein	shRNA against JMJD1C, JIB-04	RNA interference, Small molecule	n/a	↓ Ang II-induced cell hypertrophy, fibrosis, ↓ pro-fibrotic TIMP1 transcription	[176]
55	Cancer	Pancreas	Legumain	Protein	RR-11a	Small molecule	n/a	↓ Legumain → ↓ MMP-2 → ↓ PSC activation, ECM synthesis	[177]
56	Pancreatic adenocarcinoma	Pancreas	H^+/K^+-ATPase	Protein	Pantoprazole	Small molecule	n/a	↓ collagen secretion by PSC	[183]
57	Diabetic nephropathy	Kidneys	GPR43, GPR109A	Receptor proteins	Dietary fibers	Macromolecule	n/a	↓ mesangial matrix, collagen deposition, MΦ recruitment, ↓ IL-6, TNFα, CCL2, CXCL10, TGF-β, fibronectin	[184]
58	Atherosclerosis	Intestine, small intenstine epithelial cells	FABP2 mRNA	mRNA	siRNA against FABP2 mRNA	RNA interference	Lentiviral particles	↓ intestinal FABP2 → ↓ western diet-induced atherosclerosis, vascular fibrosis	[186]
59	Lung adenocarcinoma	Lungs, fibroblasts	PI3K, HDAC	Proteins	Fimepinostat	Small molecule	n/a	Attenuated TGF-β1- and bleomycin-induced fibrosis	[187]
60	Metastatic breast cancer	Lungs	CXCR4	Protein	CXCR4 antagonist (FX), Paclitaxel, PD-L1 siRNA	Macromolecule, small molecule, RNA interference	Nanocomplex	↓ tumor fibrosis, ↑ T cell infiltration, ↑ anti-PD-L1 response, ↓ α-SMA, collagen	[188]
61	Diabetic nephropathy	Kidneys, tubular cells	Proteasome	Protein complex	Proteasome inhibitor MG132	Small molecule	n/a	↓ proteasome → ↑ anti-fibrotic protein NF-E2 → ↓ CTGF, fibronectin	[189]
62	Diabetic nephropathy	Kidney, mesangial cells	RNA binding protein HuR	Protein	n/a	n/a	n/a	High glucose → ↑ HuR → HuR binds to Nox4 mRNA → ↑ Nox4 translation → ↑ ROS → ↑ matrix synthesis	[190]
63	Liver disease	Liver, MΦ	Pyruvate kinase M2	Protein	Annexin A5	Protein	n/a	Specific action in liver MΦ, ↓ α-SMA, TGF-β, Collagen IIIA1 mRNA, ↓ IL-1β, IL-6, TNFα mRNA, ↑ CD206, IL-10 (M2 polarization)	[191]
64	Liver disease	Liver, ductural reactive cells (DRC)	MCL1	Protein	S63845	Small molecule	n/a	↓ DRC, inflammation, fibrosis, collagen, fibronectin, TGF-β, α-SMA	[192]
65	Liver disease	Liver, hepatocytes, HSC	ACVR1	Protein	Momelotinib	Small molecule	n/a	↓ ACVR1 (BMP/ACVR1/SMAD pathway) → ↓ PNPLA3 mRNA → ↓ TIMP1, collagen IA2, MMP2, CXCL1, IL-6, CCL2	[193]
66	Picornavirus & cystic fibrosis	Lungs	PI4KIIIβ, CFTR	Protein, protein	"23a"	Small molecule	n/a	↓ PI4KIIIβ → ↓ picornavirus replication, stabilization of the mutated CFTR protein (mutated in patients with cystic fibrosis)	[194]
67	Rhinovirus & cystic fibrosis	Lungs, airway epithelial cells	IL-1R	Protein	n/a	n/a	n/a	IL-1R antagonism may alleviate from fibrotic material deposition	[196]
68	Cardiovascular disease, nephropathy	Heart, Kidney	Trimethylamine-N-oxide (TMAO)	Metabolite	Linaclotide	Peptide	n/a	Linaclotide → ↑ gastrointestinal transit → ↓ TMAO → ↓ renal inflammation, cardiac exposure to TMAO, collagen I, TGF-β, galectin-3, ST2.	[197]
69	Nonalcoholic steatohepatitis (NASH)	Liver	Oxidized phospholipids	Metabolite	E06-scFv	Transgenic mouse expressing neutralizing antibodies	n/a	↓ steatosis, inflammation fibrosis, hepatocyte death, progression to hepatocellular carcinoma	[200]
70	Atherosclerotic plaque	Vessels, Heart	Mitochondrial ROS	Metabolite	MitoTEMPO	Small molecule	n/a	↓ smooth muscle cell apoptosis, MMP2, matrix degradation → prevented plaque instability	[201]
71	Cancer	Prostate (in vitro)	Superoxide	Metabolite	Manganese porphyrin	Small molecule	n/a	Manganese porphyrin → converted superoxide to hydrogen peroxide → ↓ TGF-β/Smad pathway, ↓ KEAP1, ↑ NRF2	[204]

Analysis of liver samples from patients with chronic Hepatitis B infection revealed a specific T cell population to be associated with liver fibrosis (also observed in primary biliary cholangitis and autoimmune hepatitis). $KLRG1^+$ lymphocytes were identified as a strong pro-inflammatory T cell sub-population and they were positively correlated with patient worsening via progressing inflammation and fibrosis. This evidence suggests the depletion of $KLRG1^+$ lymphoid cells as a strategy against liver inflammation and fibrosis [70]. Nevertheless, the same population has also been proposed to display an anti-fibrotic role in hepatitis B, via induction of HSC death [71]. This contrasting evidence linking $KLRG1^+$ lymphocytes to fibrosis indicates that balancing this population, rather than aggressively stimulating or depleting, can achieve a fibrotic equilibrium.

Finally, related to atherosclerosis and to many other fibrotic diseases (e.g. liver fibrosis, lung fibrosis, diabetes, osteoarthritis), the targeting of senescent cells with senolytics has been described as a promising strategy against disease progression [72-74]. The engineering of CAR T cells against the urokinase-type plasminogen activator receptor (uPAR), i.e., a membrane protein expressed in senescent cells, showed a robust outcome in mice with lung adenocarcinoma and liver fibrosis, via extending the survival and restoring liver homeostasis, respectively [75].

2.3. Genes as anti-fibrotic targets

Transitioning from the cellular to the subcellular level, specific genes have been associated with fibrosis promotion. A robust example is the *ADAM10* gene (A Disintegrin and Metalloproteinase domain-containing protein 10) [76]. In an effort to inhibit its activity, the platelet-secreted exosomes carrying the microRNA miR-25-3p were used, showing that the microRNA binds to the *ADAM10* gene and reduces its expression. *In vivo*, the use of a miR-25-3p agomir resulted in downregulation of several pro-fibrotic and pro-inflammatory proteins, lipids and cytokines, including α-SMA, collagen I, collagen III, triglycerides, cholesterol, IL-1β, IL-6, and TNF-α. The agomir showed a strong efficacy in targeting the gene, as evidenced by the fact that a comparative RNA interference experiment with ADAM10 siRNA resulted in a similar magnitude of modulation [77].

Another example are the PLOD genes which are contributors in fibrosis and cancer with matrix deposition propensity [78]. Specifically, the *PLOD2* gene was silenced via the use of the DNA methyltransferase M.Sssl or the non-catalytic Krüppel associated box (KRAB) (directed in the gene promoter by the zinc finger or CRISPR/dCas9 gene editing technologies). These gene-editing systems resulted in DNA methylation and partial reduction of PLOD2 expression or in histone modifications that completely repressed gene expression. In a control experiment, the use TGF-β1 failed to re-stimulate PLOD2 expression, supporting the potential of these epigenetic editing technologies for PLOD2-targeted (or generally gene-targeted) anti-fibrotic strategies [79].

The contribution of *SULF2* gene activity in inflammation and fibrosis was evaluated in steatohepatitis and fibrosis employing a mouse model of nonalcoholic fatty liver disease (NAFLD) on high-fat diet. *In vivo* experiments in sulfatase 2 knockout and in vitro experiments with administration of short hairpin RNA (shRNA) against sulfatase 2 revealed the contribution of sulfatase 2 in worsening inflammation and fibrosis. Expression of fibrogenic protein receptors such as TGF-βR2 and PDGFRβ, and mRNA encoding for collagen IA1 and α-SMA were significantly downregulated in the absence of sulfatase 2. Interestingly, also the levels of osteopontin mRNA were reduced, supporting the pro-fibrotic role of sulfatase 2 [80].

In hepatitis C patients, three genes (*HNF4A, TAF1, CALM2*) were identified to be associated with the progression of liver fibrosis and to be major nodes in the protein–protein interaction network among 166 fibrosis-related genes [81]. While there is not much experimental support for the exact role of *TAF1* and *CALM2* genes in fibrosis, the *HNF4A* gene has been associated with fibrosis in a positive manner. Employing adeno-associated viral (AAV) particles carrying the gene encoding for HNF4A led to a positive anti-fibrotic therapy outcome, including inhibition of myofibroblast activation and induction of MET (anti-EMT) transition [82]. A similar concept, i.e., epigenetic gene activity induction, has been used for the *IL-21* gene in a hepatitis B virus (HBV) model. IL-21 has been identified as a requirement for sustaining the activity of $CD4^+$ and $CD8^+$ T cells during viral disorders [83]. Therefore, the use of a recombinant HBV loaded with a gene for IL-21 allowed the gene cargo to be delivered in infected hepatic cells and efficiently induced expression of IL-21 [84]. This approach enabled the clearance of viral particles and thus is a promising strategy against the HBV fibrotic repercussions.

2.4. Messenger RNA nucleotides as anti-fibrotic targets

The inhibition of mRNA nucleotides is the most traditional strategy of inhibiting fibrosis at the RNA level. Targets typically are mRNAs encoding for well-known pro-fibrotic proteins, e.g., TGF-β. An interesting anti-fibrotic approach against TGF-β (and also against HBV itself) was suggested for the synergistic tackling of viral fibrosis: via using AAV particles loaded with DNA encoding for shRNA against the X and S HBV coding regions as well as against TGF-β mRNA, the liver levels of total collagen, collagen I, collagen III, α-SMA, FABP1, and TGF-β would be potently reduced [85]. Mechanistically, the combination of the shRNAs resulted in direct inhibition of TGF-β, while activation of the PPAR-γ signaling pathway (involved in anti-fibrotic inhibition of TGF-β/Smad signaling [86]) enabled further TGF-β inhibition and decreased NF-κB p65 phosphorylation and activation. All together, these anti-inflammatory and anti-fibrotic modulations reduced of oxidative stress, inhibited HSC activation and suppressed ECM production.

As highlighted above, TGF-β is the cornerstone mediator of fibrosis development. There are three isoforms of TGF-β, i.e., TGF-β1, 2, and 3. A study focusing on TGF-β2 mRNA showed that its inhibition via a TGF-β2 antisense oligonucleotide (AON) resulted in collagen and α-SMA reduction, whilst also inducing the expression of anti-fibrotic PPAR-γ and limiting the infiltration of inflammatory leukocytes [87]. This example shows that the inhibition of factors closely connected to TGF-β is also a promising anti-fibrotic strategy. In this regard, histone deacetylase-4 (HDAC4) is one of the proteins required for the activation of fibroblasts via TGF-β1 [88]. Targeting the HDAC4 mRNA was investigated in diabetic nephropathy. The binding of the therapeutic microRNA miR-29b in the 3′ UTR sequence of HDAC4 mRNA resulted in reduced MΦ-mediated inflammation and less fibrosis, as apparent from the decreased levels of TGF-β and collagen IV expression, as well as the reduced fibrosis area [89].

The presence of TGF-β results in upregulation of various pro-fibrotic pathways. Inhibition of mRNA targets in these pathways has also been investigated as an anti-fibrotic therapy strategy. For example, the TGF-β-induced activation of the p38 MAPK pathway was regulated via inhibition of the MAP2K6 mRNA by a miR-375 (i.e., a cancer-suppressive microRNA [90]) mimetic, preventing lung fibroblast activation [91]. This study exemplifies the anti-fibrotic potential of microRNAs [92].

Inhibition of mRNA has been used also for preventing EMT/EndMT processes. In diabetic renal fibrosis, siRNA against the inhibitor of growth 2 (ING2) mRNA resulted in reduction of high-glucose-induced TGF-β1 and connective tissue growth factor (CTGF) mRNA levels [93]. This is an interesting outcome for the mechanisms of diabetic renal fibrosis (and perhaps unexpected),

since ING proteins are investigated for their tumor-suppressing capacities and the downregulation of fibrotic mediators (metalloproteinase 2, NF-κB signaling) in cancer [94,95]. In a high-glucose-induced cardiac fibrosis model, NLRC5 mRNA was investigated as target for its involvement in EndMT [96] (already known to be associated with liver fibrosis [97]). When exposed to high glucose, the endothelial cells undergo injury-driven morphological changes that progressively substitute their endothelial markers (cadherin, CD31) by mesenchymal ones (vimentin, α-SMA) [98]. These more mesenchymal cells together with cardiac fibroblasts overproduce ECM proteins, promoting progression of myocardial fibrosis. The inhibition of NRLC5 mRNA by siRNA ameliorated the high-glucose-induced phosphorylation of Smad-2/3 and consequently the activation of TGF-β and EndMT, by regulating the Snail and Twist expression (important transcription factors in fibrosis development [99,100]) [96].

A plethora of mRNAs have been inhibited by siRNAs or miRNAs in various diabetes and liver diseases, aiming to examine their involvement in fibrosis development. In patients with NAFLD, a protein emerging as a promising anti-fibrotic target is the methylation-controlled J protein (MCJ). The silencing of the MCJ mRNA by siRNA loaded in the lipidic transfection platform "Invivofectamine" triggered hepatocytes to oxidize fatty acids and reduce lipid accumulation in the liver [101] (NB: impaired mechanisms of fatty acid oxidation have been associated with tissue damage and fibrosis [102]). The treatment reduced steatosis and fibrosis. A protein important for the induction of liver fibrosis which is used as an anticancer target is the receptor tyrosine-protein kinase ERBB3 [103,104]. In an alcoholic liver fibrosis model, ERBB3 mRNA was inhibited by a miR-148a-3p mimetic, which induced anti-fibrotic reduction of α-SMA and collagen I and mediated apoptosis via upregulation of Bax and downregulation of Bcl2 [105], corroborating findings that indicate apoptosis induction and Bax/Bcl2 regulation in cancer as a mechanism to overcome treatment resistance [106]. Finally, the inhibition of Bach1 mRNA was used as a strategy to suppress the replication of Hepatitis C virus. Transfection of cells with plasmid encoding miR-let-7c inhibited Bach1 activity as a transcriptional suppressor of heme oxygenase 1 (HO1) expression [107]. The elevated expression of HO1 enabled antiviral activity by triggering cellular ROS to act against the infection, as observed in various viral and bacterial disorders [108,109].

2.5. miRNA, lncRNA, and sscRNA nucleotides as anti-fibrotic targets

Besides mRNA, various other RNA nucleotides, such as microRNA (miRNA), long non-coding RNA (lncRNA) and single-stranded circular RNA (sscRNA), have been investigated as anti-fibrotic targets. In cardiac fibroblasts, the miR-150-5p was examined as an anti-fibrotic target, as it is known to inactivate Smad-7 mRNA, the anti-fibrotic counterpart of pro-fibrotic Smad-3 in the TGF-β/Smad-2/3 signaling [110,111]. The miR-150-5p siRNA led to the downregulation of miR-150-5p, which reduced the protein levels of TGF-β1, of phosphorylated Smad-2 and Smad-3, α-SMA, and of collagen I and collagen III. Additional reductions were observed in the mRNA levels of CTGF and fibronectin [112]. A similar approach was followed for the inhibition of miR-410-5p, a microRNA that has been incriminated to target Smad-7 mRNA and contributing to upregulation of the TGF-β signaling [113]. An antagomir against miR-410-5p improved diabetes-affected cardiac function and reduced tissue damage [114]. Finally, a fundamental investigation on activation of stellate cells by small non-coding microRNA revealed five microRNAs, i.e., miR-21-5p, miR-222-3p, miR-221-3p, miR-181b-5p and miR-17-5p to be responsible for downregulating TIMP3 expression, which confers inflammatory and fibrotic activity in liver fibrosis and hepatocarcinogenesis [115].

Emerging investigations of lncRNAs have revealed their involvement in inflammation and fibrosis [116-118]. In a murine myocardial infarction model, the identification of lncRNA SHNG7 as a fibrosis mediator showed the lncRNA to sponge miR-34-5p, a miRNA that suppresses cardiac fibroblasts by targeting ROCK1 (a pro-fibrotic Rho kinase protein [119]). Mechanistic investigation showed that the lncRNA SHNG7 acts as competing endogenous RNA against miR-34-5p, while elevated levels of miR-34-5p resulted in easing matrix deposition, restoring cardiac function and inhibiting the transition of fibroblasts to myofibroblasts [120]. A similar pattern was observed for lncRNA PVT1 in mesangial cells, lncRNA MIAT in diabetic cardiomyopathy, and lncRNA H19 in HSC. RNA interference against these lncRNAs enabled amelioration of fibrosis and reduction of pro-inflammatory proteins [121-123].

Finally, even though their exact mechanistic role remains relatively elusive, sscRNAs have been associated with contribution to fibrosis [124]. In diabetic nephropathy, the knockdown of various sscRNAs, including circ_0123996 [125], circ_0000064 [126] and circ_WBSCR17 [127], in mesangial and tubular cells by siRNA or miRNA mimetics resulted in reduction of fibronectin, collagen, and TGF-β1. Mechanistic exploration of the role of these sscRNAs revealed that their pro-fibrotic actions rely on the sponging of endogenous regulator miRNAs that inhibit the production of fibrotic proteins.

Altogether, the identification and association of RNA nucleotides with specific diseases and disease stage, will certainly move forward diagnostic and therapeutic efficiency. Such approaches have already been in clinical trial stage. For example, in patients with hepatocellular carcinoma or liver disease, the identification of blood extracellular RNA nucleotides (exRNA) has been evaluated as a mean for accurate diagnosis (NCT02908048). Similarly, in patients with cystic fibrosis, blood miRNA signature was assessed as a strategy to reflect the pulmonary status (NCT02992080). Related to the evaluation of the treatment side-effects, in patients with breast carcinoma and fibrosis, the identification of specific lncRNA, snRNA, snoRNA, and miRNA signatures, as well as, expression patterns of heat-shock proteins (HSP) were evaluated for the prediction of pathological radiation-induced fibrosis (NCT03000764). Finally, the RNA nucleotides have been considered as therapeutic mediators. For example, in cystic fibrosis a single-stranded antisense RNA oligonucleotide has been trialed in patients with homozygous F508del cystic fibrosis patients in order to promote the correction of the CFTR expression via repairing the CFTR mRNA (NCT02532764).

2.6. TGF-β, NF-κB, Wnt/β-catenin, and p38 MAPK pathway proteins as anti-fibrotic targets

Various proteins and transcription factors in the TGF-β, NF-κB, Wnt/β-catenin, and p38 MAPK signaling pathway have been investigated as anti-fibrotic targets. In this regard, the attractive concept of blocking TGF-β1 and YAP protein (yes-associated protein; in the hippo pathway, together with Smad-2/3 involved in the TGF-β transcriptional program promoting CTGF production) for inhibiting HSC activation was investigated by the use of physalin D, a phytopharmaceutical isolated from the plant physalis. Physalin D treatment lowered the levels of various fibrotic indicators, including collagen I, α-SMA, YAP, CTGF, and phosphorylated Smad-2/3 [128]. Analogously, the ubiquitin carboxy-terminal hydrolase 1 (UCHL1) protein, i.e., a prognostic factor and promising target in neurological diseases, cancer and pulmonary fibrosis [129-131], was inhibited by the small molecule LDN-57444. UCHL1 inhibition resulted in reduced remodeling and easing of inflammation and fibrosis via modulating the TGF-β/Smad-2/3 and NF-κB signaling pathways [132]. A baicalin-lysozyme prodrug was designed to

inhibit proteins of the NF-κB and TGF-β/Smad-3 pathway in diabetic nephropathy. The conjugate improved renal impairment and reduced inflammation and fibrosis, regulating multiple pro-fibrotic proteins, and increasing the E-cadherin expression (loss of E-cadherin promotes EMT) [133]. An alternative approach is to upregulate an anti-fibrotic protein, rather than inhibiting a pro-fibrotic one. Upregulating the inhibitor of differentiation 2 (Id2) protein has been shown to have inhibitory effects against EMT after stimulation with TGF-β and attenuates pulmonary and cardiac fibrosis through regulation of Twist and TGF-β1/Smad-3 signaling, respectively [134-136]. In diabetic nephropathy, the use of the small molecule oxymatrine enabled inhibition of renal fibrosis by enhancing Id2 expression and downregulating Twist expression, which under high-glucose conditions contributes to EMT activation [137].

Focusing on the Wnt/β-catenin pathway, the use of niclosamide enabled reduction of fibrosis in and of tumor nodule size in a hepatocellular carcinoma model [138]. Even though niclosamide displays anti-cancer potential through the STAT3 signaling pathway [139], niclosamide-mediated reduction in Wnt3A mRNA, β-catenin protein and Notch1 mRNA indicates involvement of niclosamide in regulating fibrosis via affecting the Wnt/β-catenin and Notch pathways; which have both been implicated in fibrosis regulation [140,141]. Related to the interruption of Wnt/β-catenin signaling in the pancreas, the use of ICG-001, an inhibitor of the cyclic AMP response element-binding protein (CBP), resulted in blocking of the interaction between CBP and β-catenin interaction in pancreatic stellate cells, and thereby contributed to suppression of stellate cell-mediated cancer cell migration [142].

Major proteins in the pro-fibrotic p38 MAPK signaling pathway [143] have also been considered as anti-fibrotic targets. Focusing on HSC and myeloid-derived suppressor cells (MDSC) in an aggressive hepatocellular carcinoma model, SB203580 (an inhibitor of p38α and p38β proteins) abrogated the pro-fibrotic cross-talk between these two cell populations [144]. In addition to inhibiting p38 MAPK signaling, dual blockade of BET bromodomain by the Bet762 inhibitor and the anti-PD-L1 therapy inhibited the infiltration of MΦs in the liver and allowed infiltration of $CD8^+$ cytotoxic T cells, a process that is highly connected to reduction of desmoplasia. HSC are considered to be the major promotor of liver fibrosis. The use of the tyrosine kinase inhibitor neratinib in a liver fibrosis model resulted in reducing the levels of fibrotic proteins α-SMA, collagen IA2, collagen IIIA1, TGF-β and PDGFR-β. The mechanism by which neratinib promoted an anti-fibrotic phenotype and inactivation of HSC was suggested to be via inhibition of fibroblast growth factor 2 and interruption of MAPK signaling [145]. Interestingly, the inhibition of fibroblast growth factors (FGF) as an anti-fibrotic strategy has been both confirmed and challenged, with the former claimed on the basis of interruption of FGF binding to the FGF receptor, and the latter based on inhibition of p38/MAPK and TGF-β signaling [146-148].

Finally, the multi-target tyrosine kinase inhibitor sunitinib is known to block signaling in several pro-fibrotic pathways, including Wnt, TGF-β/Smad-2/3 and non-Smad signaling pathways of TGF-β (e.g., ERK1/2 and P38 pathways) [149-152]. Sunitinib activity resulted in reduced expression of pro-fibrotic markers, and together with the use of the integrin inhibitor cRGDfk peptide, it also reduced the expression of Twist [152]. The multi-target tyrosine kinase inhibition activity of sunitinib makes it a promising candidate also for desmoplastic melanoma. As an example, sunitinib formulated in polymeric micelles enabled the reduction of ECM deposition and elicited a strong cytotoxic response with elevated $CD8^+$ T cells after vaccination with BRAF peptide loaded in lipid nanoparticles. This positive outcome indicates the importance of fibrosis inhibition not only for direct anti-fibrotic activity, but also for indirectly enhancing therapeutic outcome via improving the accumulation and penetration of co-administered therapeutic agents [153].

2.7. Other proteins as anti-fibrotic targets

In addition to regulation of the above proteins and pathways, various other targets have been investigated as promising anti-fibrotic strategies. A prominent example is the inhibition of γ-secretase for inhibiting Notch activation, a concept that has been examined previously for leukemia [154,155]. The inhibition of γ-secretase prevented the translocation of Notch to the nucleus, blocking activation of pro-fibrotic HSC and pro-inflammatory MΦ. In order to prevent off-target toxicities (particularly goblet cell metaplasia), the γ-secretase inhibitor dibenzazepine was incorporated in PLGA nanoparticles for enhancing liver biodistribution [156]. Another important target is the inflammasome; an oligomer protein complex responsible for inflammatory cascades. The NLRP3 inflammasome is associated with many diseases (e.g. lung fibrosis, cardiovascular fibrosis) where its dysfunction may lead to fibrosis [157-161]. In liver disease, the use of NLRP3 knockout mice showed decreased levels of fibrosis markers and an increase in cytoprotective GATA4 [162], highlighting that therapies targeting deactivation of NLRP3 may constitute a complementary approach against liver fibrosis [163,164].

A study focusing on the autophagy pathway and pro-fibrotic extracellular vesicle (EV) production investigated the association of these features with activation of HSC and fibrosis. Several potential targets, including SHP2 mRNA and protein, mTOR mRNA and protein, ROCK protein, and REDD1 protein, were examined, in order to identify the involvement of each component in liver fibrosis with multiple therapeutic interventions, including SHP2 siRNA, SHP099 (SHP protein inhibitor), mTOR siRNA, rapamycin (mTOR inhibitor), plasmid with REDD1 gene, and fasudil (ROCK1 inhibitor). This thorough investigation showed that PDGF and SHP2 proteins are responsible for activating mTOR signaling, which promotes the release of EV with pro-fibrotic cargo. In addition, the PDGF/mTOR axis inhibited autophagy and promoted secretion of high amount of exosomes, with consequences similar to the release of EV. On top of this, mTOR was found to activate the ROCK pathway, which resulted in additional pro-fibrotic EV production. Finally, SHP2 was found to inhibit REDD1, i.e., an endogenous mTOR inhibitor and autophagy activator, and it enhanced EV release. SHP2 gene deletion in a mouse model furthermore showed reduction in fibrosis, collagen I and α-SMA levels. Importantly, TGF-β did not affect the levels of REDD1, highlighting the importance of PDGF/SHP2 signaling in the development of fibrosis. The abovementioned balance was interrupted by pharmacotherapeutic interventions (e.g., rapamycin, mTOR siRNA, fasudil) enabling autophagy promotion and inhibition of EV secretion [165].

In addition to the downregulation of pro-fibrotic proteins, the upregulation of anti-fibrotic proteins is a robust strategy to control fibrosis. Upregulation of NRF2 or inhibition of NRF2-KEAP1 interactions have allowed for alleviating fibrosis in cancer. In an interesting study in diabetic livers or steatohepatitis (which typically appear as comorbidities [166]), the production of advanced glycation end-products (AGEs) proved to accelerate liver fibrosis as their clearance receptor (AGER1) is downregulated. Enhancing the available amounts of NRF2 seems a viable anti-fibrotic strategy, as it acts as a transcription factor promoting the expression of AGER1. The use of AAV vectors carrying the NRF2 gene showed considerable transduction in hepatocytes, resulting in anti-inflammatory and anti-fibrotic responses [167]. Similarly, focusing on NRF2 in diabetic cardiomyopathy, isoliquiritigenin, a small molecule reported to reduce inflammation and fibrosis [168], was used as an NRF2 protein inducer, enabling cytoprotective effects via elevation of NRF2 levels [169]. Interestingly, even though elevation of

NRF2 levels is considered cytoprotective, and drug discovery efforts aiming at direct KEAP1-NRF2 protein–protein-interaction inhibition [170], its exact role in tumor progression remains unclear and compounds for reducing the abnormally high levels of NRF2 are under investigation [171]. Similar to the activation of the NRF2 protein, induction of the mammalian serine/threonine-protein kinase 4 (MST1) [172] and of the phosphoinositide 3-kinase p110α (PI3K(p110α)) [173] has been shown to be effective against fibrosis, in diabetic nephropathy and cardiac fibrosis remodeling, respectively.

Various other proteins have been proposed for anti-fibrotic application in the diseases addressed. In this regard, vimentin and galectin-3 have been proposed as targets for easing myofibroblast activation and cytokine storm, respectively, in viral disorders [174,175]. JMJD1C [176], legumain [177,178] and CD147 [179] have been inhibited for ameliorating fibrosis and balancing pro-fibrotic metalloproteinases (matrix proteins with fibrosis promoting and mesenchymal stem cell regulating capacities [180-182]) in cardiac fibrosis and pancreatic fibrosis. Inhibition of proteins related to homeostatic mechanisms, e.g., H^+/K^+-ATPase [183], GPR43 and GPR109A sensing receptors [184,185], intestinal fatty acid-binding protein (FABP2) [186], has also been shown to confer promising anti-fibrotic efficacy in disease models related to chronic pancreatitis, diabetic nephropathy, and atherosclerosis. Finally, promising anti-fibrotic activity profiles have been published for inhibition of other proteins, such as PI3Kα and HDAC proteins in lung adenocarcinoma [187], CXCR4 in lung metastasis [188], the proteasome and the RNA-binding protein HuR in diabetic nephropathy [189,190], the pyruvate kinase M2, MCL1, and ACVR1 in liver diseases [191-193], and PI4KIIIβ, CFTR and IL-1R in viral infections [194-196].

2.8. Metabolites as anti-fibrotic targets

Besides modulating key cell populations and genes, RNAs and proteins, also metabolic products are extensively investigated as anti-fibrotic targets. Related to cardiovascular disease and nephropathy, high levels of the intestinal bacteria-derived hepatic metabolite trimethylamine-N-oxide (TMAO) have been associated with fibrosis and inflammation. The use of linaclotide (i.e., a small peptide guanylate cyclase C agonist that accelerates gastrointestinal transit) enabled the reduction of TMAO and, consequently, renal inflammation, renal fibrosis and cardiac fibrosis [197]. Related to the regulation of gut-derived metabolites, dietary fibers can successfully stand as anti-inflammatory and anti-fibrotic mediators. Their use has been shown to significantly reduce TNF-α, IL-1β, monocyte chemotactic protein 1 (MCP1/CCL2), collagen, α-SMA, and to increase IL-10 and IFN-γ in diabetes models [198].

Oxidized phospholipids constitute another class of metabolites that accumulate in the liver and in atherosclerotic lesions, causing oxidative stress and damaging mitochondria. The development of a transgenic mouse model expressing neutralizing antibodies E06-scFv against oxidized phospholipids interrupted inflammatory signaling, improved inflammation and fibrosis, and inhibited the progression of NASH to hepatocellular carcinoma [199,200].

Overproduction of reactive oxygen species (ROS) induces oxidative stress, atherosclerotic plaque instability and fibroblast activation. In a mouse model of superoxide dismutase 2 deficiency, targeting mitochondrial ROS with the superoxide scavenger MitoTEMPO reduced the expression of MMP-2, decreased matrix degradation and prevented atherosclerotic plaque instability [201]. This result points out that anti-fibrotic strategies should aim to reconstitute a fibrotic balance (rather than complete elimination), particularly important for avoiding rupture of vulnerable atherosclerotic plaques [202,203]. Finally, in irradiated prostate fibroblasts, the use of manganese porphyrin metabolically converted superoxide to hydrogen peroxide, allowing for inhibition of the TGF-β/Smad pathway and reduction of α-SMA through sequential down-regulation of KEAP1 and activation of NRF2 [204].

3. Therapeutic outlook: Clinical status, drug repurposing and drug delivery

The exploration of anti-fibrotic targets gains more and more attention due to the understanding that inhibiting pathological fibrosis not only enables easing of the disease, but also allows for improving drug accessibility to the local microenvironment. Recent advances have explored the option to inhibit fibrotic targets at various levels of transcription and translation, aiming to holistically balance fibrotic manifestations via cutting-edge strategies, e.g., gene editing and RNA interference. The vast majority of such interventions is still under preclinical evaluation, while in clinical practice, only small molecules are typically administered and explored. On the long run, we foresee that the identification of anti-fibrotic targets and the design of specific anti-fibrotic therapies will shift the clinical landscape from unspecific to (more) cell- and molecule-specific interventions. In this respect, the utilization of nanomedicine tools which are able to deliver advanced therapeutic cargo to specific (sub)cellular targets is anticipated to further potentiate the anti-fibrotic treatment regimens.

3.1. Approved anti-fibrotic agents, clinical trials and drug repurposing

For decades, first-line anti-fibrotic interventions have been based on corticosteroids and immunosuppressants [205,206]. In recent years, two small molecules, i.e., pirfenidone and nintedanib, have been approved for IPF [207,208]. While their molecular mechanisms have not yet been completely elucidated, the evidence available suggests that pirfenidone inhibits TGF-β activity [11], while nintedanib acts as a multi-tyrosine kinase inhibitor targeting the vascular endothelial growth factor 1–3 (VEGFR1-3), fibroblast growth factor receptors 1–3 (FGFR 1–3), and the platelet-derived growth factor receptors (PDGFR) α and β [209].

Despite the capability of both nintedanib and pirfenidone to improve lung function, only limited success has been achieved with regard to prolonging the life-expectancy of patients. Consequently, exploration and clinical translation of additional pharmacotherapeutic strategies seems warranted [210]. Among them, promising results have been reported for recombinant pentraxin-2 (PTX-2), a natural amyloid protein with anti-inflammatory properties in IPF [211]. The exogenous administration of PTX-2 reversed the fibrotic phenotype and regulated MΦ accumulation, resulting in ECM remodeling and organ failure prevention in lung and kidney fibrosis [212,213], as well as significant improvements in forced vital capacity (FVC) in case of lung disease [214,215].

Additional studies investigated the role of lysophosphatidic acid (LPA), a glycerol phosphate fatty acid that acts through G protein-coupled receptor signaling. Although not involved in myofibroblast activation, it was observed that LPA induced chemotaxis of lung fibroblasts in bleomycin-induced lung fibrosis, with consequent collagen increase [216]. In a phase II clinical trial, the administration of the LPA inhibitor GLPG1690 was shown to be well tolerated in IPF patients, to improve FVC and to decrease plasma LPA concentrations [217].

Another attractive target is galectin-3, a lectin involved in cell–cell communication, which showed increased expression levels in bronchoalveolar lavage fluid of IPF patients [218]. Galectin-3 was found to be involved in EMT and myofibroblast activation, via the TGF-β and β-catenin pathway. The galectin-3 inhibitor TD139 decreased TGF-β expression and reversed the fibrogenic phenotype in a preclinical lung fibrosis model via decreasing collagen

deposition. Recently, a phase I/IIa trial showed that TD139 is safe and decreased fibrotic plasma biomarkers in patients [219].

Efforts on identifying drugs for IPF treatment have turned out to be relevant for treating other fibrotic diseases, e.g. COVID-19 [220], with three clinical trials with nintedanib and one with pirfenidone at recruiting level. However, the beneficial effect of these drugs for COVID-19 treatment is still debatable, since oral administration is incompatible with mechanical ventilation of COVID-19 patients. In this regard, pentraxin-2 and inhibitors of galectin-3 appear interesting candidates, since they are administered intravenously and display inhibitory effect against inflammatory pathways involved in COVID-19 infection.

Nintedanib is clinically approved as monotherapy for non-small cell lung cancer (NSCLC) [221], and it currently in phase III trials in combination with docetaxel [222]. This combination therapy exhibited benefits in terms of progression-free survival in patients with poor-prognosis adenocarcinoma in comparison to docetaxel monotherapy [222]. The success of the combination therapy may rely on the anti-fibrotic remodeling activities of nintedanib, which may help to improve the accumulation and intratumoral distribution of docetaxel. This idea is consistent with the results of a recent study, revealing that nintedanib has direct anti-fibrotic effects in patient-derived cancer-associated fibroblasts (CAF) of adenocarcinoma (ADC) lung cancer [223]. Upon nintedanib treatment, ADC-associated CAF exhibited reduced proliferation and invasion, as well as reduced expression of activation markers and decreases collagen content. However, only modest anti-fibrotic effects upon nintedanib treatment are observed in CAF squamous cell carcinoma (SCC). Similarly, therapeutic effects of nintedanib in terms of growth and invasion properties were consistently more robust in ADC cell lines exposed to fibroblast-activated conditioned medium than in SCC cell lines, suggesting different regulatory mechanisms of CAF activation between the two carcinoma subtypes [224]. Given such efficacy variability, nintedanib is being investigated in precision medicine setups. For example, it was evaluated in patients with metastatic pancreatic ductal adenocarcinoma (mPDAC) bearing specific mutations in oncogenes and key-modulators of fibrosis [225]. Besides cancer, nintedanib has demonstrated to reduce the expression of collagen and to affect the formation of collagen fibrils in IPF patient-derived fibroblasts [226]. In addition, nintedanib has shown efficacy in patients with systemic sclerosis, where it reduced the activation, migration and proliferation of fibroblasts as well as the expression of various ECM components. In this context, nintedanib further proved its antifibrotic properties in a sclerosis mouse model by improving dermal fibrosis and abrogating the number activation of fibroblasts to myofibroblasts [227].

Several drugs approved for other diseases and targeting upstream elements of TGF-β-signaling have been repurposed as anti-fibrotic agents. Among them is losartan, a small molecule clinically approved for treating hypertension [228]. Its mechanism of action involves inhibition of the binding of angiotensin II to the type 1 angiotensin receptor (AT1R). It was demonstrated that the losartan metabolite EXP3179 displayed potent anti-fibrotic remodeling in the myocardium in a hypertensive animal model [229]. Recently, losartan has also been proven to be beneficial in preclinical models of ovarian cancer [230]. In particular, losartan administration showed reduction of ECM components and decrease of "solid stress", resulting in decompression of vascular structures and in angiogenic normalization, thus, potentiating the accumulation of the co-administered chemotherapy. At the clinical level, losartan was found to convey benefit in hepatitis C-induced liver fibrosis [231], as well as in FOLFIRINOX (i.e. folinic acid, fluorouracil, irinotecan and oxaliplatin) -based radiochemotherapy in patients with locally advanced pancreatic adenocarcinoma [232].

An additional interesting drug under evaluation is anakinra, a recombinant protein acting as an antagonist of the IL-β1 receptor [2]. Preclinical studies in cystic fibrosis animal models have shown that by antagonizing IL-β1-pro-inflammatory activity in the lungs, anakinra reduces recruitment of neutrophils and MΦ at pulmonary sites, thereby reducing inflammation and increasing survival [233]. A phase II clinical trial (NCT03925194) for anakinra in cystic fibrosis has recently started. Furthermore, a retrospective study in COVID-19 patients revealed that only 25% of patients needed mechanical ventilation or died after receiving subcutaneous injections of anakinra, whereas these events occurred in the 73% of the control group ($p < 0.0001$) [234].

Drugs targeting intracellular factors revealed effectiveness in tuning fibrogenic reactions in multiple fibrotic diseases. Setanaxib, a small molecule targeting the NOX4 enzyme which acts downstream of canonical TGF-β/Smad-2/3 signaling, is currently in phase II clinical trial for IPF. In preclinical models of breast cancer, the inhibition of NOX4 resulted in downregulation of TGF-β, α-SMA and collagen content [235]. Interestingly, setanaxib-induced remodeling resulted in an increased infiltration of cytotoxic lymphocytes in the tumor core, with strengthened anti-tumor responses when combined with immunotherapy [235].

Additional interactions related to non-canonical TGF-β/Smad-2/3 inhibition are under investigation. In particular, interesting results have been reported by evaluating the PI3K/Akt/mTOR pathway. mTOR signaling has been demonstrated to be highly activated in all tissue components of fibrogenic kidneys in a mouse model of ischemia–reperfusion-injury (IRI) [236]. Administration of the mTOR inhibitor rapamycin decreased inflammatory cytokine release, reduced recruitment of inflammatory neutrophils, reversed MΦ inflammatory activity and decreased fibroblast activation. Recent findings exploiting CRISPR-Cas9 technology highlighted that the mTOR substrate 4E-BP1 is potently involved in TGF-β-mediated collagen synthesis and fibrogenesis in a rapamycin-insensitive way, which calls for the development of alternative mTOR inhibitors [208]. In this direction, the mTOR inhibitor MLN0128 reversed the activating phenotype of IPF patient-derived lung fibroblasts by blocking the expression of TGF-β and other fibrosis-related markers [237].

3.2. Integrating nanomedicine for targeting fibrosis

The extensive application of nanomedicine for anti-cancer purposes has resulted in the clinical translation of approximately 20 nanomedicines [238,239]. In our effort to identify therapeutic targets for alleviating fibrosis, we realized that only a small portion of studies take advantage of nanotechnology tools for enhancing the efficacy of the anti-fibrotic treatments at the research stage of target discovery and evaluation. The incorporation of nanomedicines in anti-fibrotic setups could improve the delivery of active agents specifically to the key cell populations [240,241]. Indeed, although not as widely explored as for anticancer approaches, the use of nanomedicines has already demonstrated to be able to potentiate anti-fibrotic therapies, mainly applied in liver diseases [242,243], but thus far with only minor application in atherosclerosis, diabetes, and viral diseases [244-248].

Fibrosis-targeted nanomedicines include lipid-based (e.g., liposomes), polymeric (e.g., PLGA nanoparticles), and inorganic (e.g., superparamagnetic iron oxide nanoparticles (SPIONs)) nanoparticles. The developed anti-fibrotic nanoformulations typically aim to either target fibrotic cells (e.g., fibroblasts, HSC) or the produced ECM components (e.g., collagen). These nanoparticles have seen applications in various fibrotic diseases such as pancreatic cancer, liver fibrosis, and skin fibrosis [249-251]. More specifically, the use of collagenase nanoparticles (collagozomes) resulted in ECM degradation that allowed for enhanced drug penetration on a PDAC model [249]. Similarly, a collagenase nanocapsule allowed for a prolonged release of collagenase, significantly reducing the

amount of collagen in a dermal fibrosis mouse model as well as outperforming the treatment with free-collagenase [251].

Small molecules are the most common payload. Corticosteroids (e.g., dexamethasone [252-254] or prednisolone [255-257]) have shown promising activity for tumor microenvironment remodeling, fibrosis mitigation, and attenuation of hyper-inflammation. Natural compounds (e.g., carotenoids, terpenoids [258,259]) have also been assessed as anti-fibrotic agents. In a recent approach, liposomes co-loaded with docetaxel (DTX) and dexamethasone were prepared, and were designed to enable sequential drug delivery [260]. Initial release of the corticosteroid enabled tumor stroma modulation, which contributed to increased accumulation of the DTX-liposome, outperforming the free drugs or single-loaded nanoparticle performance.

In addition to small molecules, proteins have also been evaluated as a payload in nanomedicines. TSG-6, an anti-fibrotic cytokine, was loaded into calcium phosphate-bovine serum albumin (BSA) nanoparticles and evaluated in a preclinical liver fibrosis model [261]. The TSG-6 loaded calcium phosphate-BSA NP efficiently targeted the liver, with minimal accumulation in the spleen, and exhibited improved therapeutic effects in comparison to the free cytokine. Another experiment that relied on boosting endogenous anti-fibrotic proteins used SPION to deliver the fibroblast growth factor 2 (FGF2) protein. The use of nanoparticles resulted in a higher systemic half-life FGF2, improving its anti-fibrotic efficacy [262]. In another study, SPION-conjugated relaxin (RLN) was evaluated in a pancreatic tumor model, where they demonstrated enhancement of the antitumor efficacy of gemcitabine via decreasing collagen content [263]. In a similar concept, nanoparticles containing collagenase were used as a means for reducing ECM, thereby increasing drug penetration in pancreatic tumors [249].

Several anti-fibrotic nucleotide-based therapeutics have been loaded in nanoparticles. The delivery of plasmid DNA encoding for the anti-fibrotic peptide RLN was tested against liver fibrosis and cancer metastasis [263,264]. The plasmid DNA encoding for RLN loaded in nanoparticles targeted metastatic cells and HSC, turning them into an *in situ* RLN depot [264]. The anti-fibrotic and anti-metastatic effect synergized with PD-L1 blockade immunotherapy, indicating that normalization of the ECM potentiates the accumulation and penetration of immunotherapeutics. Following the same concept, a plasmid DNA encoding for the TNFα-related apoptosis-inducing ligand (TRAIL) was co-loaded with protamine (as a facilitator of nuclear delivery) in HCC-targeted pH-responsive SP94-peptide-based nanoparticles [265]. Treatment with the nanoformulation resulted in suppression of HCC progression and liver fibrosis. AT the RNA level, loading siRNA into nanoparticles protects against degradation and improves intracellular accumulation [266]. In this regard, several studies set out to inhibit fibrosis-promoting mediators by delivering siRNA against the mRNA of the methylation-controlled J protein (MCJ) [101], gp46 [267], and Tenascin-C (TnC) [268], in liver and ovarian cancer.

Also the use of EV, i.e., cell-derived vehicles that act as intercellular molecular mediators, has been considered for anti-fibrotic therapy purposes. In light of this, a study demonstrated that EV obtained from the serum of healthy animals possess anti-fibrotic properties [269]. It was shown that these anti-fibrotic properties were due to microRNA that are abundant only in healthy mice and that their in vivo application in fibrotic mice reversed pro-fibrotic gene expression in HSC.

As alluded to above, many anti-fibrotic agents have been employed without being loaded in a nanocarrier. Such strategies are typically implemented to enhance the tumor accumulation and penetration of subsequently (or (co–)) administered nanomedicine formulations. Key examples of such anti-fibrotic priming drugs are captopril [270], losartan [230] and plerixafor [271], which have all been shown to increase tumor perfusion, dilate tumor blood vessels and normalize the tumor stroma. It should be noted in this regard that nano-formulations have been claimed to possess intrinsic anti-fibrotic properties, such as AuNPs. Treatment with AuNPs led to a reduction of CAF density in colorectal cancer models, with a consequent reduction in the expression of collagen I and other fibrosis-associated proteins, such as CTGF, TGF-β1 and VEGF [272].

Besides for delivery of active agents, other characteristics of nanoparticles such as diagnostic properties, ligand-mediated targeting and/or stimulus-responsiveness have been explored in the context of anti-fibrosis therapy. For instance, SPION loaded with indocyanine green (ICG) [273], simultaneously exhibiting magnetic resonance imaging and fluorescence imaging capacities, have aimed at visualizing hepatic fibrosis. For active targeting of fibrosis, nanocarriers have been functionalized with hyaluronic acid [274], aminoethyl anisamide [264,275] and peptides, such as RGD [273], PDGFRβ- [276], collagen-binding peptides [250]. With respect to stimulus-responsive nanoparticles, pH-sensitive nanoparticles co-loaded with hydroxychloroquine and paclitaxel have shown that nanomedicines can convey superior targeting, penetration-promoting and anti-fibrotic efficacy-enhancing effects in pancreatic cancer [277].

4. Imaging modalities for diagnostic assessment of fibrosis

While not all individuals with fibrotic disease are at equal risk of developing life-threatening organ failure, the paucity of biomarkers to detect and stage fibrosis, assess disease progression and enable longitudinal treatment monitoring constitutes a major unmet clinical need. Based on this notion, it is not surprising that intense efforts are being made towards the development of tools and technologies to advance fibrosis diagnosis. This section describes recent efforts and progress made in fibrosis staging and therapy assessment via means of anatomical and functional imaging (NB: molecular imaging of fibrosis is discussed in section 5), in atherosclerosis and cardiac disease (Fig. 7), cancer (Fig. 8), diabetes (Fig. 9), liver diseases (Fig. 10) and viral disorders (Fig. 11).

4.1. Imaging fibrosis in atherosclerosis and cardiac diseases

Early detection of anatomical abnormalities in major blood vessels can support the prediction of progression of atherosclerosis to myocardial infarction and stroke. Various imaging techniques are consequently used for visualizing fibrosis in the heart and blood vessels in (pre-)clinical settings (Fig. 7a,b).

MRI offers several sequences able to detect morphological and functional tissue alterations at image voxel resolution. In a magnetic field, different tissues exhibit specific T1 (spin–lattice) and T2 (spin–spin) relaxation time constants. T1 and T2 describe the longitudinal and transverse return rate of water protons signal to equilibrium and this process depends on the local and molecular composition of tissue environment. Therefore, disease-dependent alterations might affect characteristic and well-defined tissue relaxation times that can be qualitatively and quantitatively reported by MR contrast changes. In particular, high-resolution MRI has been used to assess the formation of mild or moderate atherosclerosis in the carotids of patients with elevated apolipoprotein B levels. A combination of time-of-flight (TOF), T1-weighted and T2-weighted MRI (Fig. 7c; image 1–3) was employed to evaluate the thickness of carotid arteries, as well as the thickness of the fibrous caps and the lipid-rich necrotic cores [278,279]. Similarly, cardiac MRI was used to assess myocardial remodeling and fibrosis in chronic inflammation [280]. Interstitial

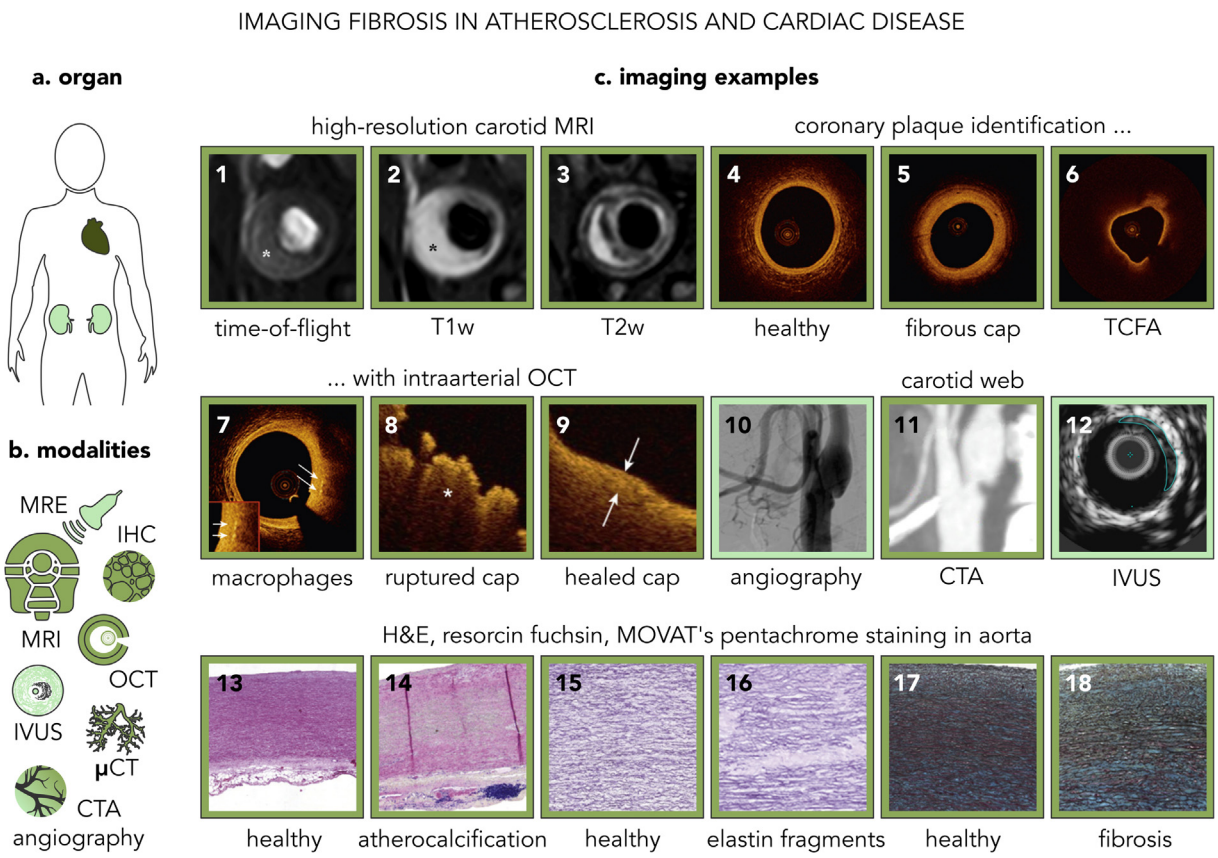

Fig. 7. Imaging fibrosis in atherosclerosis and cardiac disease. (a) The myocardium and major blood vessels are the most investigated tissues in atherosclerosis and cardiac fibrosis. (b) For visualization and detection of myocardial and vascular fibrosis, magnetic resonance imaging (MRI) and optical coherence tomography (OCT) are gold standard techniques. Other imaging modalities such as magnetic resonance elastography (MRE), intravascular ultrasound (IVUS), micro-computed tomography (μCT), computed tomography angiography (CTA), and conventional angiography are also used, for fibrosis detection and staging. Pre-clinically, post-mortem immunohistochemistry (IHC) is used to corroborate findings from (non)-invasive imaging. (c) *Image 1–3*: High-resolution carotid MRI can be used for assessing the formation of vascular plaques via time-of-flight and T1- or T2-weighted (T1w, T2w) sequences. *Image 4–9*: The gold standard method for revealing pathophysiological abnormalities in vascular diseases, i.e., intraarterial OCT, can distinguish healthy vessels, vessels with fibrous cap, and vessels with thin-cap fibro-atheroma (TCFA), which are susceptible to rupture and life-threatening thrombi formation. Intraarterial OCT can furthermore detect the presence of macrophages, ruptured caps, as well as to evaluate treatment efficacy. *Image 10–12*: A combination of conventional angiography, CTA, and IVUS shows vascular projectile protrusions, indicative of carotid intimal variant fibromuscular dysplasia (carotid web). *Image 13–18*: Hematoxylin and eosin (H&E), fuchsin and MOVAT's pentachrome stainings corroborate *ex vivo* tissue pathophysiological characteristics, such as atherocalcifications, elastin fragments, and fibrosis magnitude. Color-coding: the analysis of manuscripts described in section 4.1 revealed the frequency in which each organ and imaging modality are investigated and used for the detection of fibrosis in atherosclerosis and cardiac disease; light green = low frequency; green = medium frequency; dark green = high frequency. All images were adapted with permission [279,284,285,293,295].

myocardial fibrosis was evaluated by combining native T1 mapping and analysis of the extracellular volume (ECV), with longer T1 times and higher ECV percentages being representative for interstitial fibrosis. The MRI-derived assessment was correlated with systemic inflammation markers, showing that high levels of IL-6 are associated with higher ECV, and higher CRP levels with longer T1 times [281].

While the majority of atherosclerosis studies focus on major vessels proximal to the heart vessels, considerable attention is also given to kidney assessment, due to the development of atherosclerotic renal artery stenosis (ARAS) disease [282]. In an ARAS pig model, morphological differences between normal and atherosclerotic kidneys, as well as therapy response, were evaluated via magnetic resonance elastography (MRE), and validated by histology. The results indicated that the reduction in the stiffness of kidney parenchyma could be detected only in case of severe fibrosis, while sensitivity issues did not allow the detection of such changes in cases of mild fibrosis [283].

An important technique for visualizing structural abnormalities in blood vessels and for assessing coronary syndrome damage is intra-arterial optical coherence tomography (OCT). OCT has been used to assess fibrous cap thickness as well as ruptured fibrous caps (which promote formation of intravascular thrombi), in patient cohorts partially treated with the cholesterol-lowering drug pitavastatin. OCT revealed that treated individuals developed a thicker fibrous cap, as indicated by a larger signal-rich band which was clearly discernable from the signal-poor band indicative of the lipid core. Fibrous cap thickness was found to be significantly improved via OCT-based therapy monitoring, while lipid core thickness decreased. OCT could furthermore capture the healing of the ruptured fibrous cap and the disappearance of proximally formed thrombi [284]. In addition to the thickness of the fibrous cap and the volume of the lipid core, OCT also allows for visualizing lesions with fibrosis, calcification, thin-cap fibroatheroma and MΦ infiltration [285], as well as for correlating such morphological changes with cytometry-derived assays aiming to identify infiltrated inflammatory cell populations [286,287] (Fig. 7c; image 4–9).

As described above, the accumulation of advanced glycation end products (AGEs) contributes to fibrosis development. AGEs can be used as markers related to the severity of cardiovascular disease, since AGEs accumulation in the skin results in elevation of skin autofluorescence [288]. In an exemplary study, patients were subdivided in two groups based on skin autofluorescence

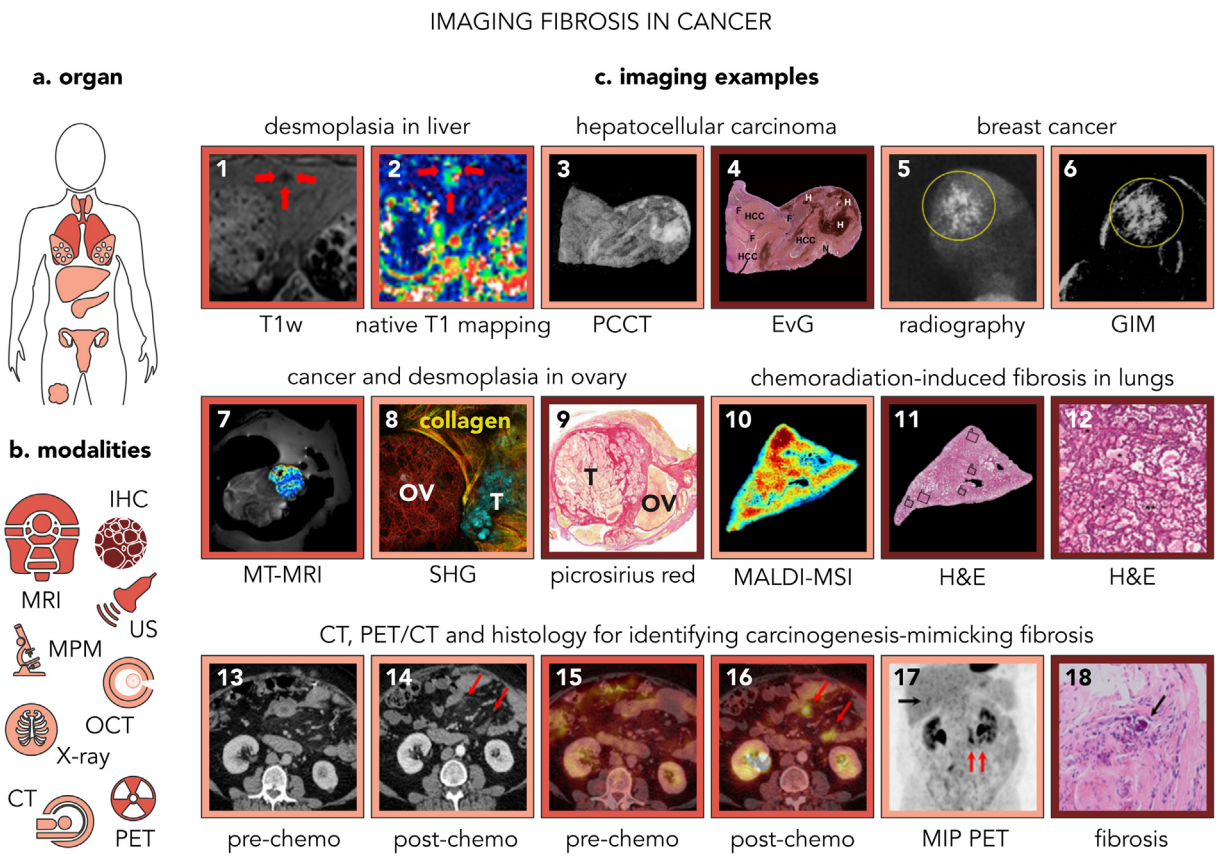

Fig. 8. Imaging fibrosis in cancer. (a) Lung carcinomas, as well as malignant manifestations in the ovaries, breast, pancreas, liver, thyroid, and skin present with a fibrotic phenotype. (b) The most commonly used imaging modalities to assess cancer-associated desmoplasia are immunohistochemical (IHC) analyses and magnetic resonance imaging MRI. (c) *Image 1–2*: T1w MRI and especially native T1 mapping are employed to detect fibrosis in liver carcinoma, with high native T1 mapping values to correlate with fibrosis (typically assessed *ex vivo* via histological staining). *Image 3–4*: Grating-based phase-contrast CT (PCCT) is a novel phase-contrast CT-based imaging method that allows for the distinction of fibrosis, hemorrhage, necrosis, and cancer cells in hepatocellular carcinoma specimens; corroborated by complementary Elastica van Gieson (EvG) histological staining. *Image 5–6*: Grating interferometry-based mammography (GIM) can detect and evaluate suspicious micro-calcifications and fibrosis of breast biopsies. *Image 7–9*: The magnetization transfer (MT) ratio in T2w MRI allows for visualizing desmoplasia in ovarian carcinoma. *Ex vivo* second harmonic generation (SHG) imaging of collagen fibers and IHC corroborates fibrotic manifestation. *Image 10–12*: Chemoradiation therapy induces severe fibrosis. To spatially map pathological alterations, treated lung tumor tissue underwent MALDI-mass spectrometry imaging together with H&E staining to unravel a correlation between N-glycan overexpression and fibrosis. *Image 13–18*: The development of masses at the post-chemotherapy stage were false-positively diagnosed as carcinogenesis via ^{18}F-FDG PET/CT; (MIP = maximum intensity projection). Subsequent *ex vivo* H&E staining and laparoscopic exploration resolved this issue, revealing the masses to be carcinogenesis-mimicking fibrosis, composed of calcified fibrotic tissue, infiltrating foamy mononuclear cells, and multinucleated giant cells. Color-coding: the analysis of manuscripts described in section 4.2 reveal the frequency in which each organ and imaging modality are investigated and used for the detection of fibrosis in cancer; light red = low frequency; red = medium frequency; dark red = high frequency. All images were adapted with permission [300,302,303,309,312,314].

and subjected to OCT and coronary angiography. The imaging results showed that only OCT was able to correlate the group with high skin autofluorescence with a thinner fibrous cap, higher thin-cap fibroatheroma, increased infiltration of MΦs, more events of ruptured plaques, increased calcification, and more thrombi [289].

Another technique that enables visualization of pathophysiological abnormalities in vessels (e.g. obstruction, dilation, stenosis) is computed tomography angiography (CTA) [290,291]. CTA was used to evaluate the pathophysiological characteristics of coronary arteries and to identify the impact of non-obstructive left main coronary artery disease (LMCA) in the overall progression of coronary artery disease. Patients with LMCA presented with a more calcified, more fibrous and more necrotic plaque, as well as with increased progression at follow-up scans. This exemplifies the value of CTA, as it contributed to the realization that the severity of LMCA is a marker for more aggressive progression of coronary artery disease [292]. Efforts to correlate CTA imaging features with histology-derived information may help to further improve the diagnostic power of this imaging modality [293,294].

Although CTA and conventional angiography are traditionally used for visualizing accumulation of atherosclerosis, alternative techniques have been investigated for detecting vascular defects. Intravascular ultrasound (IVUS) is evaluated for the potential to detect carotid web-related vascular lesions. Indeed, IVUS allowed for detection of carotid web protrusions, and was in agreement with the CTA and angiography scans. However, the low spatial resolution of IVUS does not provide further information about the physiological characteristics of the lesion, and cannot differentiate between fibrosis, thrombosis, and atherosclerosis [295] (Fig. 7c; image 10–12).

While the combination of all of the above imaging techniques in clinical practice is hardly possible, their combined use in preclinical research provides advantages in defining atherosclerosis. In a transgenic Ossabaw pig model expressing the *PCSK9* gene with D347Y mutation (which is known to promote familial hypercholesterolemia and arterial plaques), several imaging techniques were used to determine and characterize the extent of coronary and peripheral vascular atherosclerosis, mainly focusing on the heart, proximal arteries and kidneys. At the organ level, MRI and MRE nicely illustrated progressive formation of hypoxic regions in the kidneys and elevated kidney stiffness. A combination of IVUS and OCT was used to visualize the progression of plaque formation as well as volume growth in proximal heart arteries and renal arteries. To visualize vascular density, micro-computed tomography

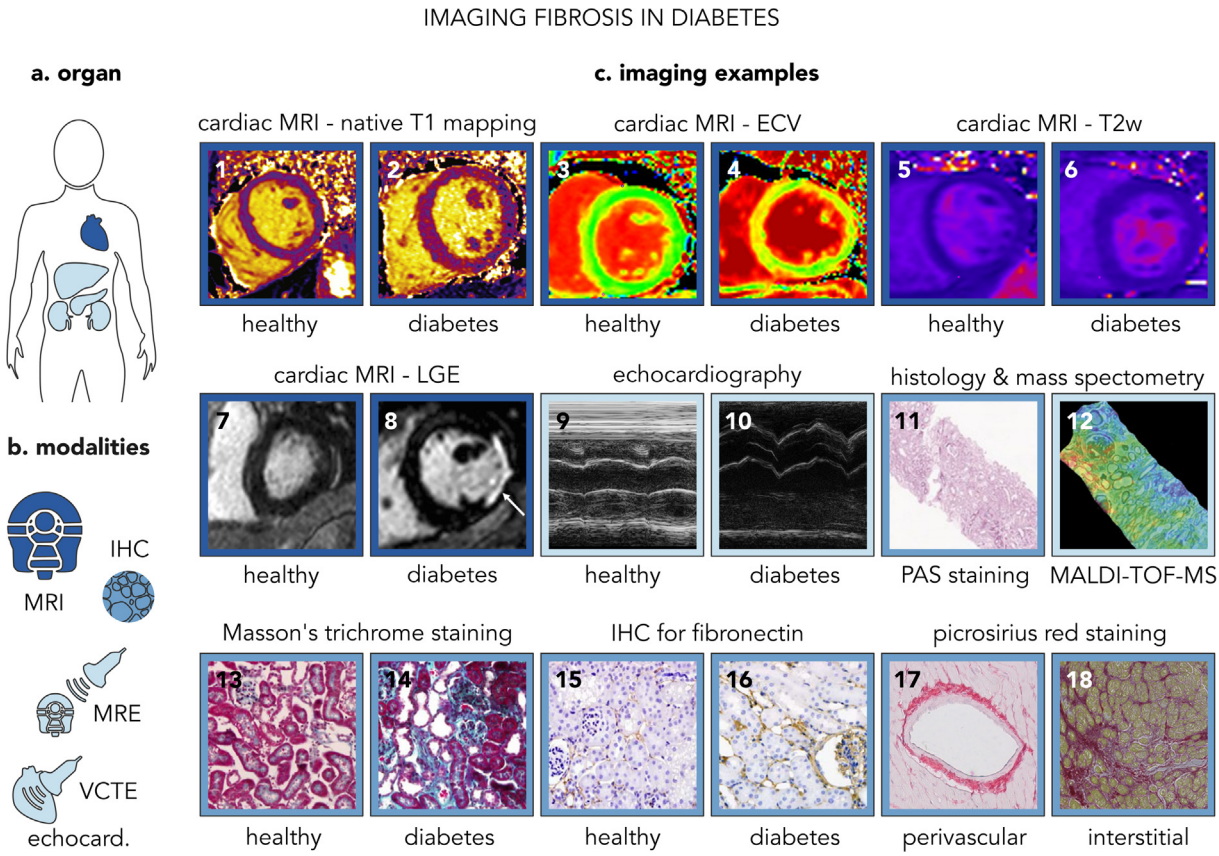

Fig. 9. Imaging fibrosis in diabetes. (a) Diabetic complications developed in the heart cause diabetic cardiomyopathy that alters myocardial functional capacity. Other organs with evident diabetic complications are the liver, pancreas, and kidneys. (b) Cardiac MRI and *ex vivo* IHC are the major modalities to diagnose diabetic fibrosis. Elastographic techniques and echocardiograms further support diagnosis. (c) *Image 1–8*: Various MRI sequences are used to assess myocardial remodeling and fibrosis in case of diabetes. Such abnormalities display a higher native T1 mapping, extracellular volume (ECV) and T2 weighted (T2w) values (appearing as more intense colors in the images), as well as late gadolinium enhancement (LGE). *Image 9–10*: Echocardiograms can inform on cardiac remodeling, evidencing increased wall thickness and alteration in cardiac pump function. *Image 11–12*: Combining IHC and MALDI-TOF-MS imaging can be employed to correlate fibrosis development with upregulation of pro-fibrotic markers. *Image 13–18*: Various histological and IHC stainings (i.e., Masson's trichrome, IHC for fibronectin, picrosirius red) are used to assess diabetes-associated fibrosis in tissues and around vessels. Color-coding: the analysis of manuscripts described in section 4.3 reveal the frequency in which each organ and imaging modality are investigated and used for the detection of fibrosis in diabetes; light blue = low frequency; blue = medium frequency; dark blue = high frequency. All images were adapted with permission [317,323,325-327,333,334].

(μCT) was employed, showing higher vessel density in the atherosclerotic model both in the myocardium and in the kidneys. In addition, regular CT allowed for identifying a loss of aortic distensibility. Finally, thorough histological analysis consisting of four different types of staining was performed to further characterize the composition of the atherosclerotic lesions in heart and vessels and to identify the plaque magnitude as well as fibrosis and calcification regions [296,297]. Overall, such histological analyses are used extensively in clinical specimens for validating cases of atherosclerosis, elastin fragmentation and fibrosis [293] (Fig. 7c; image 13–18).

4.2. Imaging fibrosis in cancer

Cancer-related fibrosis comes in multiple forms. These include an excessive stromal reaction accompanying tumor formation termed desmoplasia, as well as post-surgical scar tissue and radio- and chemotherapy-induced fibrosis. Although these fibrosis forms are heterogeneous, they do not necessarily produce substantially different radiological images, thereby challenging correct and timely diagnosis (Fig. 8a,b).

Desmoplasia refers to the formation of excess connective tissue around and within cancerous lesions as a response to smoldering tumor inflammation and/or tumor cell invasion into healthy tissue [298]. The intimate relationship between fibrosis and carcinogenesis is evidenced by the fact that desmoplastic tissue in normal breast is an important risk and prognostic factor [299]. Several imaging techniques (e.g., MRI, CT), are used in (pre)clinical practice for desmoplasia detection. For example, on the basis of different T1 relaxation times in different tumor areas, T1-mapping MRI allows for the visualization of the tumor extracellular matrix (ECM) in a preclinical rabbit model of liver cancer (Fig. 8c; image 1,2) [300]. High T1 relaxation times in tumor and short T1 relaxation times in regions surrounding the tumor suggest native T1 mapping as a possible quantitative means to assess ECM remodeling.

In certain types of cancer, such as breast and ovarian tumor, anatomical CT imaging can identify tumor-associated desmoplasia. For other tumor types, it is often challenging to distinguish fibrosis (or post-surgical scar tissue) from surrounding healthy or malignant tissue since the two entities attenuate X-rays similarly. To overcome this limited soft-tissue contrast of conventional absorption-based CT imaging, several new phase-contrast imaging methods have been developed in recent decades [301]. The signal intensities in grating-based phase-contrast CT (PCCT) images obtained with a synchrotron light source and a conventional X-ray source can be used to *ex vivo* visualize different tissue regions (e.g., fibrosis, hematoma, cancer cells, necrosis) in human liver cirrhosis and hepatocellular carcinoma (HCC) (Fig. 8c; image 3,4) [302]. Analogously, grating interferometry-based mammography (GIM) can be used to evaluate suspicious micro-calcifications and

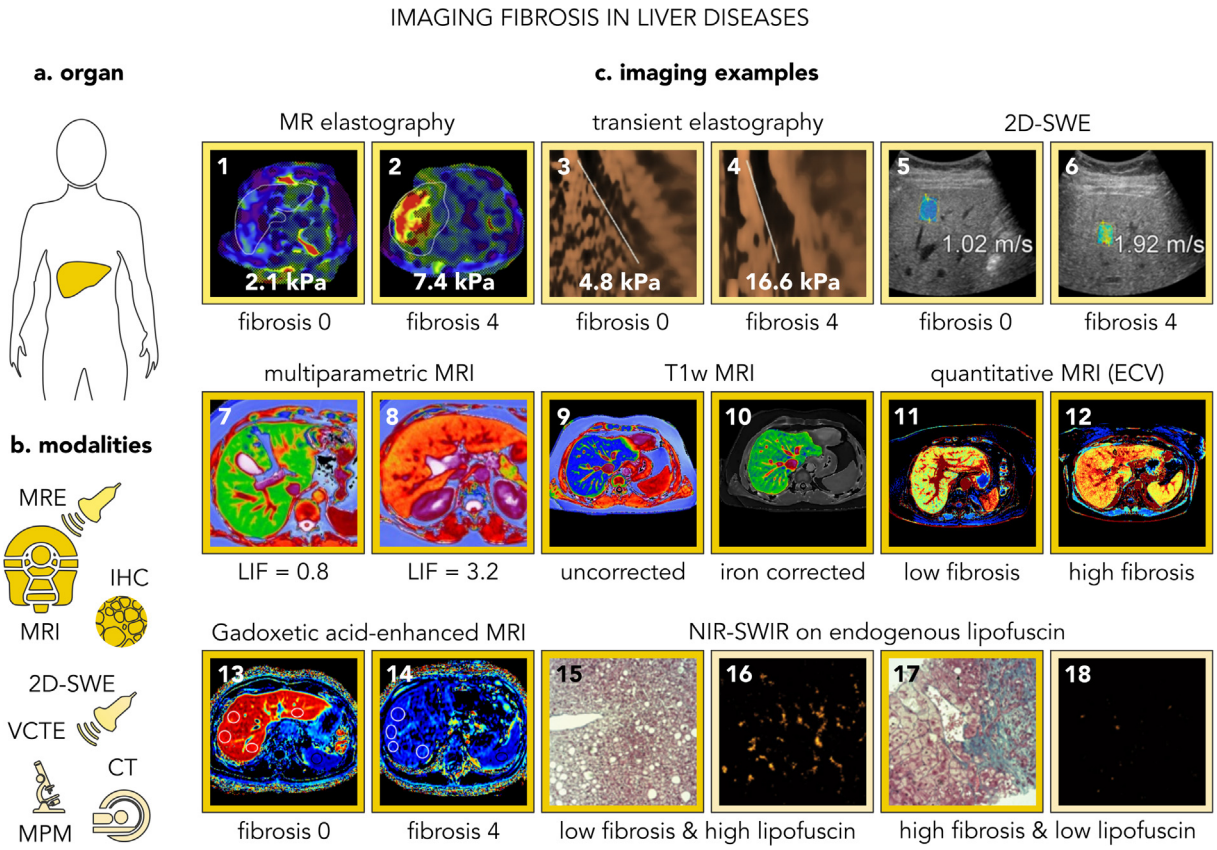

Fig. 10. Imaging fibrosis in liver diseases. (a) Non-alcoholic fatty liver disease (NAFLD) comprises a spectrum of pathological conditions affecting the liver, spanning from steatohepatitis (NASH) to more severe fibrosis and cirrhosis. (b) Staining needle-core biopsy specimens stands as the clinical reference procedure to assess liver fibrosis. In addition, MRI and MRE have recently gained preclinical attention due to the higher diagnostic performance in staging fibrosis in comparison to transient elastography (TE) or 2D ultrasound-based elastography. (c) *Image 1–6*: Elastographic techniques (i.e., MRE, transient elastography (TE), and 2D-shear wave elastography (2D-SWE)) are used to indirectly assess the extent of fibrosis via assessment of tissue stiffness. *Image 7–12*: Although conventional MRI sequences are not so precise in terms of differentiating between different fibrosis stages, novel MRI strategies including multiparametric MRI, iron-corrected T1 (cT1), and liver ECV quantification are pushing forward the efforts for accurately diagnosing patient disease stage. Such innovations appear as a strong quantitative proxy for the detection of liver inflammation and fibrosis, reducing the need for liver biopsies. *Image 13–14*: On gadoxetic acid contrast-enhanced MRI, the gadoxetic acid hepatobiliary phase uptake fraction is indicative for liver function and fibrosis stage. *Image 15–18*: Liver needle biopsies of NASH and NASH-chrirrosis patients were stained using Masson's trichrome, showing that the extent of fibrosis inversely correlates with the expression of lipofuscin. NB: the absence of cell-derived lipofuscin shows substitution of funtional tissue with desmoplastic tissue. Color-coding: the analysis of manuscripts described in section 4.4 reveal the frequency in which each organ and imaging modality are investigated and used for the detection of fibrosis in diabetes; light yellow = low frequency; yellow = medium frequency; dark yellow = high frequency. All images were adapted with permission [345,347,356,359,362,368,370].

fibrosis of breast biopsies (Fig. 8c; image 5,6) [303]. Based on X-ray absorption, refraction and scattering, in case of in-situ ductal carcinoma it was found that micro-calcifications associated with malignancy possess a lower correlation between absorption and scattering than specimens associated with fibrosis. Nevertheless, when tumor perfusion is scarce and/or hindered by dense desmoplasia, even contrast-enhanced scans might fail to differentiate between different neoplasms. For instance, in pancreatic lesions, it is difficult to differentiate fibrosis resulting from pancreatic cancer vs. fibrosis driven by other pancreatic disorders, e.g., pancreatitis [304]. In such situations, alternative modalities such as endoscopic ultrasonography (EUS) represent a better tool for differential diagnosis than contrast-enhanced CT.

Even if needle biopsies followed by histopathological staining remain to be the gold standard for diagnosing and staging cancer-associated fibrosis, non-invasive imaging is employed more and more for fibrosis detection and guiding biopsies to the right location of a targeted nodule. Such guiding techniques (e.g., endobronchial ultrasound (EBUS), however, do not allow for discrimination between cancer and desmoplasia. To resolve, in order to differentiate tumor from fibrosis during needle biopsies, polarization-sensitive OCT (PS-OCT; i.e., functional OCT) has been utilized as a guidance tool [305]. PS-OCT detects birefringent tissue component, e.g., collagen, while simultaneously generating structural OCT images, thus providing a reliable tool to quantify and characterize fibrosis [306].

Finally, pioneering work on tumor-associated collagen has resulted in establishing a previously overlooked feature of invasive breast tumors, i.e., the morphological appearance of collagen structures [307]. The tumor-associated collagen signatures (TACS) consist of a three-part system classification. In TACS-3, the presence of linear bundles of collagen fibers growing perpendicularly away from invasive breast tumor mass is causally linked to poor outcome, both in preclinical breast cancer models as well as in clinical cases [308]. The endogenous contrast generated by fibrillar collagen in second harmonic generation (SHG) microscopy has seminally contributed to the discovery that such morphological and architectural features of tumor-associated stromal tissue can be used to predict disease outcome. Based on this, due to the poor clinical translatability of in vivo microscopy, various (pre)clinical efforts are currently ongoing to correlate SHG-based microscopy features with MRI and histology features (Fig. 8c; image 7–9) [309].

Besides desmoplasia, another important and prevalent type of cancer-related fibrosis is chemo- and/or radiotherapy-induced fibrosis. These treatments induce damage not only in the tumor but also in surrounding (and distant; in the case of chemotherapy)

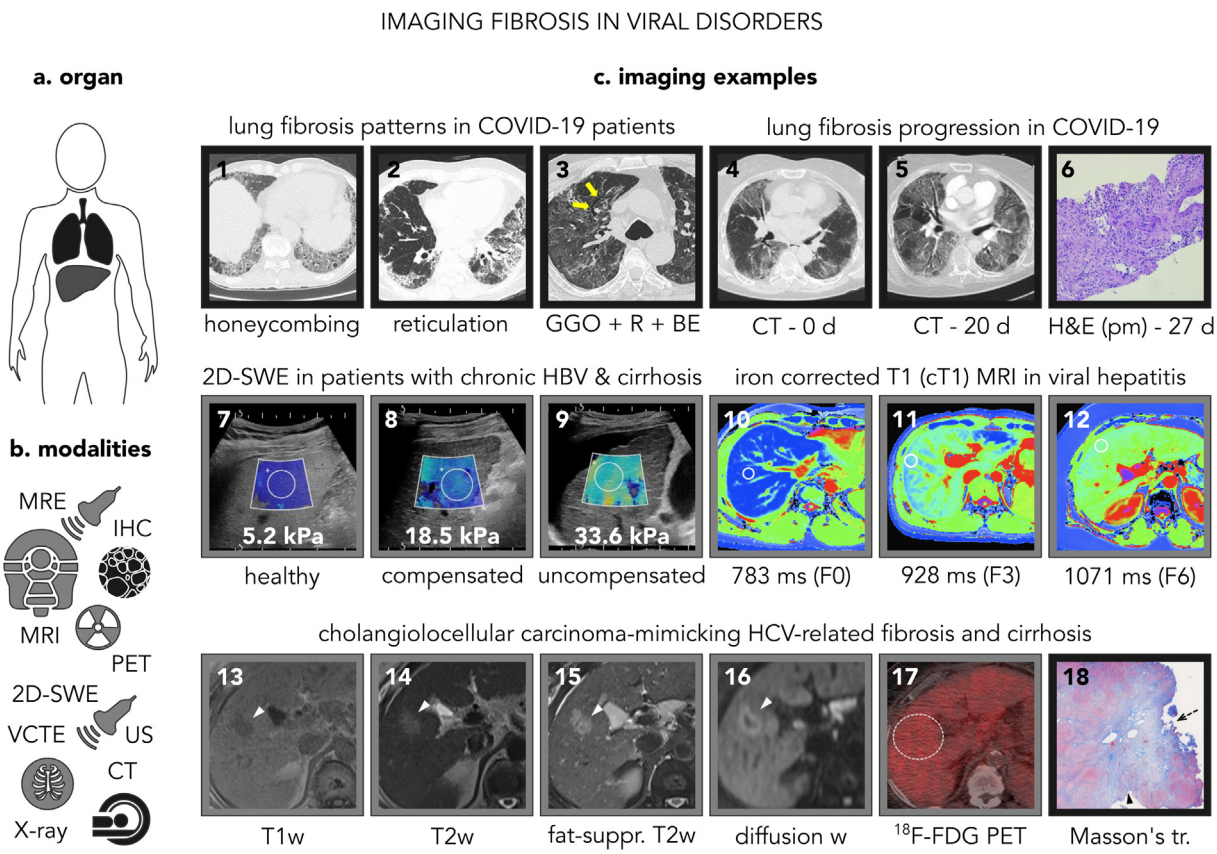

Fig. 11. Imaging fibrosis in viral disorders. (a) With the outbreak of the COVID-19 pandemic and with the ever-increasing spread of HBV/HCV infections, the main organ-focus of viral disorders are the lungs and liver. (b) Computed tomography (CT) is the most commonly used imaging modality to visualize viral-derived lungs fibrosis, whereas magnetic resonance imaging (MRI) and histology upon needle-core biopsy are most frequently used techniques for assessing fibrosis in hepatic viral disorders. (c) *Image 1–3*: The evolution of acute viral pneumonia to lung fibrosis is observed at intermediate stages of COVID-19 (14–21 days after disease symptom onset). As exemplified, CT reveals SARS-CoV-2-induced lung fibrosis appearing with different patterns, i.e., honey-combing, reticulation, or a combination of several patterns (i.e., bronchiectasis (BE) and/or reticulation (R) superimposed on areas of ground-glass opacities (GGO)). *Image 4–6*: Longitudinal chest CT allows for visualizing fibrosis evolution in COVID-19 patients. Early-stage cases (0–7 days after symptom onset) are characterized by bilateral and peripherally GGO, while more advanced-stage cases (14–21 days after symptom onset) display extensive areas of GGO with consolidation, crazy-paving appearance, and bronchiectasis. Post-mortem (pm) histology confirms the diagnosis of lung fibrosis and the destruction of alveolar structures. *Image 7–9*: Two-dimensional shear-wave elastography (2D-SWE) can distinguish fibrosis and cirrhosis severity via measuring the liver stiffness in patients with chronic HBV. Liver stiffness is higher in patients with uncompensated cirrhosis and ascites in comparison to patients with compensated cirrhosis and no ascites. *Image 10–12*: Iron-corrected T1 MRI (cT1) is a promising metric that correlates with inflammation and fibrosis, allowing for defining clear cut-off values as an indicator of the severity of viral hepatitis. *Image 13–18*: HBV/HCV infection can lead to liver fibrosis, and evolve to cirrhosis or carcinoma. In case of cholangiolocellular carcinoma (CCC), differential diagnosis of liver fibrosis vs. liver cancer is difficult to achieve via anatomical of functional imaging, as the two entities typically produce similar radiological images. In a suspected case of CCC, out of 4 imaging modalities (US, MRI, CT, PET), only ^{18}F-FDG-PET could correctly diagnose the suspected mass as fibrosis (i.e., no uptake of the probe in the suspected mass), and not as tumor (further confirmed by *ex vivo* histological analysis; fibrotic tissue appears blue in Masson's trichrome staining). Color-coding: the analysis of manuscripts described in section 4.5 reveal the frequency in which each organ and imaging modality are investigated and used for the detection of fibrosis in viral disorders; light gray = low frequency; gray = medium frequency; dark gray = high frequency. All images were adapted with permission [360,377,381,382,386,396,400].

healthy tissue. This can result in long-term fibrosis and may increase morbidity [310]. For instance, in an exemplary recent report, a case of chemotherapy-induced granulomatosis with associated fibrosis has recently been described as being erroneously identified on ^{18}F-FDG PET/CT images as metastatic progression [311]. Autopsy eventually revealed no metastatic manifestation, with the cause of death to be respiratory failure due to acute bronchopneumonia superimposed on severe parenchymal involvement by sarcoid-like granulomatosis.

In this context, emerging imaging techniques such as matrix-assisted laser desorption ionization-mass spectrometry imaging (MALDI-MSI) hold potential to visualize the spatial distribution of macromolecules which might represent distinct molecular signatures (e.g., glycan alternations) in chemoradiation-induced fibrosis (Fig. 8c; image 10–12) [312].

Finally, a diagnostically very challenging type of fibrosis is carcinogenesis-mimicking fibrosis. This is particularly evident from recent case reports. For instance, a benign fibromyxoid pseudotumor of fat resembled the radiological features of malignant liposarcoma [313]. In another example, a patient diagnosed with ovarian papillary serous carcinoma stage IIIB underwent surgery and chemotherapy, and was re-evaluated for suspected cancer relapse [314]. ^{18}F-FDG PET/CT showed a complete metabolic response, except for two left-over hypermetabolic nodules in the mesentery and the peritoneum. Rather than initiating a new line of chemotherapy, clinicians decided to surgically explore these new lesions, which were found to be calcified fibrotic lesions, proving these nodules to be peritoneal fibrosis mimicking persistent ovarian carcinomatosis (Fig. 8c; image 13–18). These examples clearly illustrate the difficulties on identifying neoplasms with non-invasive imaging, pointing out that in the majority of cases, only needle core biopsies can really "rule out" incorrect diagnosis. With the particular aim to reduce the misinterpretation of post-operative fibrosis for local recurrence, various non-invasive imaging efforts are currently taking place, including e.g., MRI and dynamic contrast-enhanced MRI (DCE-MRI) in patients with soft tissue sarcomas [315] or ultrasound in patients with breast cancer [316].

4.3. Imaging fibrosis in diabetes

Constant high-glucose exposure of major organs in diabetic patients results in progressive complications appearing as fibrosis and loss of tissue function, mainly in the heart, but also in liver, pancreas and kidneys (Fig. 9a). Since cardiomyopathy is a major complication in diabetes, various types of cardiac MRI have been established for assessing heart geometry, microcirculation, and systolic / diastolic cardiac function (Fig. 9b). In this regard, cardiac MRI reveals higher cardiac remodeling, larger ECV and brighter T2-weighted images for diabetic patients [317,318], features that reflect fibrosis and edema, respectively [319,320]. Another MRI feature that can be used to quantify interstitial myocardial remodeling is native T1 imaging, with diabetic patients showing higher T1 relaxation times [318,321,322]. Native T1 mapping has been specifically shown to capture the myocardial fibrosis and to correlate with the collagen volume fraction [323]. Cardiac MRI together with the use of gadolinium-based contrast agents is furthermore used to assess the magnitude of interstitial and replacement fibrosis. The first can be assessed via the ECV fraction, and the latter via late gadolinium enhancement (LGE; indicates tissue function impairment). Distinguishing healthy from diabetic patients using such MRI protocols is fairly straightforward, as diabetic patients have a higher ECV fraction and LGE (Fig. 9c; image 1–8) [324-326].

In addition to cardiac MRI, other imaging modalities are available at the preclinical level to evaluate diabetes-associated cardiac fibrosis. In diabetic rats, a combination of echocardiography and histology was used to assess anatomical and functional cardiac parameters (Fig. 9c; image 9,10). Echocardiography successfully captured the left atrial dimension, left ventricle internal diameter during diastole and wall thickness, while picrosirius red staining enabled assessment of interstitial and perivascular fibrosis. Echocardiography showed larger left atrial and wall thickness dimensions as well as larger left ventricle internal diameter in diabetic rats, indicative of cardiac contractility worsening. While wall thickening might allude for morphological alteration and fibrosis development, *ex vivo* picrosirius staining revealed no differences in ventricle, atrial, and perivascular fibrosis between the control and the diabetic animals [327], highlighting the value of the complementary imaging techniques for assessing tissue pathophysiology. Similarly, a study performed in rats used a combination of echocardiography, *ex vivo* confocal microscopy, and histology to identify the extent of endothelial damage, ischemia and fibrosis. Echocardiography provided functional information on systolic and diastolic performance of the left ventricle, confocal microscopy indicated the vascular permeability, and trichrome staining-based histological analysis was used to directly detect cardiac fibrosis [328].

Other tissues of interests for investigating the extent and damage of diabetes are the liver and the pancreas. Magnetic resonance elastography (MRE) has been used for assessing the stage and severity of liver fibrosis in diabetic patients via measuring liver stiffness [329,330]. Vibration-controlled transient elastography (VCTE) is an alternative technique used for assessing liver fibrosis and steatosis [331]. Even though MRE and VCTE can assess liver stiffness, they only provide indications regarding the extent of liver fibrosis, corroborating the notion that only one type of imaging technique is insufficient to fully elucidate the fibrotic signature. In case of the pancreas, MRI T1 mapping together with gadolinium-based enhanced MRI have been used to assess ECV and the magnitude of impaired pancreas functionality [320,332].

Finally, even though not directly related to detection of fibrosis, a combination of histological periodic acid-Schiff staining together with MALDI-TOF-MSI proteomic analysis can be used to define pathophysiological regions in biopsy samples of patients with diabetic nephropathy or hypertensive nephrosclerosis (Fig. 9c; image 11,12). The combination of both techniques showed that certain proteomic biomarkers primarily accumulate in fibrotic or sclerotic regions, potentially providing next-generation diagnostic tools for detecting and differentiating different disease stages [333].

All the above-mentioned techniques are typically supported by complementary histological analyses based on histological staining (e.g., Masson's trichrome staining) and immunohistochemistry (e.g., IHC for fibronectin) (Fig. 9c; image 13–18) [323,327,334].

4.4. Imaging fibrosis in liver diseases

With up to 25% of the global population at risk, non-viral and non-alcoholic liver diseases (NAFLD) are gradually developing towards a global pandemic [335]. Within the large group of NAFLD, ranging from non-alcoholic fatty liver or steatosis (NAFL) to non-alcoholic steatohepatitis (NASH) and advanced fibrosis, patients with advanced liver fibrosis are inclined to eventually develop hepatocellular carcinoma (HCC) and liver failure (Fig. 10a) [336]. Hence, there is an urgent need to establish specific and cost-effective means to stratify patients with NAFLD, to identify those who are at high risk of developing liver fibrosis and/or those progressing to cirrhosis, HCC and liver decompensation [337]. At the moment, histology upon needle aspiration biopsy is the clinical reference procedure for assessing liver fibrosis (Fig. 10b) [338,339]. Diagnosis relies on detecting excessive connective tissue deposition within the liver parenchyma via histopathological staining, with disease severity being staged using semi-quantitative scoring systems such as via Brunt́s criteria [340]. On top of such scoring systems, automated digital image analysis (DIA) can be performed with the aim to provide a more reproducible and precise methodology to assess collagen architectural changes [341].

Given the invasiveness of biopsy, elastography is a cost-effective alternative that is typically used to map liver elasticity and stiffness in case of fibrosis [342,343]. The rationale is that, while many pathological processes in the liver affect its stiffness (e.g., cholestasis, portal pressure, inflammation), fibrosis is the most frequent cause of stiffening [344]. Elastographic techniques can be implemented via both US and MRI, and are then termed as VCTE or MRE (Fig. 10c; image 1–4) [345]. VCTE is commercialized under the trade name FibroScan and considered the standard imaging technique in case of liver fibrosis [339,346]. The technique provides a quantitative one-dimensional picture of tissue stiffness, expressed in kiloPascal (kPa). Advantages of FibroScan-based VCTE are ease of use, reasonably good reproducibility, repeatability and relatively high range of stiffness values that can be recorded [347]. Nevertheless, areas of interest cannot be accurately chosen and the applicability of this technique is significantly reduced in case of obese patients or patients with ascites [348]. Additionally, the diagnostic performance of the technique only allows for differentiating "extensive" from "no" fibrosis, rather than subdividing more dynamically between "low" and "intermediate" fibrosis [349].

To overcome one of the major limitations of VCTE, i.e., the selection of ROIs, shear-wave elastography (SWE) can be used (Fig. 10c; image 5,6) [347]. In this case, the operator uses B-mode US image to find an area within the liver that is homogenous and free of vessels. A ROI with variable width and depth is then selected and as the shear-wave propagates from the emitting probe, the speed of propagation is recorded. By converting shear-wave speed into stiffness, software provides a color-coded map of the tissue stiffness, which is superimposed on the B-mode images of the ROI. If the elasticity information is obtained by "pushing" down the beam axis acoustic radiation, then the elastography technique is termed acoustic radiation force impulse imaging (ARFI). In both cases (2D-SWE and ARFI), there are no comprehensive and universal criteria to assess the measurements' quality, therefore, studies comparing

2D-SWE, ARFI, and VCTE against histology as a reference are taking place [350,351]. Overall, results obtained thus far show lower failure for ARFI, but higher diagnostic accuracy for 2D-SWE in case of intermediate and extensive fibrosis, as well as better correlation of 2D-SWE with histology.

MRE can be performed using regular MRI devices, via dedicated software and hardware. MRE uses a modified phase-contrast method with motion-encoding gradients to image the propagation characteristics of the shear waves applied anterior to the liver. Elasticity quantified by MRE is also expressed in kPa, using a formula that determines the shear modulus [339,352]. Advantages of MRE include examination of the whole liver (thereby addressing spatial heterogeneity), and the fact that MRE measurements are not significantly impacted by ascites or obesity. In comparison to VCTE, MRE has shown higher diagnostic sensitivity and specificity for patients with low, intermediate and extensive fibrosis [345,353].

In general, MRE outperforms all the other elastography techniques described thus far in terms of diagnostic performance. However, the overall diagnostic performance of MRE is still far from being optimal in differentiating the intermediate stages of liver fibrosis. The reason why imaging modalities which measure liver stiffness fail to accurately differentiate fibrosis stages is that whereas an increase in liver stiffness directly reflects an increase of connective tissue, liver fibrosis progression relies not only on increased collagen deposition, but also on the structural remodeling of collagen [354]. Such morphological modifications do not necessarily produce changes in tissue parenchyma elasticity; thus, such changes are not taken into account by measuring liver stiffness.

Because of the high costs related to the implementation of elastography features into MRI devices, several attempts have set out to validate the accuracy of standard MRI parameters (e.g., T1-weighted imaging) in comparison to MRE measurements and/or histology. Recently, it was demonstrated that for the differentiation of low-grade vs. high-stage fibrosis, the diagnostic accuracy of texture analysis (TA) on T1-weighted images combined with a machine learning (ML) algorithm is comparable to MRE [355].

Multiparametric MRI that combines anatomical and functional information for assessing the total liver inflammation and fibrosis (LIF) (i.e., T1 mapping for fibrosis/inflammation imaging, T2* mapping for liver iron quantification and proton magnetic resonance spectroscopy (^{1}H-MRS) for measuring the liver fat fraction) is gaining a lot of attention because it is fast, does not require intravenous injection of contrast agent and shows good correlation with histological parameters in the identification of the severity of various liver diseases (Fig. 10c; image 7,8) [356,357].

In a similar approach, in order to diagnose NASH in NAFLD patients, individuals have been subjected to MRI involving MR spectroscopy (MRS), MRE and T1 mapping [358]. For every patient, a multiparametric MR index was created and its diagnostic performance in staging fibrosis and NASH was assessed and compared to needle biopsy-based histology. The MR index combined the fat fraction value (FF) from MRS, the liver stiffness value from MRE, and T1 relaxation time from MRI. Despite good diagnostic performance of multiparametric MR index in discriminating NASH from non-NASH patients, the measurements were not corrected for iron content, which is one of the limitations of MRE (i.e., poor reliability of the measurements in case of patients with hepatic iron overload). Consequently, iron-corrected T1 mapping (cT1) has been established and proven to be useful to differentiate inflammation and fibrosis (Fig. 10c; image 9,10) [359,360]. It has furthermore been proposed for use in clinical trials to select patients at major risk of developing NASH among all NAFLD patients [361]. Recently, cT1 in combination with serum biomarkers (such as fasting glucose, liver enzymes) proved high diagnostic accuracy as a pre-screening biomarker to discriminate patients with high fibrosis and steatosis from lower stages of fibrosis and steatosis [359].

As liver fibrosis is defined by an increase of extracellular matrix, the acquisition of T1 values before and after administration of an extracellular contrast agent, allowed for ECV quantification, thus, for an estimation of the extent of liver fibrosis. Such an approach, which is extensively used in cardiac MRI to assess cardiac fibrosis, has been successfully employed in in pre-clinical and clinical studies [362,363]. Major findings of those studies highlighted ECV-measurements to strongly correlate with Sirius red staining on biopsies from both animal models of liver cirrhosis as well as of patients affected by liver disease. In comparison to MR elastography and TE, ECV-based fibrosis quantification does not require additional expensive equipment and it is not affected by patienťs pathological conditions (e.g., obesity, ascites). Such studies further indicate MRI-derived ECV to serve as a new tool for quantification of human liver fibrosis (Fig. 10c; image 11,12).

Another MRI-based method that has been used for detecting liver fibrosis is the intravoxel incoherent motion (IVIM) technique, which is based on diffusion-weighted MRI but allowing for better evaluation of molecular diffusion and perfusion. IVIM reflects the extent of ECM accumulation and has proven good diagnostic sensitivity in case of liver fibrosis [364].

Gadoxetic acid–enhanced MRI has gained significant attention due to its utility in diagnosing liver fibrosis and assessing hepatocytes functionality (Fig. 10c; image 13,14). Gadoxetic acid is a routinely used, gadolinium-based contrast agent for detecting and characterizing liver lesions in clinical practice [365]. Its liver uptake and excretion are directly related to hepatocyte function. As hepatocyte function is reduced during fibrotic progression, the uptake of gadoxetic acid in liver parenchyma decreases [366]. In order to obtain comparative data, the diagnostic performance of gadoxetic acid-enhanced MRI has been compared against US-based elastography. Overall, gadoxetic acid-enhanced MRI displayed similar diagnostic accuracy in staging fibrosis as compared to TE and superior accuracy versus 2D-SWE [367]. Nevertheless, the accuracy of specific MRI features needs further validation, because different MRI features (e.g., signal intensity (SI), hepatobiliary phase (HBP), contrast enhancement index (CEI)) were correlated with different fibrosis features in different studies [368,369].

In preclinical settings, the progression of NAFLD has been non-invasively monitored by near-infrared and shortwave-infrared fluorescence imaging (NIR-SWIR). The rationale for this is based on the endogenous autofluorescence of lipofuscin, whose production increases following oxidative stress. As oxidative stress and increased ROS mediate liver injury and drive fibrosis, lipofuscin deposition might correlate with fibrosis progression. NIR-SWIR lipofuscin autofluorescence was detected both in vivo and *ex vivo*, in four murine models simulate different types of liver damage. The applicability of NIR-SWIR imaging of lipofuscin was also evaluated in a cohort of patient-derived NASH and NASH-cirrhosis biopsies (Fig. 10c; image 15–18). Because the production of lipofuscin follows ROS production, the absolute liver autofluorescence signal in choline-deficient L-amino acid-defined high-fat diet mice was substantially less pronounced than in the CCl_4 mouse model, reflecting the etiology of the disease. In addition, the signal was abundant in NASH patients and reduced in NASH-cirrhosis patients, suggesting lipofuscin imaging to indirectly correlate with fibrosis progression [370].

Other endogenous autofluorescent molecules such as NAD(P)H and flavin coenzymes can also act as label-free reporters of morphological and metabolic liver changes. Using *in vivo* multiphoton fluorescence lifetime imaging (FLIM), the redox ratio in healthy and fibrotic livers was analyzed and proven to be a sensitive measure to differentiate disease states [371]. By means of second harmonic generation (SHG), the autofluorescence lifetime associated

with collagen was used to image and study fibrotic collagen deposition in CCl_4-induced liver fibrosis, fatty liver disease and HCC. It was shown that fibrosis results in significant changes in NAD(P)H and collagen architecture and that these changes were reflected in the outcome of several metabolic-related measurements.

Next to imaging biomarkers, significant effort has been made towards the research and establishment of serum biomarkers of liver fibrosis, such as bilirubin, liver enzymes, platelet count, hyaluronic acid, pro-collagen, and laminin. Whereas serum biomarkers of liver fibrosis are well-validated in patients with chronic viral hepatitis (more prominently for HCV than for HBV and HIV), they are less well validated and clinically used in NAFLD and not validated in other chronic liver diseases [346]. The two most frequently applied panels of serum biomarkers in NAFLD, are the NAFLD Fibrosis Score (NFS) and the BARD score. The NFS is a composite score of age, hyperglycemia, body mass index (BMI), platelet count, albumin, and aspartate aminotransferase and alanine aminotransferase (AST/ALT) ratio and it identifies NAFLD patients with and without advanced fibrosis at initial NAFLD diagnosis. The BARD score accounts for three variables, i.e., the AST/ALT ratio, the BMI and the presence of diabetes [346].

4.5. Imaging fibrosis in viral disorders

Acute viral pneumonia and chronic viral liver infections cause sustained immune responses (Fig. 11a). While host defense mechanisms may clear or halt the virus, they can also cause tissue damage and dysfunctional tissue repair, i.e., fibrosis. Pulmonary fibrosis is one of the most severe consequences of viral pneumonia [372]. Progressive and irreversible interstitial pulmonary fibrosis are characterized by declining lung function, reduction of quality-of-life, and increased mortality [373]. Thus, it is important to diagnose and stage lung fibrosis resulting viral pneumonia, including – very prominently – in case of coronavirus infection [374]. Severe acute respiratory syndrome coronavirus 2 (SARS-CoV-2) is the causative pathogen of the current COVID-19 pandemic. Severe COVID-19 infection is characterized by respiratory symptoms, which progress to respiratory failure in a substantial proportion of cases, thus requiring intensive care in up to a third of hospitalized patients [375]. These findings are continuously monitored and comprehensively summarized in the real-time "living systematic review" of the Cochrane Database of Systematic Reviews, whose aim is to evaluate the accuracy of chest imaging (CT, X-ray and ultrasound) for diagnosing COVID-19 in suspected cases [376]. Up until the latest update, the authors systematically analyzed 34 studies with 9339 COVID-19 suspected cases. Most studies (31 studies; 8014 participants) utilized chest CT, followed by chest X-ray imaging (3 studies; 1243 participants) and lung ultrasound (1 study; 100 participants). Although solid conclusions cannot be drawn, it seems obvious chest CT is a sensitive and properly specific imaging technique to visualize COVID-19 repercussion in the lungs (Fig. 11b).

In one of the first retrospective studies published on SARS-CoV-2 [377], patients were subjected to high-resolution computed tomography (HR-CT) on the day of admission and 60 days after discharge from the hospital. Approximately one third of patients developed pulmonary fibrosis and specific fibrotic and inflammatory patterns were detected (e.g., honeycombing, reticulation, architectural distortion, traction bronchiectasis, and architectural distortion superimposed to areas of bronchiectasis). Other important patterns detected in the lungs of COVID-19 infected individuals were ground glass opacity (GGO; i.e., patchy or diffuse X-ray attenuation in the lungs, with preserved bronchial and vascular structures [378]), and consolidation (i.e., a homogenous increase in lung parenchymal attenuation that obscures both bronchial and vascular structures [379]) (Fig. 11c; image 1–3) [380-382]. The detection of these radiological patterns appears to be a very useful clinical tool, since the worsening of the disease can be better predicted via these radiological patterns than via viral load (e.g., via RT-PCR) [383]. In this regard, it is important to note that the development of fibrosis, as revealed by CT, correlated not only with longer hospitalization time but also with increased inflammation [384]. Patients who eventually developed fibrosis showed a larger, irregular interface and parenchymal band in the initial CT scan, larger interstitial thickening coarse reticular pattern, parenchymal band and pleural effusion in the worst-state CT, and more segments involved in both CT scans. In severe or critically severe patients, multiple patches or an integrated larger patch of GGO, consolidation and fibrosis were present in both lungs.

One of the largest post-mortem studies reported in Europe described that focal patterns of mural and microcystic-honeycombing fibrosis were present in 63% and 39% of cases, respectively [385]. Needle core lung biopsies from intensive care unit (ICU) COVID-19 patients that eventually deceased revealed the major histopathological patterns to be fibrosis, organized pneumonia (OP) with acute fibrinous exudate, and diffuse alveolar damage (DAD) [386,387]. The first histopathological report pinpointed diffuse alveolar damage as the predominant pattern (at 7 days post-hospitalization) and the second report described OP and fibrosis as the most common histopathological features (at 23 days post-hospitalization). In some cases, patients were reported to rapidly progress from acute pneumonia to OP, with evident signs of fibrosis and reduced lung volume as revealed by chest X-ray and CT (Fig. 11c; image 4–6) [388].

As for other virus-induced acute respiratory distress syndrome (ARDS), e.g., SARS-CoV-1, MERS-CoV, COVID-19 progresses to severe cases at different speeds in different patients. In addition, lung fibrosis is unlikely to regress in surviving patients affected by severe disease. Thus, long-term follow-up CT scans are needed for identifying long-term functional impairment. Taking into account the time-factor in COVID-19-associated fibrosis development, CT findings across different patients and time points throughout disease progression reveal a relatively well-preserved pattern [389]. The typical CT pattern in asymptomatic patients was unilateral and multifocal GGO. Within one week after symptom onset, lesions rapidly evolved to bilateral and diffuse, with a relative decrease in the frequency of GGO areas and a transition to consolidation. GGO further decreased in frequency throughout the second week after symptom onset, while consolidation became even more abundant. A reticular pattern associated with bronchiectasis (i.e., irreversible dilation of the bronchial tree [390]), and irregular interlobular or septal thickening were increased from the second week onwards. These findings indicate extensive interstitial changes, pointing towards the development of severe fibrosis. As the disease progressed in the third week after onset, consolidation and mixed patterns became more apparent, while GGO decreased further. Of note, CT scans could reveal lung abnormalities due to SARS-CoV-2 infection even before onset of symptoms, encouraging the use of CT in combination with laboratory findings for early diagnosis [391].

Whereas chest CT has been fundamental in identifying SARS-COV-2-induced lung fibrosis, for other types of organ fibrosis following sustained virus-induced inflammation, such as hepatitis B and C, several different complementary approaches exist. Liver fibrosis is a key predictive factor for progression of viral disease towards liver failure, cirrhosis and hepatocellular carcinoma (HCC). Therefore, the management of liver fibrosis (i.e., accurate fibrosis imaging, staging, treatment and monitoring) has become the new surrogate goal of HBV/HCV therapy [392]. In this regard, various imaging techniques are employed as means to detect virus-induced liver fibrosis.

The most widely used and validated imaging technique to assess liver fibrosis in patients with viral hepatitis is transient

elastography (TE), which is performed with an ultrasound transducer mounted on the axis of a vibrator. TE gives a 1-dimensional quantitative readout of the velocity which relates to tissue stiffness [393]. Despite the ease of use and decent reproducibility for cirrhosis, TE cannot distinguish between intermediate stages of fibrosis, and its applicability is less good than serum biomarkers in obese or ascitic patients [394]. As such, and as shown for non-viral liver diseases, point shear wave elastography (pSWE) and two-dimensional shear wave elastography (2D-SWE) are used as alternatives (Fig. 11c; image 7–9). Despite the advantages of these SWE techniques in comparison to TE (e.g., ROI selection), meta-analyses indicate that SWE and TE to have comparable diagnostic accuracies in cases of severe fibrosis, with TE being more accurate in case of significant fibrosis or liver cirrhosis [395]. Currently, only a few studies have evaluated 2D-SWE for the staging of liver fibrosis in patients with chronic hepatitis B and C [396-398]. Consequently, definitive liver stiffness cut-off values for staging liver fibrosis are not yet established. In addition to ultrasound elastography, also MRI and MRE are increasingly used for viral hepatitis, providing the possibility to visualize the entire liver and displaying good performance in obese and ascitic patients [352,399]. Similarly to non-viral liver fibrosis, iron corrected and multiparametric MRI gains a lot of ground considering the accurate diagnosis of patients' fibrosis magnitude (Fig. 11c; image 10–12) [360]. In case of MRE, the relatively high cost and low signal-to-noise ratio in iron-overloaded livers limit its applicability [342,346].

Finally, despite the utilization the abovementioned imaging techniques to accurately detect fibrosis, needle core biopsy is the only diagnostic tool that can ultimately rule out the malignant nature of a lesion. This realization became apparent in an example of a patient previously diagnosed with HCV-related cirrhosis and diabetes with a mass which resembled cholangiolocarcinoma on US, CT, and MRI (Fig. 11c; image 13–16). In contrast, ^{18}F-FDG-PET could correctly diagnose the suspected mass as fibrosis, as no tracer uptake was observed in the mass (Fig. 11c; image 17). After laparoscopic resection of the suspicious liver tissue, histological analysis revealed a mass comprising of abundant fibrosis and dilated blood vessels, but no evidence of tumor cells (Fig. 11c; image 18) [400].

Among the different available strategies for the clinical management of HCV and HBV patients, the combination of imaging biomarkers (i.e., TE-measurement of liver stiffness) with serum biomarkers is the most efficient, as it allows for rapid staging of liver disease without the need for liver biopsy [346,401]. The most validated panels of serum biomarkers of liver fibrosis in HCV/HBV patients are those which reflect the changes in the fibrogenic cascade upon progression of viral disease as well as the changes in the release of hepatic enzymes. Among others, FibroTest®, combining six different serum markers (Alpha-2-macroglobulin, haptoglobin, apolipoprotein A1, gamma-glutamyl transpeptidase (GGT), total bilirubin, and ALT) with age and gender of the patients and the AST to Platelet Ratio Index (APRI) are the most validated ones.

5. Diagnostic outlook: Multimodality and molecular probes for imaging fibrosis

Accurate diagnosis and staging of fibrosis require a comprehensive imaging-based approach. Within the umbrella of diagnostic techniques, histopathological stainings of biopsy specimens stands as the gold standard reference procedure. Chemical staining (e.g., Masson's trichrome) reveal important features of pathological fibrosis, such as the extension of connective tissue deposition (i.e., collagen amount) and architectural distribution and/or remodeling of collagen (e.g., perivascular vs. interstitial fibrosis). The downside of this is that histology requires an invasive medical procedure to acquire tissue specimens, which can be painful and dangerous, and which notoriously results in sampling variability. These features make biopsy-based histological examination an imperfect gold standard for fibrosis assessment, and they underline the need for establishing more elegant and more advanced methods [338,402].

Such insights have boosted the development of multimodality imaging approaches, in which two or more complementary imaging techniques are used together. This is because a single imaging modality may not be capable of assessing fibrosis in a reliable and holistic manner. For example, both IPF and viral pneumonia-induced lung fibrosis can be diagnosed and staged via chest CT [376]. However, on CT images, cases of confluent HCV-induced fibrosis can be mistaken for malignancy [400]. Another example shows that although sonography and angiography can straightforwardly identify obstructed vessels and heart functionality, only the combination of intra-arterial OCT with MRI can accurately assess distinct morphological alterations in vessels and the magnitude of cardiac remodeling. Intra-arterial OCT, however, is hardly applied in clinical routine, due to its high invasiveness.

Pitfalls for using single imaging modalities are also obvious in the case of cancer. While they are typically relatively easy to employ, non-invasive imaging techniques to detect lung, liver, heart, and thyroid fibrosis are less sensitive at assessing cancer-related fibrosis in these organs [403]. In such cases, the combination of two imaging modalities (e.g., anatomical or functional CT, US and MRI) followed by needle biopsy and histology are required to properly diagnose cancer-associated fibrosis (i.e., desmoplasia, chemoradiation-induced fibrosis, local recurrence). The main reason for combining different techniques is that single-used imaging modalities oftentimes fail to discriminate different fibrotic entities (e.g., tumor progression from chemotherapy-induced fibrosis [311]), because of the fact that they display unclear radiological features.

Since the direct visualization of fibrosis can be challenging, tissue function readouts rather than anatomical features are used to indirectly capture fibrosis. A prominent example is the assessment of liver stiffness [346]. As liver fibrosis is the most common cause of liver stiffening [344], increased liver stiffness is used as an indirect marker of fibrosis. An increase in liver stiffness directly reflects an increase of connective tissue content [354]. However, liver fibrosis progression does not uniquely rely on an increase in collagen content, but also on structural remodeling of collagen [340,354]. This morphological modification of the collagen network does not necessarily produce changes in tissue elasticity. Thus, such alterations are not taken into account by measuring stiffness only. In fact, between "no" fibrosis and "mild-to-significant" fibrosis, the amount of collagen does not necessarily increase, while it does exponentially increase once the patient progresses to advanced fibrosis. This explains why most elastography-based methods which measure liver stiffness fail to differentiate mild from significant liver fibrosis, and thereby also why histology still stands as the gold standard diagnostic method.

Despite "smart" multimodal imaging combinations, anatomical and functional approaches may not be sensitive or specific enough to detect early-stage fibrotic disease and/or to distinguish active fibrosis from scar tissue. Employing molecular imaging via targeted probes may provide a solution in such situations [404,405]. Indeed, for various diseases (e.g., pulmonary fibrosis, liver fibrosis and atherosclerosis), there are a number of fibrosis molecular imaging agents available [406,407]. These fibrosis-specific probes can be used against several molecular and cell targets. Prominent examples are the FDA approved PET probe ^{111}In-octreotide and the SPECT probe ^{68}Ga-DOTANOC, which target activated fibroblasts via their affinity for the somatostatin receptor, and the PET or

SPECT probes ^{18}F-FEDAC, ^{99m}Tc-Glc-NAc-PEI, ^{99m}Tc-3RPGD2, which target HSC via their affinity for the translocator protein TSPO, desmin, vimentin, and $\alpha_v\beta_3$ integrin, respectively [408-412]. Other cells that are targeted due to their involvement in fibrosis-associated processes are macrophages, via the PET probes ^{64}Cu- or ^{68}Ga-BMV101, as well as neutrophils via the MRI probe MPO-Gd (which tracks the neutrophil degranulation process) [413,414]. In addition to cell-targets, dedicated PET, SPECT, and MRI probes are developed to visualize deposition of ECM components. Prominent examples of this include targeting of collagen I by the MRI probes EP-3533 and CM-101, and the PET / SPECT probes ^{68}Ga-CBP8, ^{99m}TC-collagelin, and ^{99m}TC-CBP1495. Collagen I and III are co-addressed using optical imaging probe CNA-35. Last but not least, elastin can be targeted using the MRI probe Gd-ESMA [415-422].

In the case of cancer, the heterogeneity of fibrosis manifestation complicates the development and utilization of molecular probes for non-invasive imaging. Until several years ago, fibrosis-related molecular imaging in cancer was hardly performed, except via the use of ^{18}F-FDG-PET which can be used to distinguish malignant from fibrotic masses (with tumor lesions typically showing higher uptake). Recently, however, very prominent progress has been made with regard to fibroblast-activation protein (FAP) imaging, using PET and radiolabeled FAP inhibitors. Proof-of-concept has been provided in multiple different cancer entities, and ^{68}Ga-FAPI PET imaging is suggested to become complementary to ^{18}F-FDG PET/CT for identifying and characterising the cancerous lesions [423].

6. Concluding remarks

Experimentation on the discovery of anti-fibrotic targets will enable a better understanding, diagnosis and treatment of fibrogenic disorders. The elucidation of specific genes, RNA components, proteins and metabolites as fibrotic contributors will help to design therapies fighting fibrosis from multiple angles. In this regard, nanotechnological tools will potentiate the specific targeting of therapeutic agents. This notion will result in a transition of the clinical landscape from the use of broad / unspecific therapies to complementary cell- or molecule-specific treatments. In this therapeutic effort, improving image-guided diagnostics will assure the early detection, staging, and overall assessment of fibrosis contributing to the application of treatments at early stages of the disease progression. In this regard, the discovery of dedicated molecular probes against different pro-fibrotic cells or ECM components will further improve the diagnosis and monitoring of fibrosis. Taken together, examining fibrosis as major co-morbidity in many diseases rather than as a singular disease symptom/aftermath will contribute to a paradigm shift from easing the symptoms to establishing a solid therapeutic and diagnostic anti-fibrotic strategy.

Declaration of Competing Interest

The authors declare that they have no known competing financial interests or personal relationships that could have appeared to influence the work reported in this paper.

Acknowledgements

A.M.S., F.DL., Y.S. and T.L., acknowledge financial support from the European Research Council (ERC: Meta-Targeting (864121)), the European Union (European Fund for Regional Development: TAKTIRA (EFRE-0801767)), the German Research Foundation (DFG: LA 2937/4-1, SH 1223/1-1, SFB/TRR57, SFB1066, GRK/RTG 2375 (Tumor-targeted Drug Delivery; Project number: 331065168)), the German Federal Ministry of Education and Research (BMBF: PP-TNBC, Project number: 16GW 0319K), and the Excellence Strategy of the Federal Government and the Länder (G:(DE-82)EXS-SF-OPSF580). L.C. acknowledges the Italian Association for Cancer Research (AIRC) fellowship for abroad "Monica Broggi". J.W.W. and G.S. acknowledge funding from the Singapore Ministry of Health's National Medical Research Council (NMRC/OFYIRG/0081/2018) and the National University of Singapore NanoNASH Program (NUHSRO/2020/002/NanoNash/LOA).

References

[1] R.M. du Bois, Strategies for treating idiopathic pulmonary fibrosis, Nat. Rev. Drug Discov. 9 (2010) 129–140, https://doi.org/10.1038/nrd2958.
[2] T.-H. Lan, X.-Q. Huang, H.-M. Tan, Vascular fibrosis in atherosclerosis, Cardiovasc. Pathol. 22 (2013) 401–407, https://doi.org/10.1016/J.CARPATH.2013.01.003.
[3] S. Hinderer, K. Schenke-Layland, Cardiac fibrosis – a short review of causes and therapeutic strategies, Adv. Drug Deliv. Rev. 146 (2019) 77–82, https://doi.org/10.1016/J.ADDR.2019.05.011.
[4] A. Piek, R.A. de Boer, H.H.W. Silljé, The fibrosis-cell death axis in heart failure, Heart Fail. Rev. 21 (2016) 199–211, https://doi.org/10.1007/s10741-016-9536-9.
[5] D. Chen, Dually efficacious medicine against fibrosis and cancer, Med. Sci. 7 (2019) 41, https://doi.org/10.3390/medsci7030041.
[6] J.M. Oldham, H.R. Collard, Comorbid conditions in idiopathic pulmonary fibrosis: recognition and management, Front. Med. 4 (2017) 123, https://doi.org/10.3389/fmed.2017.00123.
[7] J.-H. Zhao, Mesangial Cells and Renal Fibrosis, in, Springer, Singapore, 2019, pp. 165–194.
[8] D. Wang, Y. Ma, X. Tong, Y. Zhang, H. Fan, Diabetes mellitus contributes to idiopathic pulmonary fibrosis: a review from clinical appearance to possible pathogenesis, Front. Public Heal. 8 (2020) 196, https://doi.org/10.3389/fpubh.2020.00196.
[9] X. Li, Y. Jiao, Y. Xing, P. Gao, Diabetes mellitus and risk of hepatic fibrosis/cirrhosis, Biomed Res. Int. 2019 (2019) 1–8, https://doi.org/10.1155/2019/5308308.
[10] S. Twigg, S.M. Twigg, Fibrosis in diabetes complications: pathogenic mechanisms and circulating and urinary markers, Vasc. Health Risk Manag. 4 (2008) 575–596, https://doi.org/10.2147/VHRM.S1991.
[11] N.C. Henderson, F. Rieder, T.A. Wynn, Fibrosis: from mechanisms to medicines, Nature 587 (2020) 555–566, https://doi.org/10.1038/s41586-020-2938-9.
[12] M. Yamauchi, T.H. Barker, D.L. Gibbons, J.M. Kurie, The fibrotic tumor stroma, J. Clin. Invest. 128 (2018) 16–25, https://doi.org/10.1172/JCI93554.
[13] T.A. Wynn, T.R. Ramalingam, Mechanisms of fibrosis: therapeutic translation for fibrotic disease, Nat. Med. 18 (2012) 1028–1040, https://doi.org/10.1038/nm.2807.
[14] X. Li, L. Zhu, B. Wang, M. Yuan, R. Zhu, Drugs and targets in fibrosis, Front. Pharmacol. 8 (2017) 855, https://doi.org/10.3389/fphar.2017.00855.
[15] N.G. Frangogiannis, Transforming growth factor–β in tissue fibrosis, J. Exp. Med. 217 (2020), https://doi.org/10.1084/jem.20190103.
[16] W.A. Border, N.A. Noble, Transforming growth factor β in tissue fibrosis, N. Engl. J. Med. 331 (1994) 1286–1292, https://doi.org/10.1056/NEJM199411103311907.
[17] X. Meng, D.J. Nikolic-Paterson, H.Y. Lan, TGF-β: the master regulator of fibrosis, Nat. Rev. Nephrol. 12 (2016) 325–338, https://doi.org/10.1038/nrneph.2016.48.
[18] Y.E. Zhang, Non-smad pathways in TGF-β signaling, Cell Res. 19 (2009) 128–139, https://doi.org/10.1038/cr.2008.328.
[19] B. Costanza, I. Umelo, J. Bellier, V. Castronovo, A. Turtoi, Stromal modulators of TGF-β in cancer, J. Clin. Med. 6 (2017) 7, https://doi.org/10.3390/jcm6010007.
[20] C. Neuzillet, A. Tijeras-Raballand, R. Cohen, J. Cros, S. Faivre, E. Raymond, A. De Gramont, Targeting the TGFβ pathway for cancer therapy, Pharmacol. Ther. 147 (2015) 22–31, https://doi.org/10.1016/j.pharmthera.2014.11.001.
[21] S. Kim, H. Iwao, Molecular and cellular mechanisms of angiotensin II-mediated cardiovascular and renal diseases, Pharmacol. Rev. 52 (2000) 11–34 (accessed January 28, 2021) https://pharmrev.aspetjournals.org/content/52/1/11/tab-article-info.
[22] A.R. Brasier, A. Recinos, M.S. Eledrisi, M.S. Runge, Vascular inflammation and the renin-angiotensin system, Arterioscler. Thromb. Vasc. Biol. 22 (2002) 1257–1266, https://doi.org/10.1161/01.ATV.0000021412.56621.A2.
[23] L.A. Borthwick, L. Barron, K.M. Hart, K.M. Vannella, R.W. Thompson, S. Oland, A. Cheever, J. Sciurba, T.R. Ramalingam, A.J. Fisher, T.A. Wynn, Macrophages are critical to the maintenance of IL-13-dependent lung inflammation and fibrosis, Mucosal Immunol. 9 (2016) 38–55, https://doi.org/10.1038/mi.2015.34.
[24] M. Kaviratne, M. Hesse, M. Leusink, A.W. Cheever, S.J. Davies, J.H. McKerrow, L.M. Wakefield, J.J. Letterio, T.A. Wynn, IL-13 activates a mechanism of tissue

fibrosis that is completely TGF-beta independent, J. Immunol. 173 (2004) 4020–4029, https://doi.org/10.4049/jimmunol.173.6.4020.
[25] S. Fichtner-Feigl, W. Strober, K. Kawakami, R.K. Puri, A. Kitani, IL-13 signaling through the IL-13α2 receptor is involved in induction of TGF-β1 production and fibrosis, Nat. Med. 12 (2006) 99–106, https://doi.org/10.1038/nm1332.
[26] Y. Zhang, T.C. Lee, B. Guillemin, M.C. Yu, W.N. Rom, Enhanced IL-1 beta and tumor necrosis factor-alpha release and messenger RNA expression in macrophages from idiopathic pulmonary fibrosis or after asbestos exposure, J. Immunol. 150 (1993) 4188–4196.
[27] M. Natsume, H. Tsuji, A. Harada, M. Akiyama, T. Yano, H. Ishikura, I. Nakanishi, K. Matsushima, S.I. Kaneko, N. Mukaida, Attenuated liver fibrosis and depressed serum albumin levels in carbon tetrachloride-treated IL-6-deficient mice, J. Leukoc. Biol. 66 (1999) 601–608, https://doi.org/10.1002/jlb.66.4.601.
[28] M. Brown, S. O'Reilly, The immunopathogenesis of fibrosis in systemic sclerosis, Clin. Exp. Immunol. 195 (2019) 310–321, https://doi.org/10.1111/cei.13238.
[29] G.J. Prud'homme, Pathobiology of transforming growth factor β in cancer, fibrosis and immunologic disease, and therapeutic considerations, Lab. Investig. 87 (2007) 1077–1091. DOI: 10.1038/labinvest.3700669.
[30] Y.Y. Wan, R.A. Flavell, TGF-β and regulatory T cell in immunity and autoimmunity, J. Clin. Immunol. 28 (2008) 647–659, https://doi.org/10.1007/s10875-008-9251-y.
[31] M.M. Mia, M. Boersema, R.A. Bank, Interleukin-1β attenuates myofibroblast formation and extracellular matrix production in dermal and lung fibroblasts exposed to transforming growth factor-β1, PLoS ONE 9 (2014), https://doi.org/10.1371/journal.pone.0091559 e91559.
[32] T.J. Keane, C.M. Horejs, M.M. Stevens, Scarring vs. functional healing: matrix-based strategies to regulate tissue repair, Adv. Drug Deliv. Rev. 129 (2018) 407–419, https://doi.org/10.1016/j.addr.2018.02.002.
[33] G. Stokman, A.M. Hoek, D. Denker Thorbekk, E.J. Pieterman, S. Skovgård Veidal, B. Basta, M. Iruarrizaga-Lejarreta, J.W. Hoorn, L. Verschuren, J.F.P. Berbée, P.C.N. Rensen, T. Skjæret, C. Alonso, M. Feigh, J.J.P. Kastelein, S.L. Friedman, H.M.G. Princen, D.A. Fraser, Dual targeting of hepatic fibrosis and atherogenesis by icosabutate, an engineered eicosapentaenoic acid derivative, Liver Int. 40 (2020) 2860–2876, https://doi.org/10.1111/liv.14643.
[34] S.P. Levick, D.C. Loch, S.M. Taylor, J.S. Janicki, J.M. Samet, F.H. Chilton, Arachidonic acid metabolism as a potential mediator of cardiac fibrosis associated with inflammation, J. Immunol. 178 (2007) 641–646, https://doi.org/10.4049/jimmunol.178.2.641.
[35] J.J. Tomasek, G. Gabbiani, B. Hinz, C. Chaponnier, R.A. Brown, Myofibroblasts and mechano-regulation of connective tissue remodelling, Nat. Rev. Mol. Cell Biol. 3 (2002) 349–363, https://doi.org/10.1038/nrm809.
[36] C.A. Fielding, G.W. Jones, R.M. McLoughlin, L. McLeod, V.J. Hammond, J. Uceda, A.S. Williams, M. Lambie, T.L. Foster, C.-T. Liao, C.M. Rice, C.J. Greenhill, C.S. Colmont, E. Hams, B. Coles, A. Kift-Morgan, Z. Newton, K.J. Craig, J.D. Williams, G.T. Williams, S.J. Davies, I.R. Humphreys, V.B. O'Donnell, P.R. Taylor, B.J. Jenkins, N. Topley, S.A. Jones, Interleukin-6 signaling drives fibrosis in unresolved inflammation, Immunity 40 (2014) 40–50, https://doi.org/10.1016/J.IMMUNI.2013.10.022.
[37] A. Fujiwara, S. Funaki, E. Fukui, K. Kimura, T. Kanou, N. Ose, M. Minami, Y. Shintani, Effects of pirfenidone targeting the tumor microenvironment and tumor-stroma interaction as a novel treatment for non-small cell lung cancer, Sci. Rep. 10 (2020) 10900, https://doi.org/10.1038/s41598-020-67904-8.
[38] T. Yamanaka, N. Harimoto, T. Yokobori, R. Muranushi, K. Hoshino, K. Hagiwara, D. Gantumur, T. Handa, N. Ishii, M. Tsukagoshi, T. Igarashi, H. Tanaka, A. Watanabe, N. Kubo, K. Araki, K. Shirabe, Nintedanib inhibits intrahepatic cholangiocarcinoma aggressiveness via suppression of cytokines extracted from activated cancer-associated fibroblasts, Br. J. Cancer. 122 (2020) 986–994, https://doi.org/10.1038/s41416-020-0744-7.
[39] M. Sha, S. Jeong, B. Qiu, Y. Tong, L. Xia, N. Xu, J. Zhang, Q. Xia, Isolation of cancer-associated fibroblasts and its promotion to the progression of intrahepatic cholangiocarcinoma, Cancer Med. 7 (2018) 4665–4677, https://doi.org/10.1002/cam4.1704.
[40] E.A. Kosmacek, R.E. Oberley-Deegan, Adipocytes protect fibroblasts from radiation-induced damage by adiponectin secretion, Sci. Rep. 10 (2020) 12616, https://doi.org/10.1038/s41598-020-69352-w.
[41] W. Udomsinprasert, S. Honsawek, Y. Poovorawan, Adiponectin as a novel biomarker for liver fibrosis, World J. Hepatol. 10 (2018) 708–718, https://doi.org/10.4254/wjh.v10.i10.708.
[42] K.K. Vidya Vijayan, K.P. Karthigeyan, S.P. Tripathi, L.E. Hanna, Pathophysiology of CD4+ T-cell depletion in HIV-1 and HIV-2 infections, Front. Immunol. 8 (2017) 580, https://doi.org/10.3389/fimmu.2017.00580.
[43] C. Trautwein, S.L. Friedman, D. Schuppan, M. Pinzani, Hepatic fibrosis: concept to treatment, J. Hepatol. 62 (2015) S15–S24, https://doi.org/10.1016/j.jhep.2015.02.039.
[44] L. Zhang, M.B. Bansal, Role of kupffer cells in driving hepatic inflammation and fibrosis in HIV infection, Front. Immunol. 11 (2020) 1086, https://doi.org/10.3389/fimmu.2020.01086.
[45] J. Hou, J. Shi, L. Chen, Z. Lv, X. Chen, H. Cao, Z. Xiang, X. Han, M2 macrophages promote myofibroblast differentiation of LR-MSCs and are associated with pulmonary fibrogenesis, Cell Commun. Signal. 16 (2018) 89, https://doi.org/10.1186/s12964-018-0300-8.
[46] L. Kaps, N. Leber, A. Klefenz, N. Choteschovsky, R. Zentel, L. Nuhn, D. Schuppan, In vivo siRNA delivery to immunosuppressive liver macrophages by α-mannosyl-functionalized cationic nanohydrogel particles, Cells. 9 (2020) 1905, https://doi.org/10.3390/cells9081905.
[47] N. Leber, L. Kaps, A. Yang, M. Aslam, M. Giardino, A. Klefenz, N. Choteschovsky, S. Rosigkeit, A. Mostafa, L. Nuhn, D. Schuppan, R. Zentel, α-mannosyl-functionalized cationic nanohydrogel particles for targeted gene knockdown in immunosuppressive macrophages, Macromol. Biosci. 19 (2019) 1900162, https://doi.org/10.1002/mabi.201900162.
[48] P. An, L.-L. Wei, S. Zhao, D.Y. Sverdlov, K.A. Vaid, M. Miyamoto, K. Kuramitsu, M. Lai, Y.V. Popov, Hepatocyte mitochondria-derived danger signals directly activate hepatic stellate cells and drive progression of liver fibrosis, Nat. Commun. 11 (2020) 2362, https://doi.org/10.1038/s41467-020-16092-0.
[49] E. Zigmond, C. Varol, Two roads diverge in the sick liver, Monocytes Travel Both, Immunity. 53 (2020) 479–481, https://doi.org/10.1016/J.IMMUNI.2020.08.006.
[50] Y. Wen, J. Lambrecht, C. Ju, F. Tacke, Hepatic macrophages in liver homeostasis and diseases-diversity, plasticity and therapeutic opportunities, Cell. Mol. Immunol. 18 (2021) 45–56, https://doi.org/10.1038/s41423-020-00558-8.
[51] Vanhockerhout, M. Binte Abdul Latib, L. Devisscher, A. Hoorens, J. Bonnardel, N. Vandamme, A. Kremer, P. Borghgraef, H. Van Vlierberghe, S. Lippens, E. Pearce, Y. Saeys, C.L. Scott, Osteopontin Expression Identifies a Subset of Recruited Macrophages Distinct from Kupffer Cells in the Fatty Liver, Immunity. 53 (2020) 641-657.e14. DOI: 10.1016/J.IMMUNI.2020.08.004.
[52] D. Zhang, R. Zhuang, Z. Guo, M. Gao, L. Huang, L. You, P. Zhang, J. Li, X. Su, H. Wu, X. Chen, X. Zhang, Desmin- and vimentin-mediated hepatic stellate cell-targeting radiotracer ^{99m}Tc-GlcNAc-PEI for liver fibrosis imaging with SPECT, Theranostics. 8 (2018) 1340–1349, https://doi.org/10.7150/thno.22806.
[53] A. Pardo, K. Gibson, J. Cisneros, T.J. Richards, Y. Yang, C. Becerril, S. Yousem, I. Herrera, V. Ruiz, M. Selman, N. Kaminski, Up-regulation and profibrotic role of osteopontin in human idiopathic pulmonary fibrosis, PLoS Med. 2 (2005), https://doi.org/10.1371/journal.pmed.0020251 e251.
[54] T.-M. Leung, X. Wang, N. Kitamura, M.I. Fiel, N. Nieto, Osteopontin delays resolution of liver fibrosis, Lab. Investig. 93 (2013) 1082–1089, https://doi.org/10.1038/labinvest.2013.104.
[55] G. Song, M. Pacher, A. Balakrishnan, Q. Yuan, H.-C. Tsay, D. Yang, J. Reetz, S. Brandes, Z. Dai, B.M. Pützer, M.J. Araúzo-Bravo, D. Steinemann, T. Luedde, R.F. Schwabe, M.P. Manns, H.R. Schöler, A. Schambach, T. Cantz, M. Ott, A.D. Sharma, Direct reprogramming of hepatic myofibroblasts into hepatocytes in vivo attenuates liver fibrosis, Cell Stem Cell 18 (2016) 797–808, https://doi.org/10.1016/J.STEM.2016.01.010.
[56] O.Z. Cheng, N. Palaniyar, NET balancing: a problem in inflammatory lung diseases, Front. Immunol. 4 (2013) 1, https://doi.org/10.3389/fimmu.2013.00001.
[57] B.N. Porto, R.T. Stein, Neutrophil extracellular traps in pulmonary diseases: too much of a good thing?, Front. Immunol. 7 (2016) 311, https://doi.org/10.3389/fimmu.2016.00311.
[58] K. Ritis, K. Kambas, neutrophil extracellular traps - the invisible inflammatory mediator in fibrosis, J. Clin. Exp. Pathol. 05 (2015) 1–2, https://doi.org/10.4172/2161-0681.1000239.
[59] M. Suzuki, J. Ikari, R. Anazawa, N. Tanaka, Y. Katsumata, A. Shimada, E. Suzuki, K. Tatsumi, Neutrophil extracellular traps contribute to pulmonary fibrosis induced by bleomycin, in: Mech. Lung Inj. Repair, European Respiratory Society, 2019: p. PA2414. DOI: 10.1183/13993003.congress-2019.PA2414.
[60] A.D. Gregory, C.R. Kliment, H.E. Metz, K.-H. Kim, J. Kargl, B.A. Agostini, L.T. Crum, E.A. Oczypok, T.A. Oury, A.M. Houghton, Neutrophil elastase promotes myofibroblast differentiation in lung fibrosis, J. Leukoc. Biol. 98 (2015) 143–152, https://doi.org/10.1189/jlb.3HI1014-493R.
[61] C. Carmona-Rivera, W. Zhao, S. Yalavarthi, M.J. Kaplan, Neutrophil extracellular traps induce endothelial dysfunction in systemic lupus erythematosus through the activation of matrix metalloproteinase-2, Ann. Rheum. Dis. 74 (2015) 1417–1424, https://doi.org/10.1136/annrheumdis-2013-204837.
[62] E. Frangou, D. Vassilopoulos, J. Boletis, D.T. Boumpas, An emerging role of neutrophils and NETosis in chronic inflammation and fibrosis in systemic lupus erythematosus (SLE) and ANCA-associated vasculitides (AAV): Implications for the pathogenesis and treatment, Autoimmun. Rev. 18 (2019) 751–760, https://doi.org/10.1016/j.autrev.2019.06.011.
[63] S. Ling, J.W. Xu, NETosis as a pathogenic factor for heart failure, Oxid. Med. Cell. Longev. 2021 (2021), https://doi.org/10.1155/2021/6687096.
[64] M. Dwyer, Q. Shan, S. D'Ortona, R. Maurer, R. Mitchell, H. Olesen, S. Thiel, J. Huebner, M. Gadjeva, Cystic fibrosis Sputum DNA has NETosis characteristics and neutrophil extracellular trap release is regulated by macrophage migration-inhibitory factor, J. Innate Immun. 6 (2014) 765–779, https://doi.org/10.1159/000363242.
[65] C. Radermecker, N. Detrembleur, J. Guiot, E. Cavalier, M. Henket, C. d'Emal, C. Vanwinge, D. Cataldo, C. Oury, P. Delvenne, T. Marichal, Neutrophil extracellular traps infiltrate the lung airway, interstitial, and vascular compartments in severe COVID-19, J. Exp. Med. 217 (2020), https://doi.org/10.1084/jem.20201012.
[66] M. Sharma, M.P. Schlegel, M.S. Afonso, E.J. Brown, K. Rahman, A. Weinstock, B. E. Sansbury, E.M. Corr, C. van Solingen, G.J. Koelwyn, L.C. Shanley, L. Beckett, D. Peled, J.J. Lafaille, M. Spite, P. Loke, E.A. Fisher, K.J. Moore, Regulatory T cells license macrophage pro-resolving functions during atherosclerosis regression, Circ. Res. 127 (2020) 335–353, https://doi.org/10.1161/CIRCRESAHA.119.316461.

[67] A.C. Foks, A.H. Lichtman, J. Kuiper, Treating atherosclerosis with regulatory T cells, Arterioscler. Thromb. Vasc. Biol. 35 (2015) 280–287, https://doi.org/10.1161/ATVBAHA.114.303568.

[68] H. Bartolomaeus, A. Balogh, M. Yakoub, S. Homann, L. Markó, S. Höges, D. Tsvetkov, A. Krannich, S. Wundersitz, E.G. Avery, N. Haase, K. Kräker, L. Hering, M. Maase, K. Kusche-Vihrog, M. Grandoch, J. Fielitz, S. Kempa, M. Gollasch, Z. Zhumadilov, S. Kozhakhmetov, A. Kushugulova, K.-U. Eckardt, R. Dechend, L.C. Rump, S.K. Forslund, D.N. Müller, J. Stegbauer, N. Wilck, Short-chain fatty acid propionate protects from hypertensive cardiovascular damage, Circulation 139 (2019) 1407–1421, https://doi.org/10.1161/CIRCULATIONAHA.118.036652.

[69] P.M. Smith, M.R. Howitt, N. Panikov, M. Michaud, C.A. Gallini, M. Bohlooly-Y, J. N. Glickman, W.S. Garrett, The microbial metabolites, short-chain fatty acids, regulate colonic Treg cell homeostasis, Science 341 (2013) 569–573, https://doi.org/10.1126/science.1241165.

[70] Y. Li, B. Li, Z. You, J. Zhang, Y. Wei, Y. Li, Y. Chen, B. Huang, Q. Wang, Q. Miao, Y. Peng, J. Fang, M.E. Gershwin, R. Tang, S.A. Greenberg, X. Ma, Cytotoxic KLRG1 expressing lymphocytes invade portal tracts in primary biliary cholangitis, J. Autoimmun. 103 (2019), https://doi.org/10.1016/J.JAUT.2019.06.004 102293.

[71] R.S. Wijaya, S.A. Read, S. Schibeci, M. Eslam, M.K. Azardaryany, K. El-Khobar, D. van der Poorten, R. Lin, L. Yuen, V. Lam, J. George, M.W. Douglas, G. Ahlenstiel, KLRG1+ natural killer cells exert a novel antifibrotic function in chronic hepatitis B, J. Hepatol. 71 (2019) 252–264, https://doi.org/10.1016/J.JHEP.2019.03.012.

[72] M. Serrano, N. Barzilai, Targeting senescence, Nat. Med. 24 (2018) 1092–1094, https://doi.org/10.1038/s41591-018-0141-4.

[73] M.R. Bennett, M.C.H. Clarke, Killing the old: cell senescence in atherosclerosis, Nat. Rev. Cardiol. 14 (2017) 8–9, https://doi.org/10.1038/nrcardio.2016.195.

[74] L. Wang, R. Chen, G. Li, Z. Wang, J. Liu, Y. Liang, J.-P. Liu, FBW7 mediates senescence and pulmonary fibrosis through telomere uncapping, Cell Metab. 32 (2020) 860–877.e9, https://doi.org/10.1016/J.CMET.2020.10.004.

[75] C. Amor, J. Feucht, J. Leibold, Y.-J. Ho, C. Zhu, D. Alonso-Curbelo, J. Mansilla-Soto, J.A. Boyer, X. Li, T. Giavridis, A. Kulick, S. Houlihan, E. Peerschke, S.L. Friedman, V. Ponomarev, A. Piersigilli, M. Sadelain, S.W. Lowe, Senolytic CAR T cells reverse senescence-associated pathologies, Nature 583 (2020) 127–132, https://doi.org/10.1038/s41586-020-2403-9.

[76] D. Lagares, P. Ghassemi-Kakroodi, C. Tremblay, A. Santos, C.K. Probst, A. Franklin, D.M. Santos, P. Grasberger, N. Ahluwalia, S.B. Montesi, B.S. Shea, K.E. Black, R. Knipe, M. Blati, M. Baron, B. Wu, H. Fahmi, R. Gandhi, A. Pardo, M. Selman, J. Wu, J.-P. Pelletier, J. Martel-Pelletier, A.M. Tager, M. Kapoor, ADAM10-mediated ephrin-B2 shedding promotes myofibroblast activation and organ fibrosis, Nat. Med. 23 (2017) 1405–1415, https://doi.org/10.1038/nm.4419.

[77] Y. Yao, W. Sun, Q. Sun, B. Jing, S. Liu, X. Liu, G. Shen, R. Chen, H. Wang, Platelet-derived exosomal MicroRNA-25-3p inhibits coronary vascular endothelial cell inflammation through adam10 via the NF-κB signaling pathway in ApoE−/− Mice, Front. Immunol. 10 (2019) 2205, https://doi.org/10.3389/fimmu.2019.02205.

[78] Y. Qi, R. Xu, Roles of PLODs in collagen synthesis and cancer progression, Front. Cell Dev. Biol. 6 (2018) 66, https://doi.org/10.3389/fcell.2018.00066.

[79] R.A.F. Gjaltema, D. Goubert, C. Huisman, C. del Pilar García, M. Tobilla, P.G. Koncz, D. Jellema, U. Wu, A. Brouwer, P.J. Kiss, R.A. Verschure, M.G. Rots Bank, KRAB-induced heterochromatin effectively silences PLOD2 gene expression in somatic cells and is resilient to TGFβ1 activation, Int. J. Mol. Sci. 21 (2020) 3634, https://doi.org/10.3390/ijms21103634.

[80] T.H. Kim, B.A. Banini, F.Z. Asumda, N.A. Campbell, C. Hu, C.D. Moser, A.M. Shire, S. Han, C. Ma, A. Krishnan, T. Mounajjed, T.A. White, G.J. Gores, N.K. LeBrasseur, M.R. Charlton, L.R. Roberts, Knockout of sulfatase 2 is associated with decreased steatohepatitis and fibrosis in a mouse model of nonalcoholic fatty liver disease, Am. J. Physiol. Liver Physiol. 319 (2020) G333–G344, https://doi.org/10.1152/ajpgi.00150.2019.

[81] D. Ji, G. Chen, J. Wang, L. Cao, F. Lu, X. Mu, X. Zhang, X. Lu, Identification of TAF1, HNF4A, and CALM2 as potential therapeutic target genes for liver fibrosis, J. Cell. Physiol. 234 (2019) 9045–9051, https://doi.org/10.1002/jcp.27579.

[82] H.-Y. Yue, C. Yin, J.-L. Hou, X. Zeng, Y.-X. Chen, W. Zhong, P.-F. Hu, X. Deng, Y.-X. Tan, J.-P. Zhang, B.-F. Ning, J. Shi, X. Zhang, H.-Y. Wang, Y. Lin, W.-F. Xie, Hepatocyte nuclear factor 4alpha attenuates hepatic fibrosis in rats, Gut 59 (2010) 236–246, https://doi.org/10.1136/gut.2008.174904.

[83] H. Elsaesser, K. Sauer, D.G. Brooks, IL-21 is required to control chronic viral infection, Science 324 (2009) 1569–1572, https://doi.org/10.1126/science.1174182.

[84] Z. Shen, J. Wu, Z. Gao, J. Wang, H. Zhu, R. Mao, X. Wang, J. Zhang, Y. Xie, J. Liu, Characterization of IL-21-expressing recombinant hepatitis B virus (HBV) as a therapeutic agent targeting persisting HBV infection, Theranostics. 10 (2020) 5600–5612, https://doi.org/10.7150/thno.44715.

[85] L. Ye, T. Chen, J. Cao, L. Sun, W. Li, C. Zhang, Short hairpin RNA attenuates liver fibrosis by regulating the PPAR-γ and NF-κB pathways in HBV-induced liver fibrosis in mice, Int. J. Oncol. 57 (2020) 1116–1128, https://doi.org/10.3892/ijo.2020.5125.

[86] A.T. Dantas, M.C. Pereira, M.J.B. de Melo Rego, L.F. da Rocha, I. da R. Pitta, C.D. L. Marques, A.L.B.P. Duarte, M.G. da R. Pitta, The Role of PPAR Gamma in Systemic Sclerosis, PPAR Res. 2015 (2015) 1–12. DOI: 10.1155/2015/124624.

[87] A. Dropmann, S. Dooley, B. Dewidar, S. Hammad, T. Dediulia, J. Werle, V. Hartwig, S. Ghafoory, S. Woelfl, H. Korhonen, M. Janicot, K. Wosikowski, T. Itzel, A. Teufel, D. Schuppan, A. Stojanovic, A. Cerwenka, S. Nittka, A. Piiper, T. Gaiser, N. Beraza, M. Milkiewicz, P. Milkiewicz, J.G. Brain, D.E.J. Jones, T.S. Weiss, U.M. Zanger, M. Ebert, N.M. Meindl-Beinker, TGF-β2 silencing to target biliary-derived liver diseases, Gut 69 (2020) 1677–1690, https://doi.org/10.1136/gutjnl-2019-319091.

[88] W. Glenisson, V. Castronovo, D. Waltregny, Histone deacetylase 4 is required for TGFβ1-induced myofibroblastic differentiation, Biochim. Biophys. Acta - Mol. Cell Res. 1773 (2007) 1572–1582, https://doi.org/10.1016/J.BBAMCR.2007.05.016.

[89] P. Gondaliya, A.P. Dasare, K. Jash, R.K. Tekade, A. Srivastava, K. Kalia, miR-29b attenuates histone deacetylase-4 mediated podocyte dysfunction and renal fibrosis in diabetic nephropathy, J. Diabetes Metab. Disord. 19 (2020) 13–27, https://doi.org/10.1007/s40200-019-00469-0.

[90] J.-W. Yan, J.-S. Lin, X.-X. He, The emerging role of miR-375 in cancer, Int. J. Cancer. 135 (2014) 1011–1018, https://doi.org/10.1002/ijc.28563.

[91] X. Zhang, Q. Chen, H. Song, W. Jiang, S. Xie, J. Huang, G. Kang, MicroRNA-375 prevents TGF-β-dependent transdifferentiation of lung fibroblasts via the MAP2K6/P38 pathway, Mol. Med. Rep. 22 (2020) 1803–1810, https://doi.org/10.3892/mmr.2020.11261.

[92] Y. Peng, C.M. Croce, The role of MicroRNAs in human cancer, Signal Transduct. Target. Ther. 1 (2016) 15004, https://doi.org/10.1038/sigtrans.2015.4.

[93] Y. Ma, R. Yan, Q. Wan, B. Lv, Y. Yang, T. Lv, W. Xin, Inhibitor of growth 2 regulates the high glucose-induced cell cycle arrest and epithelial-to-mesenchymal transition in renal proximal tubular cells, J. Physiol. Biochem. 76 (2020) 373–382, https://doi.org/10.1007/s13105-020-00743-3.

[94] D. Larrieu, D. Ythier, R. Binet, C. Brambilla, E. Brambilla, S. Sengupta, R. Pedeux, ING2 controls the progression of DNA replication forks to maintain genome stability, EMBO Rep. 10 (2009) 1168–1174, https://doi.org/10.1038/embor.2009.180.

[95] M. Li, Y. Zhu, H. Zhang, L. Li, P. He, H. Xia, Y. Zhang, C. Mao, Delivery of inhibitor of growth 4 (ING4) gene significantly inhibits proliferation and invasion and promotes apoptosis of human osteosarcoma cells, Sci. Rep. 4 (2015) 7380, https://doi.org/10.1038/srep07380.

[96] B. Wang, Y. Wu, Z. Ge, X. Zhang, Y. Yan, Y. Xie, NLRC5 deficiency ameliorates cardiac fibrosis in diabetic cardiomyopathy by regulating EndMT through Smad2/3 signaling pathway, Biochem. Biophys. Res. Commun. 528 (2020) 545–553, https://doi.org/10.1016/J.BBRC.2020.05.151.

[97] X. Liu, Y. Wu, Y. Yang, W. Li, C. Huang, X. Meng, J. Li, Role of NLRC5 in progression and reversal of hepatic fibrosis, Toxicol. Appl. Pharmacol. 294 (2016) 43–53, https://doi.org/10.1016/J.TAAP.2016.01.012.

[98] J.C. Kovacic, S. Dimmeler, R.P. Harvey, T. Finkel, E. Aikawa, G. Krenning, A.H. Baker, Endothelial to mesenchymal transition in cardiovascular disease: JACC state-of-the-art review, J. Am. Coll. Cardiol. 73 (2019) 190–209, https://doi.org/10.1016/J.JACC.2018.09.089.

[99] D. Medici, S. Potenta, R. Kalluri, Transforming growth factor-β2 promotes Snail-mediated endothelial–mesenchymal transition through convergence of Smad-dependent and Smad-independent signalling, Biochem. J. 437 (2011) 515–520, https://doi.org/10.1042/BJ20101500.

[100] G. Sánchez-Duffhues, A. García de Vinuesa, P. ten Dijke, Endothelial-to-mesenchymal transition in cardiovascular diseases: developmental signaling pathways gone awry, Dev. Dyn. 247 (2018) 492–508, https://doi.org/10.1002/dvdy.24589.

[101] L. Barbier-Torres, K.A. Fortner, P. Iruzubieta, T.C. Delgado, E. Giddings, Y. Chen, D. Champagne, D. Fernández-Ramos, D. Mestre, B. Gomez-Santos, M. Varela-Rey, V.G. de Juan, P. Fernández-Tussy, I. Zubiete-Franco, C. García-Monzón, Á. González-Rodríguez, D. Oza, F. Valença-Pereira, Q. Fang, J. Crespo, P. Aspichueta, F. Tremblay, B.C. Christensen, J. Anguita, M.L. Martínez-Chantar, M. Rincón, Silencing hepatic MCJ attenuates non-alcoholic fatty liver disease (NAFLD) by increasing mitochondrial fatty acid oxidation, Nat. Commun. 11 (2020) 3360, https://doi.org/10.1038/s41467-020-16991-2.

[102] K.W. Chung, E.K. Lee, M.K. Lee, G.T. Oh, B.P. Yu, H.Y. Chung, Impairment of PPARα and the fatty acid oxidation pathway aggravates renal fibrosis during aging, J. Am. Soc. Nephrol. 29 (2018) 1223–1237, https://doi.org/10.1681/ASN.2017070802.

[103] G. Sithanandam, L.M. Anderson, The ERBB3 receptor in cancer and cancer gene therapy, Cancer Gene Ther. 15 (2008) 413–448, https://doi.org/10.1038/cgt.2008.15.

[104] L.A. Scheving, X. Zhang, D.W. Threadgill, W.E. Russell, Hepatocyte ERBB3 and EGFR are required for maximal CCl_4 -induced liver fibrosis, Am. J. Physiol. Liver Physiol. 311 (2016) G807–G816, https://doi.org/10.1152/ajpgi.00423.2015.

[105] J. Xiong, J. Ni, C. Chen, K. Wang, miR-148a-3p regulates alcoholic liver fibrosis through targeting ERBB3, Int. J. Mol. Med. 46 (2020) 1003–1012, https://doi.org/10.3892/ijmm.2020.4655.

[106] M.H. Naseri, M. Mahdavi, J. Davoodi, S.H. Tackallou, M. Goudarzvand, S.H. Neishabouri, Up regulation of Bax and down regulation of Bcl2 during 3-NC mediated apoptosis in human cancer cells, Cancer Cell Int. 15 (2015) 55, https://doi.org/10.1186/s12935-015-0204-2.

[107] W. Chen, C. Wei, J. Lee, Micro RNA -let-7c suppresses hepatitis C virus replication by targeting Bach1 for induction of haem oxygenase-1 expression, J. Viral Hepat. 26 (2019) 655–665, https://doi.org/10.1111/jvh.13072.

[108] A.-M. Mitterstiller, D. Haschka, S. Dichtl, M. Nairz, E. Demetz, H. Talasz, M.P. Soares, E. Einwallner, H. Esterbauer, F.C. Fang, S. Geley, G. Weiss, Heme oxygenase 1 controls early innate immune response of macrophages to *Salmonella* Typhimurium infection, Cell. Microbiol. 18 (2016) 1374–1389, https://doi.org/10.1111/cmi.12578.

[109] A. Zhang, B. Wan, D. Jiang, Y. Wu, P. Ji, Y. Du, G. Zhang, The cytoprotective enzyme heme oxygenase-1 suppresses pseudorabies virus replication in vitro, Front. Microbiol. 11 (2020) 412, https://doi.org/10.3389/fmicb.2020.00412.
[110] X.-M. Meng, P.M.-K. Tang, J. Li, H.Y. Lan, TGF-β/Smad signaling in renal fibrosis, Front. Physiol. 6 (2015) 82, https://doi.org/10.3389/fphys.2015.00082.
[111] L. Zhu, S. Chen, Y. Chen, Unraveling the biological functions of Smad7 with mouse models, Cell Biosci. 1 (2011) 44, https://doi.org/10.1186/2045-3701-1-44.
[112] H. Che, Y. Wang, Y. Li, J. Lv, H. Li, Y. Liu, R. Dong, Y. Sun, X. Xu, J. Zhao, L. Wang, Inhibition of microRNA-150-5p alleviates cardiac inflammation and fibrosis via targeting Smad7 in high glucose-treated cardiac fibroblasts, J. Cell. Physiol. 235 (2020) 7769–7779, https://doi.org/10.1002/jcp.29386.
[113] T. Zou, M. Zhu, Y.-C. Ma, F. Xiao, X. Yu, L. Xu, L.-Q. Ma, J. Yang, J.-Z. Dong, MicroRNA-410-5p exacerbates high-fat diet-induced cardiac remodeling in mice in an endocrine fashion, Sci. Rep. 8 (2018) 8780, https://doi.org/10.1038/s41598-018-26646-4.
[114] X. Xia, Y. Liang, W. Zheng, D. Lin, S. Sun, miR-410-5p promotes the development of diabetic cardiomyopathy by suppressing PIM1-induced anti-apoptosis, Mol. Cell. Probes. 52 (2020), https://doi.org/10.1016/J.MCP.2020.101558 101558.
[115] F. Azar, K. Courtet, B. Dekky, D. Bonnier, O. Dameron, A. Colige, V. Legagneux, N. Théret, Integration of miRNA-regulatory networks in hepatic stellate cells identifies TIMP3 as a key factor in chronic liver disease, Liver Int. 40 (2020) 2021–2033, https://doi.org/10.1111/liv.14476.
[116] R.-W. Yao, Y. Wang, L.-L. Chen, Cellular functions of long noncoding RNAs, Nat. Cell Biol. 21 (2019) 542–551, https://doi.org/10.1038/s41556-019-0311-8.
[117] M.R. Hadjicharalambous, B.T. Roux, C.A. Feghali-Bostwick, L.A. Murray, D.L. Clarke, M.A. Lindsay, Long non-coding RNAs are central regulators of the IL-1β-induced inflammatory response in normal and idiopathic pulmonary lung fibroblasts, Front. Immunol. 9 (2018) 2906, https://doi.org/10.3389/fimmu.2018.02906.
[118] J. Lin, Z. Jiang, C. Liu, D. Zhou, J. Song, Y. Liao, J. Chen, Emerging roles of long non-coding RNAs in renal fibrosis, Life. 10 (2020) 131, https://doi.org/10.3390/life10080131.
[119] R.S. Knipe, A.M. Tager, J.K. Liao, The Rho kinases: critical mediators of multiple profibrotic processes and rational targets for new therapies for pulmonary fibrosis, Pharmacol. Rev. 67 (2015) 103–117, https://doi.org/10.1124/pr.114.009381.
[120] J. Wang, S. Zhang, X. Li, M. Gong, LncRNA SNHG7 promotes cardiac remodeling by upregulating ROCK1 via sponging miR-34-5p., Aging (Albany NY) 12 (2020) 10441–10456, https://doi.org/10.18632/aging.103269.
[121] W. Zhong, J. Zeng, J. Xue, A. Du, Y. Xu, Knockdown of lncRNA PVT1 alleviates high glucose-induced proliferation and fibrosis in human mesangial cells by miR-23b-3p/WT1 axis, Diabetol. Metab. Syndr. 12 (2020) 33, https://doi.org/10.1186/s13098-020-00539-x.
[122] Y. Qi, H. Wu, C. Mai, H. Lin, J. Shen, X. Zhang, Y. Gao, Y. Mao, X. Xie, LncRNA-MIAT-mediated miR-214-3p silencing is responsible for IL-17 production and cardiac fibrosis in diabetic cardiomyopathy, Front. Cell Dev. Biol. 8 (2020) 243, https://doi.org/10.3389/fcell.2020.00243.
[123] Z. Wang, X. Yang, J. Kai, F. Wang, Z. Wang, J. Shao, S. Tan, A. Chen, F. Zhang, S. Wang, Z. Zhang, S. Zheng, HIF-1α-upregulated lncRNA-H19 regulates lipid droplet metabolism through the AMPKα pathway in hepatic stellate cells, Life Sci. 255 (2020), https://doi.org/10.1016/J.LFS.2020.117818 117818.
[124] J. Yao, Q. Dai, Z. Liu, L. Zhou, J. Xu, Circular RNAs in Organ Fibrosis, in: Springer, Singapore, 2018: pp. 259–273. DOI: DOI: 10.1007/978-981-13-1426-1_21.
[125] W. Wang, J. Feng, H. Zhou, Q. Li, Circ_0123996 promotes cell proliferation and fibrosis in mouse mesangial cells through sponging miR-149-5p and inducing Bach1 expression, Gene 761 (2020), https://doi.org/10.1016/J.GENE.2020.144971 144971.
[126] X. Ge, L. Xi, Q. Wang, H. Li, L. Xia, Z. Cang, W. Peng, S. Huang, Circular RNA Circ_0000064 promotes the proliferation and fibrosis of mesangial cells via miR-143 in diabetic nephropathy, Gene 758 (2020), https://doi.org/10.1016/J.GENE.2020.144952 144952.
[127] G. Li, Y. Qin, S. Qin, X. Zhou, W. Zhao, D. Zhang, Circ_WBSCR17 aggravates inflammatory responses and fibrosis by targeting miR-185-5p/SOX6 regulatory axis in high glucose-induced human kidney tubular cells, Life Sci. 259 (2020), https://doi.org/10.1016/J.LFS.2020.118269 118269.
[128] D. Xiang, J. Zou, X. Zhu, X. Chen, J. Luo, L. Kong, H. Zhang, Physalin D attenuates hepatic stellate cell activation and liver fibrosis by blocking TGF-β/Smad and YAP signaling, Phytomedicine 78 (2020), https://doi.org/10.1016/J.PHYMED.2020.153294 153294.
[129] Y. Gu, F. Lv, M. Xue, K. Chen, C. Cheng, X. Ding, M. Jin, G. Xu, Y. Zhang, Z. Wu, L. Zheng, Y. Wu, The deubiquitinating enzyme UCHL1 is a favorable prognostic marker in neuroblastoma as it promotes neuronal differentiation, J. Exp. Clin. Cancer Res. 37 (2018) 258, https://doi.org/10.1186/s13046-018-0931-z.
[130] C. Jin, W. Yu, X. Lou, F. Zhou, X. Han, N. Zhao, B. Lin, UCHL1 is a putative tumor suppressor in ovarian cancer cells and contributes to cisplatin resistance, J. Cancer. 4 (2013) 662–670, https://doi.org/10.7150/jca.6641.
[131] N. Panyain, A. Godinat, T. Lanyon-Hogg, S. Lachiondo-Ortega, E.J. Will, C. Soudy, M. Mondal, K. Mason, S. Elkhalifa, L.M. Smith, J.A. Harrigan, E.W. Tate, Discovery of a potent and selective covalent inhibitor and activity-based probe for the deubiquitylating enzyme UCHL1, with Antifibrotic activity, J. Am. Chem. Soc. 142 (2020) 12020–12026, https://doi.org/10.1021/jacs.0c04527.
[132] X. Han, Y.-L. Zhang, T. Fu, P.-B. Li, T. Cong, H.-H. Li, Blockage of UCHL1 activity attenuates cardiac remodeling in spontaneously hypertensive rats, Hypertens. Res. 43 (2020) 1089–1098, https://doi.org/10.1038/s41440-020-0486-1.
[133] X. Zheng, Q. Nie, J. Feng, X. Fan, Y. Jin, G. Chen, J. Du, Kidney-targeted baicalin-lysozyme conjugate ameliorates renal fibrosis in rats with diabetic nephropathy induced by streptozotocin, BMC Nephrol. 21 (2020) 174, https://doi.org/10.1186/s12882-020-01833-6.
[134] M. Kondo, E. Cubillo, K. Tobiume, T. Shirakihara, N. Fukuda, H. Suzuki, K. Shimizu, K. Takehara, A. Cano, M. Saitoh, K. Miyazono, A role for Id in the regulation of TGF-β-induced epithelial–mesenchymal transdifferentiation, Cell Death Differ. 11 (2004) 1092–1101, https://doi.org/10.1038/sj.cdd.4401467.
[135] J. Yang, M. Velikoff, M. Agarwal, S. Disayabutr, P.J. Wolters, K.K. Kim, Overexpression of inhibitor of DNA-binding 2 attenuates pulmonary fibrosis through regulation of c-Abl and twist, Am. J. Pathol. 185 (2015) 1001–1011, https://doi.org/10.1016/J.AJPATH.2014.12.008.
[136] L. Yin, M. Liu, W. Li, F. Wang, Y. Tang, C. Huang, Over-expression of inhibitor of differentiation 2 attenuates post-infarct cardiac fibrosis through inhibition of TGF-β1/Smad3/HIF-1α/IL-11 signaling pathway, Front. Pharmacol. 10 (2019) 1349, https://doi.org/10.3389/fphar.2019.01349.
[137] Y. Xiao, C. Peng, Y. Xiao, D. Liang, Z. Yuan, Z. Li, M. Shi, Y. Wang, F. Zhang, B. Guo, Oxymatrine Inhibits twist-mediated renal tubulointerstitial fibrosis by upregulating Id2 expression, Front. Physiol. 11 (2020) 599, https://doi.org/10.3389/fphys.2020.00599.
[138] M.S. Zeyada, N. Abdel-Rahman, A. El-Karef, S. Yahia, I.M. El-Sherbiny, L.A. Eissa, Niclosamide-loaded polymeric micelles ameliorate hepatocellular carcinoma in vivo through targeting Wnt and Notch pathways, Life Sci. 261 (2020), https://doi.org/10.1016/J.LFS.2020.118458 118458.
[139] C. Wang, X. Zhou, H. Xu, X. Shi, J. Zhao, M. Yang, L. Zhang, X. Jin, Y. Hu, X. Li, X. Xiao, M. Liao, Niclosamide inhibits cell growth and enhances drug sensitivity of hepatocellular carcinoma cells via STAT3 signaling pathway, J. Cancer. 9 (2018) 4150–4155, https://doi.org/10.7150/jca.26948.
[140] A.P. Lam, C.J. Gottardi, β-catenin signaling, Curr. Opin. Rheumatol. 23 (2011) 562–567, https://doi.org/10.1097/BOR.0b013e32834b3309.
[141] B. Hu, S.H. Phan, Notch in fibrosis and as a target of anti-fibrotic therapy, Pharmacol. Res. 108 (2016) 57–64, https://doi.org/10.1016/J.PHRS.2016.04.010.
[142] M. Che, S.-M. Kweon, J.-L. Teo, Y.-C. Yuan, L.G. Melstrom, R.T. Waldron, A. Lugea, R.A. Urrutia, S.J. Pandol, K.K.Y. Lai, Targeting the CBP/β-catenin interaction to suppress activation of cancer-promoting pancreatic stellate cells, Cancers (Basel). 12 (2020) 1476, https://doi.org/10.3390/cancers12061476.
[143] N. Sugiyama, M. Kohno, T. Yokoyama, Inhibition of the p38 MAPK pathway ameliorates renal fibrosis in an NPHP2 mouse model, Nephrol. Dial. Transplant. 27 (2012) 1351–1358, https://doi.org/10.1093/ndt/gfr550.
[144] M. Liu, J. Zhou, X. Liu, Y. Feng, W. Yang, F. Wu, O.K.-W. Cheung, H. Sun, X. Zeng, W. Tang, M.T.S. Mok, J. Wong, P.C. Yeung, P.B.S. Lai, Z. Chen, H. Jin, J. Chen, S.L. Chan, A.W.H. Chan, K.F. To, J.J.Y. Sung, M. Chen, A.S.-L. Cheng, Targeting monocyte-intrinsic enhancer reprogramming improves immunotherapy efficacy in hepatocellular carcinoma, Gut 69 (2020) 365–379, https://doi.org/10.1136/gutjnl-2018-317257.
[145] Y.J. Park, H.-T. An, J.-S. Park, O. Park, A.J. Duh, K. Kim, K.H. Chung, K.C. Lee, Y. Oh, S. Lee, Tyrosine kinase inhibitor neratinib attenuates liver fibrosis by targeting activated hepatic stellate cells, Sci. Rep. 10 (2020) 14756, https://doi.org/10.1038/s41598-020-71688-2.
[146] N. Lin, S. Chen, W. Pan, L. Xu, K. Hu, R. Xu, NP603, a novel and potent inhibitor of FGFR1 tyrosine kinase, inhibits hepatic stellate cell proliferation and ameliorates hepatic fibrosis in rats, Am. J. Physiol. Physiol. 301 (2011) C469–C477, https://doi.org/10.1152/ajpcell.00452.2010.
[147] D.M. Dolivo, S.A. Larson, T. Dominko, Fibroblast growth factor 2 as an antifibrotic: antagonism of myofibroblast differentiation and suppression of pro-fibrotic gene expression, Cytokine Growth Factor Rev. 38 (2017) 49–58, https://doi.org/10.1016/J.CYTOGFR.2017.09.003.
[148] D.M. Dolivo, S.A. Larson, T. Dominko, FGF2-mediated attenuation of myofibroblast activation is modulated by distinct MAPK signaling pathways in human dermal fibroblasts, J. Dermatol. Sci. 88 (2017) 339–348, https://doi.org/10.1016/J.JDERMSCI.2017.08.013.
[149] C. Le Tourneau, E. Raymond, S. Faivre, Sunitinib: a novel tyrosine kinase inhibitor. A brief review of its therapeutic potential in the treatment of renal carcinoma and gastrointestinal stromal tumors (GIST), Ther. Clin. Risk Manag. 3 (2007) 341–348, https://doi.org/10.2147/tcrm.2007.3.2.341.
[150] G. Aparicio-Gallego, M. Blanco, A. Figueroa, R. García-Campelo, M. Valladares-Ayerbes, E. Grande-Pulido, L. Antón-Aparicio, New insights into molecular mechanisms of sunitinib-associated side effects, Mol. Cancer Ther. 10 (2011) 2215–2223, https://doi.org/10.1158/1535-7163.MCT-10-1124.
[151] Y.E. Zhang, Non-smad signaling pathways of the TGF-β family, Cold Spring Harb Perspect. Biol. 9 (2017), https://doi.org/10.1101/cshperspect.a022129 a022129.
[152] K.-Y. Park, J. Kim, Cyclic pentapeptide cRGDfK enhances the inhibitory effect of sunitinib on TGF-β1-induced epithelial-to-mesenchymal transition in human non-small cell lung cancer cells, PLoS ONE 15 (2020), https://doi.org/10.1371/journal.pone.0232917 e0232917.

[153] H. Zhu, Q. Liu, L. Miao, S. Musetti, M. Huo, L. Huang, Remodeling the fibrotic tumor microenvironment of desmoplastic melanoma to facilitate vaccine immunotherapy, Nanoscale. 12 (2020) 3400–3410, https://doi.org/10.1039/C9NR09610H.
[154] G.C. Grosveld, γ-secretase inhibitors: Notch so bad, Nat. Med. 15 (2009) 20–21, https://doi.org/10.1038/nm0109-20.
[155] P.J. Real, V. Tosello, T. Palomero, M. Castillo, E. Hernando, E. de Stanchina, M.L. Sulis, K. Barnes, C. Sawai, I. Homminga, J. Meijerink, I. Aifantis, G. Basso, C. Cordon-Cardo, W. Ai, A. Ferrando, γ-secretase inhibitors reverse glucocorticoid resistance in T cell acute lymphoblastic leukemia, Nat. Med. 15 (2009) 50–58, https://doi.org/10.1038/nm.1900.
[156] L.R. Richter, Q. Wan, D. Wen, Y. Zhang, J. Yu, J. ku Kang, C. Zhu, E.L. McKinnon, Z. Gu, L. Qiang, U.B. Pajvani, Targeted Delivery of Notch Inhibitor Attenuates Obesity-Induced Glucose Intolerance and Liver Fibrosis, ACS Nano. 14 (2020) 6878–6886. DOI: DOI: 10.1021/acsnano.0c01007.
[157] Y. Yang, H. Wang, M. Kouadir, H. Song, F. Shi, Recent advances in the mechanisms of NLRP3 inflammasome activation and its inhibitors, Cell Death Dis. 10 (2019) 128, https://doi.org/10.1038/s41419-019-1413-8.
[158] I. Lasithiotaki, I. Giannarakis, E. Tsitoura, K.D. Samara, G.A. Margaritopoulos, C. Choulaki, E. Vasarmidi, N. Tzanakis, A. Voloudaki, P. Sidiropoulos, N.M. Siafakas, K.M. Antoniou, NLRP3 inflammasome expression in idiopathic pulmonary fibrosis and rheumatoid lung, Eur. Respir. J. 47 (2016) 910–918, https://doi.org/10.1183/13993003.00564-2015.
[159] E. De Nardo, Dominic; De Nardo, Christine M.; Latz, New Insights into Mechanisms Controlling the NLRP3 Inflammasome and Its Role in Lung Disease, Am. J. Pathol. 184 (2014) 42–54. DOI: 10.1016/J.AJPATH.2013.09.007.
[160] A.A. Pinar, T.E. Scott, B.M. Huuskes, F.E. Tapia Cáceres, B.K. Kemp-Harper, C.S. Samuel, Targeting the NLRP3 inflammasome to treat cardiovascular fibrosis, Pharmacol. Ther. 209 (2020) 107511. DOI: 10.1016/J.PHARMTHERA.2020.107511.
[161] A.A.A. Alyaseer, M.H.S. de Lima, T.T. Braga, The role of NLRP3 inflammasome activation in the epithelial to mesenchymal transition process during the fibrosis, Front. Immunol. 11 (2020) 883, https://doi.org/10.3389/fimmu.2020.00883.
[162] P. Gallego, B. Castejón-Vega, J.A. del Campo, M.D. Cordero, The absence of NLRP3-inflammasome modulates hepatic fibrosis progression, lipid metabolism, and inflammation in KO NLRP3 mice during aging, Cells 9 (2020) 2148, https://doi.org/10.3390/cells9102148.
[163] C. Hao, Z. Lu, Y. Zhao, Z. Chen, C. Shen, G. Ma, L. Chen, Overexpression of GATA4 enhances the antiapoptotic effect of exosomes secreted from cardiac colony-forming unit fibroblasts via miRNA221-mediated targeting of the PTEN/PI3K/AKT signaling pathway, Stem Cell Res. Ther. 11 (2020) 251, https://doi.org/10.1186/s13287-020-01759-8.
[164] E. Bisping, S. Ikeda, S.W. Kong, O. Tarnavski, N. Bodyak, J.R. McMullen, S. Rajagopal, J.K. Son, Q. Ma, Z. Springer, P.M. Kang, S. Izumo, W.T. Pu, Gata4 is required for maintenance of postnatal cardiac function and protection from pressure overload-induced heart failure, Proc. Natl. Acad. Sci. USA 103 (2006) 14471–14476, https://doi.org/10.1073/pnas.0602543103.
[165] J. Gao, B. Wei, T.M. de Assuncao, Z. Liu, X. Hu, S. Ibrahim, S.A. Cooper, S. Cao, V. H. Shah, E. Kostallari, Hepatic stellate cell autophagy inhibits extracellular vesicle release to attenuate liver fibrosis, J. Hepatol. 73 (2020) 1144–1154, https://doi.org/10.1016/J.JHEP.2020.04.044.
[166] S. Tomah, N. Alkhouri, O. Hamdy, Nonalcoholic fatty liver disease and type 2 diabetes: where do Diabetologists stand?, Clin. Diabetes Endocrinol. 6 (2020) 9, https://doi.org/10.1186/s40842-020-00097-1.
[167] A. Dehnad, W. Fan, J.X. Jiang, S.R. Fish, Y. Li, S. Das, G. Mozes, K.A. Wong, K.A. Olson, G.W. Charville, M. Ali, N.J. Török, AGER1 downregulation associates with fibrosis in nonalcoholic steatohepatitis and type 2 diabetes, J. Clin. Invest. 130 (2020) 4320–4330, https://doi.org/10.1172/JCI133051.
[168] Y. Watanabe, Y. Nagai, H. Honda, N. Okamoto, S. Yamamoto, T. Hamashima, Y. Ishii, M. Tanaka, T. Suganami, M. Sasahara, K. Miyake, K. Takatsu, Isoliquiritigenin attenuates adipose tissue inflammation in vitro and adipose tissue fibrosis through inhibition of innate immune responses in mice, Sci. Rep. 6 (2016) 23097, https://doi.org/10.1038/srep23097.
[169] X. Gu, Y. Shi, X. Chen, Z. Sun, W. Luo, X. Hu, G. Jin, S. You, Y. Qian, W. Wu, G. Liang, G. Wu, Z. Chen, X. Chen, Isoliquiritigenin attenuates diabetic cardiomyopathy via inhibition of hyperglycemia-induced inflammatory response and oxidative stress, Phytomedicine 78 (2020), https://doi.org/10.1016/J.PHYMED.2020.153319 153319.
[170] D.A. Abed, S. Lee, L. Hu, Discovery of disubstituted xylylene derivatives as small molecule direct inhibitors of Keap1-Nrf2 protein-protein interaction, Bioorg. Med. Chem. 28 (2020), https://doi.org/10.1016/J.BMC.2020.115343 115343.
[171] S. Pompili, R. Sferra, E. Gaudio, A. Viscido, G. Frieri, A. Vetuschi, G. Latella, Can Nrf2 modulate the development of intestinal fibrosis and cancer in inflammatory bowel disease?, Int. J. Mol. Sci. 20 (2019), https://doi.org/10.3390/ijms20164061.
[172] T. Yang, C. Heng, Y. Zhou, Y. Hu, S. Chen, H. Wang, H. Yang, Z. Jiang, S. Qian, Y. Wang, J. Wang, X. Zhu, L. Du, X. Yin, Q. Lu, Targeting mammalian serine/threonine-protein kinase 4 through Yes-associated protein/TEA domain transcription factor-mediated epithelial-mesenchymal transition ameliorates diabetic nephropathy orchestrated renal fibrosis, Metabolism. 108 (2020), https://doi.org/10.1016/J.METABOL.2020.154258 154258.
[173] D. Prakoso, M.J. De Blasio, M. Tate, H. Kiriazis, D.G. Donner, H. Qian, D. Nash, M. Deo, K.L. Weeks, L.J. Parry, P. Gregorevic, J.R. McMullen, R.H. Ritchie, Gene therapy targeting cardiac phosphoinositide 3-kinase (p110α) attenuates cardiac remodeling in type 2 diabetes, Am. J. Physiol. Circ. Physiol. 318 (2020) H840–H852, https://doi.org/10.1152/ajpheart.00632.2019.
[174] Z. Li, D. Paulin, P. Lacolley, D. Coletti, O. Agbulut, Vimentin as a target for the treatment of COVID-19, BMJ Open Respir Res. 7 (2020), https://doi.org/10.1136/bmjresp-2020-000623 e000623.
[175] J. Garcia-Revilla, T. Deierborg, J.L. Venero, A. Boza-Serrano, Hyperinflammation and fibrosis in severe COVID-19 patients: galectin-3, a target molecule to consider, Front. Immunol. 11 (2020) 2069, https://doi.org/10.3389/fimmu.2020.02069.
[176] S. Zhang, Y. Lu, C. Jiang, Inhibition of histone demethylase JMJD1C attenuates cardiac hypertrophy and fibrosis induced by angiotensin II, J. Recept. Signal Transduct. 40 (2020) 339–347, https://doi.org/10.1080/10799893.2020.1734819.
[177] Y.-C. Ren, Q. Zhao, Y. He, B. Li, Z. Wu, J. Dai, L. Wen, X. Wang, G. Hu, Legumain promotes fibrogenesis in chronic pancreatitis via activation of transforming growth factor β1, J. Mol. Med. 98 (2020) 863–874, https://doi.org/10.1007/s00109-020-01911-0.
[178] O. Zbodakova, K. Chalupsky, J. Tureckova, R. Sedlacek, Metalloproteinases in liver fibrosis: current insights, Met. Med. 4 (2017) 25–35, https://doi.org/10.2147/MNM.S124363.
[179] D. Guindolet, E.E. Gabison, Role of CD147 (EMMPRIN/Basigin) in tissue remodeling, Anat. Rec. 303 (2020) 1584–1589, https://doi.org/10.1002/ar.24089.
[180] A. Takawale, P. Zhang, V.B. Patel, X. Wang, G. Oudit, Z. Kassiri, Tissue inhibitor of matrix metalloproteinase-1 promotes myocardial fibrosis by mediating CD63–integrin β1 interaction, Hypertension 69 (2017) 1092–1103, https://doi.org/10.1161/HYPERTENSIONAHA.117.09045.
[181] V. Egea, S. Zahler, N. Rieth, P. Neth, T. Popp, K. Kehe, M. Jochum, C. Ries, Tissue inhibitor of metalloproteinase-1 (TIMP-1) regulates mesenchymal stem cells through let-7f microRNA and Wnt/β-catenin signaling, Proc. Natl. Acad. Sci. U. S. A. 109 (2012) E309–E316, https://doi.org/10.1073/pnas.1115083109.
[182] M. Wang, D. Zhao, G. Spinetti, J. Zhang, L.-Q. Jiang, G. Pintus, R. Monticone, E. G. Lakatta, Matrix metalloproteinase 2 activation of transforming growth factor-β1 (TGF-β1) and TGF-β1–Type II receptor signaling within the aged arterial wall, Arterioscler. Thromb. Vasc. Biol. 26 (2006) 1503–1509, https://doi.org/10.1161/01.ATV.0000225777.58488.f2.
[183] M. Tozzi, C.E. Sørensen, L. Magni, N.M. Christensen, R. Bouazzi, C.M. Buch, M. Stefanini, C. Duranti, A. Arcangeli, I. Novak, Proton pump inhibitors reduce pancreatic adenocarcinoma progression by selectively targeting H+, K+-ATPases in pancreatic cancer and stellate cells, Cancers (Basel). 12 (2020) 640, https://doi.org/10.3390/cancers12030640.
[184] Y.J. Li, X. Chen, T.K. Kwan, Y.W. Loh, J. Singer, Y. Liu, J. Ma, J. Tan, L. Macia, C.R. Mackay, S.J. Chadban, H. Wu, Dietary fiber protects against diabetic nephropathy through short-chain fatty acid-mediated activation of G protein-coupled receptors GPR43 and GPR109A, J. Am. Soc. Nephrol. 31 (2020) 1267–1281, https://doi.org/10.1681/ASN.2019101029.
[185] L. Macia, J. Tan, A.T. Vieira, K. Leach, D. Stanley, S. Luong, M. Maruya, C. Ian McKenzie, A. Hijikata, C. Wong, L. Binge, A.N. Thorburn, N. Chevalier, C. Ang, E. Marino, R. Robert, S. Offermanns, M.M. Teixeira, R.J. Moore, R.A. Flavell, S. Fagarasan, C.R. Mackay, Metabolite-sensing receptors GPR43 and GPR109A facilitate dietary fibre-induced gut homeostasis through regulation of the inflammasome, Nat. Commun. 6 (2015) 6734, https://doi.org/10.1038/ncomms7734.
[186] L. Zhang, F. Wang, J. Wang, Y. Wang, Y. Fang, Intestinal fatty acid-binding protein mediates atherosclerotic progress through increasing intestinal inflammation and permeability, J. Cell. Mol. Med. 24 (2020) 5205–5212, https://doi.org/10.1111/jcmm.15173.
[187] W. Zhang, Y. Zhang, T. Tu, S. Schmull, Y. Han, W. Wang, H. Li, Dual inhibition of HDAC and tyrosine kinase signaling pathways with CUDC-907 attenuates TGFβ1 induced lung and tumor fibrosis, Cell Death Dis. 11 (2020) 765, https://doi.org/10.1038/s41419-020-02916-w.
[188] Z. Li, Y. Wang, Y. Shen, C. Qian, D. Oupicky, M. Sun, Targeting pulmonary tumor microenvironment with CXCR4-inhibiting nanocomplex to enhance anti–PD-L1 immunotherapy, Sci. Adv. 6 (2020) eaaz9240, https://doi.org/10.1126/sciadv.aaz9240.
[189] S. Jin, J. Li, M. Barati, S. Rane, Q. Lin, Y. Tan, Z. Zheng, L. Cai, M.J. Rane, Loss of NF-E2 expression contributes to the induction of profibrotic signaling in diabetic kidneys, Life Sci. 254 (2020), https://doi.org/10.1016/J.LFS.2020.117783 117783.
[190] Q. Shi, D.-Y. Lee, D. Féliers, H.E. Abboud, M.A. Bhat, Y. Gorin, Interplay between RNA-binding protein HuR and Nox4 as a novel therapeutic target in diabetic kidney disease, Mol. Metab. 36 (2020), https://doi.org/10.1016/J.MOLMET.2020.02.011 100968.
[191] F. Xu, M. Guo, W. Huang, L. Feng, J. Zhu, K. Luo, J. Gao, B. Zheng, L.-D. Kong, T. Pang, X. Wu, Q. Xu, Annexin A5 regulates hepatic macrophage polarization via directly targeting PKM2 and ameliorates NASH, Redox Biol. 36 (2020), https://doi.org/10.1016/J.REDOX.2020.101634 101634.
[192] A.I. Azad, A. Krishnan, L. Troop, Y. Li, T. Katsumi, K. Pavelko, E. Kostallari, M.E. Guicciardi, G.J. Gores, Targeted apoptosis of ductular reactive cells reduces hepatic fibrosis in a mouse model of cholestasis, Hepatology 72 (2020) 1013–1028, https://doi.org/10.1002/hep.31211.
[193] B.E. Schwartz, V. Rajagopal, C. Smith, E. Cohick, G. Whissell, M. Gamboa, R. Pai, A. Sigova, I. Grossman, D. Bumcrot, K. Sasidharan, S. Romeo, A. Sehgal, P. Pingitore, Discovery and targeting of the signaling controls of PNPLA3 to effectively reduce transcription, Expression, and Function in Pre-Clinical

NAFLD/NASH Settings, Cells. 9 (2020) 2247, https://doi.org/10.3390/cells9102247.
[194] S. Tassini, E. Langron, L. Delang, C. Mirabelli, K. Lanko, E. Crespan, M. Kissova, G. Tagliavini, G. Fontò, S. Bertoni, S. Palese, C. Giorgio, F. Ravanetti, L. Ragionieri, C. Zamperini, A. Mancini, E. Dreassi, G. Maga, P. Vergani, J. Neyts, M. Radi, Multitarget CFTR modulators endowed with multiple beneficial side effects for cystic fibrosis patients: toward a simplified therapeutic approach, J. Med. Chem. 62 (2019) 10833–10847, https://doi.org/10.1021/acs.jmedchem.9b01416.
[195] H. England, H.R. Summersgill, M.E. Edye, N.J. Rothwell, D. Brough, Release of interleukin-1α or interleukin-1β depends on mechanism of cell death, J. Biol. Chem. 289 (2014) 15942–15950, https://doi.org/10.1074/jbc.M114.557561.
[196] S.T. Montgomery, D.L. Frey, M.A. Mall, S.M. Stick, A. Kicic, A. CF, Rhinovirus Infection Is Associated With Airway Epithelial Cell Necrosis and Inflammation via Interleukin-1 in Young Children With Cystic Fibrosis, Front. Immunol. 11 (2020) 596. DOI: 10.3389/fimmu.2020.00596.
[197] F. Nanto-Hara, Y. Kanemitsu, S. Fukuda, K. Kikuchi, K. Asaji, D. Saigusa, T. Iwasaki, H.-J. Ho, E. Mishima, T. Suzuki, C. Suzuki, T. Tsukimi, T. Matsuhashi, Y. Oikawa, Y. Akiyama, S. Kure, Y. Owada, Y. Tomioka, T. Soga, S. Ito, T. Abe, The guanylate cyclase C agonist linaclotide ameliorates the gut–cardio–renal axis in an adenine-induced mouse model of chronic kidney disease, Nephrol. Dial. Transplant. 35 (2019) 250–264, https://doi.org/10.1093/ndt/gfz126.
[198] M. Li, Y. Zhou, L. Zuo, D. Nie, X. Li, Dietary fiber regulates intestinal flora and suppresses liver and systemic inflammation to alleviate liver fibrosis in mice, Nutrition. 81 (2021), https://doi.org/10.1016/J.NUT.2020.110959 110959.
[199] X. Que, M.-Y. Hung, C. Yeang, A. Gonen, T.A. Prohaska, X. Sun, C. Diehl, A. Määttä, D.E. Gaddis, K. Bowden, J. Pattison, J.G. MacDonald, S. Ylä-Herttuala, P.L. Mellon, C.C. Hedrick, K. Ley, Y.I. Miller, C.K. Glass, K.L. Peterson, C.J. Binder, S. Tsimikas, J.L. Witztum, Oxidized phospholipids are proinflammatory and proatherogenic in hypercholesterolaemic mice, Nature 558 (2018) 301–306, https://doi.org/10.1038/s41586-018-0198-8.
[200] X. Sun, J.S. Seidman, P. Zhao, T.D. Troutman, N.J. Spann, X. Que, F. Zhou, Z. Liao, M. Pasillas, X. Yang, J.A. Magida, T. Kisseleva, D.A. Brenner, M. Downes, R. M. Evans, A.R. Saltiel, S. Tsimikas, C.K. Glass, J.L. Witztum, Neutralization of oxidized phospholipids ameliorates non-alcoholic steatohepatitis, Cell Metab. 31 (2020) 189–206.e8, https://doi.org/10.1016/J.CMET.2019.10.014.
[201] A.E. Vendrov, M.D. Stevenson, S. Alahari, H. Pan, S.A. Wickline, N.R. Madamanchi, M.S. Runge, Attenuated superoxide dismutase 2 activity induces atherosclerotic plaque instability during aging in hyperlipidemic mice, J. Am. Heart Assoc. 6 (2017), https://doi.org/10.1161/JAHA.117.006775.
[202] S. Holm Nielsen, L. Jonasson, K. Kalogeropoulos, M.A. Karsdal, A.L. Reese-Petersen, U. Keller, F. Genovese, J. Nilsson, I. Goncalves, Exploring the role of extracellular matrix proteins to develop biomarkers of plaque vulnerability and outcome, J. Intern. Med. 287 (2020) 493–513. DOI: 10.1111/joim.13034.
[203] P.K. Shah, Z.S. Galis, Matrix metalloproteinase hypothesis of plaque rupture, Circulation 104 (2001) 1878–1880, https://doi.org/10.1161/circ.104.16.1878.
[204] S. Shrishrimal, A. Chatterjee, E.A. Kosmacek, P.J. Davis, J.T. McDonald, R.E. Oberley-Deegan, Manganese porphyrin, MnTE-2-PyP, treatment protects the prostate from radiation-induced fibrosis (RIF) by activating the NRF2 signaling pathway and enhancing SOD2 and sirtuin activity, Free Radic. Biol. Med. 152 (2020) 255–270, https://doi.org/10.1016/J.FREERADBIOMED.2020.03.014.
[205] L. Richeldi, H.R.H.R. Davies, P. Spagnolo, F. Luppi, Corticosteroids for idiopathic pulmonary fibrosis, Cochrane Database Syst. Rev. (2003), https://doi.org/10.1002/14651858.CD002880.
[206] H.R.H.R. Davies, L. Richeldi, E.H. Walters, Immunomodulatory agents for idiopathic pulmonary fibrosis, in: H.R.H.R. Davies (Ed.), Cochrane Database Syst. Rev., John Wiley & Sons, Ltd, Chichester, UK, 2003. DOI: 10.1002/14651858.CD003134.
[207] T.E. King, W.Z. Bradford, S. Castro-Bernardini, E.A. Fagan, I. Glaspole, M.K. Glassberg, E. Gorina, P.M. Hopkins, D. Kardatzke, L. Lancaster, D.J. Lederer, S. D. Nathan, C.A. Pereira, S.A. Sahn, R. Sussman, J.J. Swigris, P.W. Noble, A phase 3 trial of pirfenidone in patients with idiopathic pulmonary fibrosis, N. Engl. J. Med. 370 (2014) 2083–2092, https://doi.org/10.1056/NEJMoa1402582.
[208] H.V. Woodcock, J.D. Eley, D. Guillotin, M. Platé, C.B. Nanthakumar, M. Martufi, S. Peace, G. Joberty, D. Poeckel, R.B. Good, A.R. Taylor, N. Zinn, M. Redding, E.J. Forty, R.E. Hynds, C. Swanton, M. Karsdal, T.M. Maher, A. Fisher, G. Bergamini, R.P. Marshall, A.D. Blanchard, P.F. Mercer, R.C. Chambers, The mTORC1/4E-BP1 axis represents a critical signaling node during fibrogenesis, Nat. Commun. 10 (2019) 6, https://doi.org/10.1038/s41467-018-07858-8.
[209] L. Wollin, E. Wex, A. Pautsch, G. Schnapp, K.E. Hostettler, S. Stowasser, M. Kolb, Mode of action of nintedanib in the treatment of idiopathic pulmonary fibrosis, Eur. Respir. J. 45 (2015) 1434–1445, https://doi.org/10.1183/09031936.00174914.
[210] C. Sheridan, Drugmakers turn sights on scarred lungs, Nat. Biotechnol. 38 (2020) 118–120, https://doi.org/10.1038/s41587-020-0415-5.
[211] L.A. Murray, Q. Chen, M.S. Kramer, D.P. Hesson, R.L. Argentieri, X. Peng, M. Gulati, R.J. Homer, T. Russell, N. van Rooijen, J.A. Elias, C.M. Hogaboam, E.L. Herzog, TGF-beta driven lung fibrosis is macrophage dependent and blocked by Serum amyloid P, Int. J. Biochem. Cell Biol. 43 (2011) 154–162, https://doi.org/10.1016/J.BIOCEL.2010.10.013.
[212] N. Nakagawa, L. Barron, I.G. Gomez, B.G. Johnson, A.M. Roach, S. Kameoka, R. M. Jack, M.L. Lupher, S.A. Gharib, J.S. Duffield, Pentraxin-2 suppresses c-Jun/AP-1 signaling to inhibit progressive fibrotic disease, JCI Insight. 1 (2016), https://doi.org/10.1172/JCI.INSIGHT.87446.
[213] D. Pilling, R.H. Gomer, Persistent Lung Inflammation and Fibrosis in Serum Amyloid P Component (Apcs-/-) Knockout Mice, PLoS ONE 9 (2014), https://doi.org/10.1371/journal.pone.0093730 e93730.
[214] G. Raghu, B. van den Blink, M.J. Hamblin, A.W. Brown, J.A. Golden, L.A. Ho, M. S. Wijsenbeek, M. Vasakova, A. Pesci, D.E. Antin-Ozerkis, K.C. Meyer, M. Kreuter, D. Moran, H. Santin-Janin, F. Aubin, G.-J. Mulder, R. Gupta, L. Richeldi, Long-term treatment with recombinant human pentraxin 2 protein in patients with idiopathic pulmonary fibrosis: an open-label extension study, Lancet Respir. Med. 7 (2019) 657–664, https://doi.org/10.1016/S2213-2600(19)30172-9.
[215] A. Tzouvelekis, V. Tzilas, K.M. Antoniou, D. Bouros, Human pentraxin 2 protein treatment for IPF, Lancet Respir. Med. 7 (2019) 640–641, https://doi.org/10.1016/S2213-2600(19)30173-0.
[216] A.M. Tager, P. LaCamera, B.S. Shea, G.S. Campanella, M. Selman, Z. Zhao, V. Polosukhin, J. Wain, B.A. Karimi-Shah, N.D. Kim, W.K. Hart, A. Pardo, T.S. Blackwell, Y. Xu, J. Chun, A.D. Luster, The lysophosphatidic acid receptor LPA1 links pulmonary fibrosis to lung injury by mediating fibroblast recruitment and vascular leak, Nat. Med. 14 (2008) 45–54, https://doi.org/10.1038/nm1685.
[217] T.M. Maher, E.M. van der Aar, O. Van de Steen, L. Allamassey, J. Desrivot, S. Dupont, L. Fagard, P. Ford, A. Fieuw, W. Wuyts, Safety, tolerability, pharmacokinetics, and pharmacodynamics of GLPG1690, a novel autotaxin inhibitor, to treat idiopathic pulmonary fibrosis (FLORA): a phase 2a randomised placebo-controlled trial, Lancet Respir. Med. 6 (2018) 627–635, https://doi.org/10.1016/S2213-2600(18)30181-4.
[218] A.C. MacKinnon, M.A. Gibbons, S.L. Farnworth, H. Leffler, U.J. Nilsson, T. Delaine, A.J. Simpson, S.J. Forbes, N. Hirani, J. Gauldie, T. Sethi, Regulation of Transforming Growth Factor-β1–driven Lung Fibrosis by Galectin-3, Am. J. Respir. Crit. Care Med. 185 (2012) 537–546, https://doi.org/10.1164/rccm.201106-0965OC.
[219] N. Hirani, A.C. MacKinnon, L. Nicol, P. Ford, H. Schambye, A. Pedersen, U.J. Nilsson, H. Leffler, T. Sethi, S. Tantawi, L. Gavelle, R.J. Slack, R. Mills, U. Karmakar, D. Humphries, F. Zetterberg, L. Keeling, L. Paul, P.L. Molyneaux, F. Li, W. Funston, I.A. Forrest, A.J. Simpson, M.A. Gibbons, T.M. Maher, Target-inhibition of galectin-3 by inhaled TD139 in patients with idiopathic pulmonary fibrosis, Eur. Respir. J. (2020), https://doi.org/10.1183/13993003.02559-2020.
[220] P.M. George, A.U. Wells, R.G. Jenkins, Pulmonary fibrosis and COVID-19: the potential role for antifibrotic therapy, Lancet Respir. Med. 8 (2020) 807–815, https://doi.org/10.1016/S2213-2600(20)30225-3.
[221] A. Alshangiti, G. Chandhoke, P.M. Ellis, Antiangiogenic therapies in non-small-cell lung cancer, Curr. Oncol. 25 (2018) S45–S58, https://doi.org/10.3747/co.25.3747.
[222] M. Reck, R. Kaiser, A. Mellemgaard, J.-Y. Douillard, S. Orlov, M. Krzakowski, J. von Pawel, M. Gottfried, I. Bondarenko, M. Liao, C.-N. Gann, J. Barrueco, B. Gaschler-Markefski, S. Novello, Docetaxel plus nintedanib versus docetaxel plus placebo in patients with previously treated non-small-cell lung cancer (LUME-Lung 1): a phase 3, double-blind, randomised controlled trial, Lancet Oncol. 15 (2014) 143–155, https://doi.org/10.1016/S1470-2045(13)70586-2.
[223] M. Gabasa, R. Ikemori, F. Hilberg, N. Reguart, J. Alcaraz, Nintedanib selectively inhibits the activation and tumour-promoting effects of fibroblasts from lung adenocarcinoma patients, Br. J. Cancer. 117 (2017) 1128–1138, https://doi.org/10.1038/bjc.2017.270.
[224] R. Ikemori, M. Gabasa, P. Duch, M. Vizoso, P. Bragado, M. Arshakyan, I.-C. Luis, A. Marín, S. Morán, M. Castro, G. Fuster, S. Gea-Sorli, T. Jauset, L. Soucek, L.M. Montuenga, M. Esteller, E. Monsó, V.I. Peinado, P. Gascon, C. Fillat, F. Hilberg, N. Reguart, J. Alcaraz, Epigenetic *SMAD3* repression in tumor-associated fibroblasts impairs fibrosis and response to the antifibrotic drug nintedanib in lung squamous cell carcinoma, Cancer Res. 80 (2020) 276–290, https://doi.org/10.1158/0008-5472.CAN-19-0637.
[225] H. Taghizadeh, L. Müllauer, R.M. Mader, M. Schindl, G.W. Prager, Applied precision medicine in metastatic pancreatic ductal adenocarcinoma., Ther. Adv. Med. Oncol. 12 (2020) 1758835920938611. DOI: 10.1177/1758835920938611.
[226] L. Knuppel, Y. Ishikawa, M. Aichler, K. Heinzelmann, R. Hatz, J. Behr, A. Walch, H.P. Bachinger, O. Eickelberg, C.A. Staab-Weijnitz, A novel antifibrotic mechanism of nintedanib and pirfenidone inhibition of collagen fibril assembly, Am. J. Respir. Cell Mol. Biol. 57 (2017) 77–90, https://doi.org/10.1165/rcmb.2016-0217OC.
[227] J. Huang, C. Beyer, K. Palumbo-Zerr, Y. Zhang, A. Ramming, A. Distler, K. Gelse, O. Distler, G. Schett, L. Wollin, J.H.W. Distler, Nintedanib inhibits fibroblast activation and ameliorates fibrosis in preclinical models of systemic sclerosis, Ann. Rheum. Dis. 75 (2016) 883–890, https://doi.org/10.1136/annrheumdis-2014-207109.
[228] E. Ripley, A. Hirsch, Fifteen years of losartan: what have we learned about losartan that can benefit chronic kidney disease patients?, Int. J. Nephrol. Renovasc. Dis. 3 (2010) 93–98, https://doi.org/10.2147/ijnrd.s7038.
[229] J.L. Miguel-Carrasco, J. Beaumont, G. San José, M.U. Moreno, B. López, A. González, G. Zalba, J. Díez, A. Fortuño, S. Ravassa, Mechanisms underlying the cardiac antifibrotic effects of losartan metabolites, Sci. Rep. 7 (2017) 41865, https://doi.org/10.1038/srep41865.
[230] Y. Zhao, J. Cao, A. Melamed, M. Worley, A. Gockley, D. Jones, H.T. Nia, Y. Zhang, T. Stylianopoulos, A.S. Kumar, F. Mpekris, M. Datta, Y. Sun, L. Wu, X. Gao, O. Yeku, M.G. Del Carmen, D.R. Spriggs, R.K. Jain, L. Xu, M.G. del Carmen, D.R. Spriggs, R.K. Jain, L. Xu, Losartan treatment enhances chemotherapy efficacy and reduces ascites in ovarian cancer models by normalizing the tumor

stroma, 116 (2019) 2210–2219. https://www.pnas.org/content/116/6/2210.long (accessed December 28, 2020).
[231] J. Colmenero, R. Bataller, P. Sancho-Bru, M. Domínguez, M. Moreno, X. Forns, M. Bruguera, V. Arroyo, D.A. Brenner, P. Ginès, Effects of losartan on hepatic expression of nonphagocytic NADPH oxidase and fibrogenic genes in patients with chronic hepatitis C, Am. J. Physiol. Liver Physiol. 297 (2009) G726–G734, https://doi.org/10.1152/ajpgi.00162.2009.
[232] J.E. Murphy, J.Y. Wo, D.P. Ryan, J.W. Clark, W. Jiang, B.Y. Yeap, L.C. Drapek, L. Ly, C.V. Baglini, L.S. Blaszkowsky, C.R. Ferrone, A.R. Parikh, C.D. Weekes, R.D. Nipp, E.L. Kwak, J.N. Allen, R.B. Corcoran, D.T. Ting, J.E. Faris, A.X. Zhu, L. Goyal, D.L. Berger, M. Qadan, K.D. Lillemoe, N. Talele, R.K. Jain, T.F. Delaney, D.G. Duda, Y. Boucher, C. Fernández-Del Castillo, T.S. Hong, Total neoadjuvant therapy with FOLFIRINOX in combination with losartan followed by chemoradiotherapy for locally advanced pancreatic cancer: a phase 2 clinical trial, JAMA Oncol. 5 (2019) 1020–1027, https://doi.org/10.1001/jamaoncol.2019.0892.
[233] R.G. Iannitti, V. Napolioni, V. Oikonomou, A. De Luca, C. Galosi, M. Pariano, C. Massi-Benedetti, M. Borghi, M. Puccetti, V. Lucidi, C. Colombo, E. Fiscarelli, C. Lass-Flörl, F. Majo, L. Cariani, M. Russo, L. Porcaro, G. Ricciotti, H. Ellemunter, L. Ratclif, F.M. De Benedictis, V.N. Talesa, C.A. Dinarello, F.L. van de Veerdonk, L. Romani, IL-1 receptor antagonist ameliorates inflammasome-dependent inflammation in murine and human cystic fibrosis, Nat. Commun. 7 (2016) 10791, https://doi.org/10.1038/ncomms10791.
[234] T. Huet, H. Beaussier, O. Voisin, S. Jouveshomme, G. Dauriat, I. Lazareth, E. Sacco, J.-M. Naccache, Y. Bézie, S. Laplanche, A. Le Berre, J. Le Pavec, S. Salmeron, J. Emmerich, J.-J. Mourad, G. Chatellier, G. Hayem, Anakinra for severe forms of COVID-19: a cohort study, Lancet Rheumatol. 2 (2020) e393–e400, https://doi.org/10.1016/S2665-9913(20)30164-8.
[235] K. Ford, C.J. Hanley, M. Mellone, C. Szyndralewiez, F. Heitz, P. Wiesel, O. Wood, M. Machado, M.-A. Lopez, A.-P. Ganesan, C. Wang, A. Chakravarthy, T. R. Fenton, E.V. King, P. Vijayanand, C.H. Ottensmeier, A. Al-Shamkhani, N. Savelyeva, G.J. Thomas, NOX4 inhibition potentiates immunotherapy by overcoming cancer-associated fibroblast-mediated CD8 T-cell exclusion from tumors, Cancer Res. 80 (2020) 1846–1860, https://doi.org/10.1158/0008-5472.CAN-19-3158.
[236] G. Chen, H. Chen, C. Wang, Y. Peng, L. Sun, H. Liu, F. Liu, Rapamycin Ameliorates Kidney Fibrosis by Inhibiting the Activation of mTOR Signaling in Interstitial Macrophages and Myofibroblasts, PLoS ONE 7 (2012), https://doi.org/10.1371/journal.pone.0033626 e33626.
[237] W. Chang, K. Wei, L. Ho, G.J. Berry, S.S. Jacobs, C.H. Chang, G.D. Rosen, A critical role for the mTORC2 pathway in lung fibrosis, PLoS ONE 9 (2014), https://doi.org/10.1371/journal.pone.0106155.
[238] A.M. Sofias, M. Dunne, G. Storm, C. Allen, The battle of "nano" paclitaxel, Adv. Drug Deliv. Rev. 122 (2017) 20–30, https://doi.org/10.1016/J.ADDR.2017.02.003.
[239] A.C. Anselmo, S. Mitragotri, Nanoparticles in the clinic: An update, Bioeng. Transl. Med. 4 (2019), https://doi.org/10.1002/btm2.10143 e10143.
[240] M.J. Mitchell, M.M. Billingsley, R.M. Haley, M.E. Wechseler, N.A. Peppas, R. Langer, Engineering precision nanoparticles for drug delivery, Nat. Rev. Drug Discov. (2020).
[241] R. van der Meel, E. Sulheim, Y. Shi, F. Kiessling, W.J.M. Mulder, T. Lammers, Smart cancer nanomedicine, Nat. Nanotechnol. 14 (2019) 1007–1017, https://doi.org/10.1038/s41565-019-0567-y.
[242] X. Bai, G. Su, S. Zhai, Recent advances in nanomedicine for the diagnosis and therapy of liver fibrosis, Nanomaterials. 10 (2020) 1945, https://doi.org/10.3390/nano10101945.
[243] X. Han, Y. Xu, M. Geranpayehvaghei, G.J. Anderson, Y. Li, G. Nie, Emerging nanomedicines for anti-stromal therapy against desmoplastic tumors, Biomaterials 232 (2020), https://doi.org/10.1016/j.biomaterials.2019.119745 119745.
[244] P. Chen, X. Zhang, A. Venosa, I.H. Lee, D. Myers, J.A. Holloway, R.K. Prud'homme, D. Gao, Z. Szekely, J.D. Laskin, D.L. Laskin, P.J. Sinko, A Novel Bivalent Mannosylated Targeting Ligand Displayed on Nanoparticles Selectively Targets Anti-Inflammatory M2 Macrophages, Pharmaceutics. 12 (2020) 243. DOI: 10.3390/pharmaceutics12030243.
[245] I.S. Meyer, C.C. Goetzke, M. Kespohl, M. Sauter, A. Heuser, V. Eckstein, H.P. Vornlocher, D.G. Anderson, J. Haas, B. Meder, H.A. Katus, K. Klingel, A. Beling, F. Leuschner, Silencing the CSF-1 axis using nanoparticle encapsulated siRNA mitigates viral and autoimmune myocarditis, Front. Immunol. 9 (2018), https://doi.org/10.3389/fimmu.2018.02303.
[246] A.D. Abdel-Mageid, M.E.S. Abou-Salem, N.M.H.A. Salaam, H.A.S. El-Garhy, The potential effect of garlic extract and curcumin nanoparticles against complication accompanied with experimentally induced diabetes in rats, Phytomedicine 43 (2018) 126–134, https://doi.org/10.1016/j.phymed.2018.04.039.
[247] K. Manna, S. Mishra, M. Saha, S. Mahapatra, C. Saha, G. Yenge, N. Gaikwad, R. Pal, D. Oulkar, K. Banerjee, K. Das Saha, Amelioration of diabetic nephropathy using pomegranate peel extract-stabilized gold nanoparticles: assessment of NF-κB and Nrf2 signaling system , Int. J. Nanomedicine. Volume 14 (2019) 1753–1777. DOI: 10.2147/IJN.S176013.
[248] X. Yang, Design and optimization of crocetin loaded PLGA nanoparticles against diabetic nephropathy via suppression of inflammatory biomarkers: a formulation approach to preclinical study, Drug Deliv. 26 (2019) 849–859, https://doi.org/10.1080/10717544.2019.1642417.
[249] A. Zinger, L. Koren, O. Adir, M. Poley, M. Alyan, Z. Yaari, N. Noor, N. Krinsky, A. Simon, H. Gibori, M. Krayem, Y. Mumblat, S. Kasten, S. Ofir, E. Fridman, N. Milman, M.M. Lübtow, L. Liba, J. Shklover, J. Shainsky-Roitman, Y. Binenbaum, D. Hershkovitz, Z. Gil, T. Dvir, R. Luxenhofer, R. Satchi-Fainaro, A. Schroeder, Collagenase nanoparticles enhance the penetration of drugs into pancreatic tumors, ACS Nano 13 (2019) 11008–11021, https://doi.org/10.1021/acsnano.9b02395.
[250] S. El-Safy, S.N. Tammam, M. Abdel-Halim, M.E. Ali, J. Youshia, M.A. Shetab Boushehri, A. Lamprecht, S. Mansour, Collagenase loaded chitosan nanoparticles for digestion of the collagenous scar in liver fibrosis: The effect of chitosan intrinsic collagen binding on the success of targeting, Eur. J. Pharm. Biopharm. 148 (2020) 54–66, https://doi.org/10.1016/j.ejpb.2020.01.003.
[251] M.R. Villegas, A. Baeza, A. Usategui, P.L. Ortiz-Romero, J.L. Pablos, M. Vallet-Regí, Collagenase nanocapsules: An approach to fibrosis treatment, Acta Biomater. 74 (2018) 430–438, https://doi.org/10.1016/J.ACTBIO.2018.05.007.
[252] J. Kroon, J.T. Buijs, G. van der Horst, H. Cheung, M. van der Mark, L. van Bloois, L.Y. Rizzo, T. Lammers, R.C. Pelger, G. Storm, G. van der Pluijm, J.M. Metselaar, Liposomal delivery of dexamethasone attenuates prostate cancer bone metastatic tumor growth In Vivo, Prostate 75 (2015) 815–824, https://doi.org/10.1002/pros.22963.
[253] A.K. Deshantri, M.H. Fens, R.W.J. Ruiter, J.M. Metselaar, G. Storm, L. van Bloois, A. Varela-Moreira, S.N. Mandhane, T. Mutis, A.C.M. Martens, R.W.J. Groen, R. M. Schiffelers, Liposomal dexamethasone inhibits tumor growth in an advanced human-mouse hybrid model of multiple myeloma, J. Control. Release. 296 (2019) 232–240, https://doi.org/10.1016/J.JCONREL.2019.01.028.
[254] L. Quan, Y. Zhang, B.J. Crielaard, A. Dusad, S.M. Lele, C.J.F. Rijcken, J.M. Metselaar, H. Kostková, T. Etrych, K. Ulbrich, F. Kiessling, T.R. Mikuls, W.E. Hennink, G. Storm, T. Lammers, D. Wang, Nanomedicines for inflammatory arthritis: head-to-head comparison of glucocorticoid-containing polymers, micelles, and liposomes, ACS Nano. 8 (2014) 458–466, https://doi.org/10.1021/nn4048205.
[255] M. Banciu, J.M. Metselaar, R.M. Schiffelers, G. Storm, Liposomal glucocorticoids as tumor-targeted anti-angiogenic nanomedicine in B16 melanoma-bearing mice, J. Steroid Biochem. Mol. Biol. 111 (2008) 101–110, https://doi.org/10.1016/J.JSBMB.2008.05.004.
[256] J.M. van den Hoven, W. Hofkens, M.H.M. Wauben, J.P.A. Wagenaar-Hilbers, J. H. Beijnen, B. Nuijen, J.M. Metselaar, G. Storm, Optimizing the therapeutic index of liposomal glucocorticoids in experimental arthritis, Int. J. Pharm. 416 (2011) 471–477, https://doi.org/10.1016/J.IJPHARM.2011.03.025.
[257] J.M. Metselaar, M.H.M. Wauben, J.P.A. Wagenaar-Hilbers, O.C. Boerman, G. Storm, Complete remission of experimental arthritis by joint targeting of glucocorticoids with long-circulating liposomes, Arthritis Rheum. 48 (2003) 2059–2066, https://doi.org/10.1002/art.11140.
[258] X. Chen, Y. Zhang, P. Zhao, Y. Chen, Y. Zhou, S. Wang, L. Yin, Preparation and evaluation of PEGylated asiatic acid nanostructured lipid carriers on anti-fibrosis effects, Drug Dev. Ind. Pharm. 46 (2020) 57–69, https://doi.org/10.1080/03639045.2019.1701002.
[259] Y. Wu, Y. Wu, I.-F. Chen, Y.-L. Wu, C. Chuang, H. Huang, S. Kuo, Reparative effects of astaxanthin-hyaluronan nanoaggregates against retrorsine-CCl4-induced liver fibrosis and necrosis, Molecules 23 (2018) 726, https://doi.org/10.3390/molecules23040726.
[260] L. Zhang, H. Su, Y. Liu, N. Pang, J. Li, X.R. Qi, Enhancing solid tumor therapy with sequential delivery of dexamethasone and docetaxel engineered in a single carrier to overcome stromal resistance to drug delivery, J. Control. Release. 294 (2019) 1–16, https://doi.org/10.1016/j.jconrel.2018.12.004.
[261] M. Wang, M. Zhang, L. Fu, J. Lin, X. Zhou, P. Zhou, P. Huang, H. Hu, Y. Han, Liver-targeted delivery of TSG-6 by calcium phosphate nanoparticles for the management of liver fibrosis, Theranostics. 10 (2020) 36–49, https://doi.org/10.7150/thno.37301.
[262] D.W. Kurniawan, R. Booijink, L. Pater, I. Wols, A. Vrynas, G. Storm, J. Prakash, R. Bansal, Fibroblast growth factor 2 conjugated superparamagnetic iron oxide nanoparticles (FGF2-SPIONs) ameliorate hepatic stellate cells activation in vitro and acute liver injury in vivo, J. Control. Release. 328 (2020) 640–652, https://doi.org/10.1016/j.jconrel.2020.09.041.
[263] D.F. Mardhian, G. Storm, R. Bansal, J. Prakash, Nano-targeted relaxin impairs fibrosis and tumor growth in pancreatic cancer and improves the efficacy of gemcitabine in vivo, J. Control. Release. 290 (2018) 1–10, https://doi.org/10.1016/j.jconrel.2018.09.031.
[264] M. Hu, Y. Wang, L. Xu, S. An, Y. Tang, X. Zhou, J. Li, R. Liu, L. Huang, Relaxin gene delivery mitigates liver metastasis and synergizes with check point therapy, Nat. Commun. 10 (2019) 2993.
[265] C.H. Liu, G.J. Chern, F.F. Hsu, K.W. Huang, Y.C. Sung, H.C. Huang, J.T. Qiu, S.K. Wang, C.C. Lin, C.H. Wu, H.C. Wu, J.Y. Liu, Y. Chen, A multifunctional nanocarrier for efficient TRAIL-based gene therapy against hepatocellular carcinoma with desmoplasia in mice, Hepatology 67 (2018) 899–913, https://doi.org/10.1002/hep.29513.
[266] M.A. Subhan, V. Torchilin, siRNA based drug design, quality, delivery and clinical translation, Nanomed. Nanotechnol. Biol. Med. 29 (2020), https://doi.org/10.1016/J.NANO.2020.102239 102239.
[267] Z. Jia, Y. Gong, Y. Pi, X. Liu, L. Gao, L. Kang, J. Wang, F. Yang, J. Tang, W. Lu, Q. Li, W. Zhang, Z. Yan, L. Yu, PPB peptide-mediated siRNA-loaded stable nucleic acid lipid nanoparticles on targeting therapy of hepatic fibrosis, Mol. Pharm. 15 (2018) 53–62, https://doi.org/10.1021/acs.molpharmaceut.7b00709.
[268] J.L. Vivero-Escoto, H. Vadarevu, R. Juneja, L.W. Schrum, J.H. Benbow, Nanoparticle mediated silencing of tenascin C in hepatic stellate cells:

Effect on inflammatory gene expression and cell migration, J. Mater. Chem. B. 7 (2019) 7396–7405, https://doi.org/10.1039/c9tb01845j.
[269] L. Chen, R. Chen, S. Kemper, M. Cong, H. You, D.R. Brigstock, Therapeutic effects of serum extracellular vesicles in liver fibrosis, J. Extracell. Vesicles. 7 (2018) 1461505, https://doi.org/10.1080/20013078.2018.1461505.
[270] B. Zhang, T. Jiang, Y. Tuo, K. Jin, Z. Luo, W. Shi, H. Mei, Y. Hu, Z. Pang, X. Jiang, Captopril improves tumor nanomedicine delivery by increasing tumor blood perfusion and enlarging endothelial gaps in tumor blood vessels, Cancer Lett. 410 (2017) 12–19, https://doi.org/10.1016/j.canlet.2017.09.007.
[271] I.X. Chen, V.P. Chauban, J. Posada, M.R. Ng, M.W. Wu, P. Adstamongkonkul, P. Huang, N. Lindeman, R. Langer, R.K. Jain, Blocking CXCR4 alleviates desmoplasia, increases T-lymphocyte infiltration, and improves immunotherapy in metastatic breast cancer, Proc. Natl. Acad. Sci. United States Am. 5 (2019) 4558–4566.
[272] X. Zhao, J. Pan, W. Li, W. Yang, L. Qin, Y. Pan, Gold nanoparticles enhance cisplatin delivery and potentiate chemotherapy by decompressing colorectal cancer vessels, Int. J. Nanomedicine. 13 (2018) 6207–6221, https://doi.org/10.2147/IJN.S176928.
[273] Y. Li, W. Shang, X. Liang, C. Zeng, M. Liu, S. Wang, H. Li, J. Tian, The diagnosis of hepatic fibrosis by magnetic resonance and near-infrared imaging using dual-modality nanoparticles, RSC Adv. 8 (2018) 6699–6708, https://doi.org/10.1039/c7ra10847h.
[274] H. Liang, Z. Li, Z. Ren, Q. Jia, L. Guo, S. Li, H. Zhang, S. Hu, D. Zhu, D. Shen, Z. Yu, K. Cheng, Light-triggered NO-releasing nanoparticles for treating mice with liver fibrosis, Nano Res. 13 (2020) 2197–2202, https://doi.org/10.1007/s12274-020-2833-6.
[275] Q. Liu, F. Chen, L. Hou, L. Shen, X. Zhang, D. Wang, L. Huang, Nanocarrier-mediated chemo-immunotherapy arrested cancer progression and induced tumor dormancy in desmoplastic melanoma, ACS Nano 12 (2018) 7812–7825, https://doi.org/10.1021/acsnano.8b01890.
[276] M. Deshmukh, S. Nakagawa, T. Higashi, A. Vincek, A. Venkatesh, M. Ruiz de Galarreta, A.P. Koh, N. Goossens, H. Hirschfield, C.B. Bian, N. Fujiwara, A. Ono, H. Hoshida, M. El-Abtah, N.B. Ahmad, A. Lujambio, R. Sanchez, B.C. Fuchs, K. Poelstra, J. Prakash, Y. Hoshida, Cell type-specific pharmacological kinase inhibition for cancer chemoprevention, Nanomed. Nanotechnol. Biol. Med. 14 (2018) 317–325, https://doi.org/10.1016/j.nano.2017.11.004.
[277] X. Chen, Q. Yu, Y. Liu, Q. Sheng, K. Shi, Y. Wang, M. Li, Z. Zhang, Q. He, Synergistic cytotoxicity and co-autophagy inhibition in pancreatic tumor cells and cancer-associated fibroblasts by dual functional peptide-modified liposomes, Acta Biomater. 99 (2019) 339–349, https://doi.org/10.1016/j.actbio.2019.09.003.
[278] T. Han, P. Paramsothy, J. Hong, D. Isquith, D. Xu, H. Bai, M. Neradilek, E. Gill, X.-Q. Zhao, High-resolution MRI assessed carotid atherosclerotic plaque characteristics comparing men and women with elevated ApoB levels, Int. J. Cardiovasc. Imaging. 36 (2020) 481–489, https://doi.org/10.1007/s10554-019-01600-1.
[279] R.M. Kwee, M.T.B. Truijman, R.J. van Oostenbrugge, W.H. Mess, M.H. Prins, C. L. Franke, A.G.G.C. Korten, J.E. Wildberger, M.E. Kooi, Longitudinal MRI study on the natural history of carotid artery plaques in symptomatic patients, PLoS ONE 7 (2012) 42472, https://doi.org/10.1371/journal.pone.0042472.
[280] S. Steven, K. Frenis, M. Oelze, S. Kalinovic, M. Kuntic, M.T. Bayo Jimenez, K. Vujacic-Mirski, J. Helmstädter, S. Kröller-Schön, T. Münzel, A. Daiber, Vascular inflammation and oxidative stress: major triggers for cardiovascular disease, Oxid. Med. Cell. Longev. (2019 (2019)) 1–26, https://doi.org/10.1155/2019/7092151.
[281] M.D. Marques, V. Nauffal, B. Ambale-Venkatesh, H.D. Vasconcellos, C. Wu, H. Bahrami, R.P. Tracy, M. Cushman, D.A. Bluemke, J.A.C. Lima, Association between inflammatory markers and myocardial fibrosis, Hypertension 72 (2018) 902–908, https://doi.org/10.1161/HYPERTENSIONAHA.118.11463.
[282] R.G. Woolfson, Renal failure in atherosclerotic renovascular disease: pathogenesis, diagnosis, and intervention, Postgrad. Med. J. 77 (2001) 68–74, https://doi.org/10.1136/PMJ.77.904.68.
[283] X. Zhang, X. Zhu, C.M. Ferguson, K. Jiang, T. Burningham, A. Lerman, L.O. Lerman, Magnetic resonance elastography can monitor changes in medullary stiffness in response to treatment in the swine ischemic kidney, Magn. Reson. Mater. Physics, Biol. Med. 31 (2018) 375–382, https://doi.org/10.1007/s10334-017-0671-7.
[284] T. Nishiguchi, T. Kubo, T. Tanimoto, Y. Ino, Y. Matsuo, T. Yamano, K. Terada, H. Emori, Y. Katayama, A. Taruya, Y. Ozaki, Y. Shiono, K. Shimamura, T. Kameyama, H. Kitabata, T. Yamaguchi, A. Tanaka, T. Hozumi, T. Akasaka, Effect of early pitavastatin therapy on coronary fibrous-cap thickness assessed by optical coherence tomography in patients with acute coronary syndrome: the ESCORT study, JACC Cardiovasc. Imaging. 11 (2018) 829–838, https://doi.org/10.1016/J.JCMG.2017.07.011.
[285] L. Räber, K.C. Koskinas, K. Yamaji, M. Taniwaki, M. Roffi, L. Holmvang, H.M. Garcia Garcia, T. Zanchin, R. Maldonado, A. Moschovitis, G. Pedrazzini, S. Zaugg, J. Dijkstra, C.M. Matter, P.W. Serruys, T.F. Lüscher, H. Kelbaek, A. Karagiannis, M.D. Radu, S. Windecker, Changes in coronary plaque composition in patients with acute myocardial infarction treated with high-intensity statin therapy (IBIS-4): a serial optical coherence tomography study, JACC Cardiovasc. Imaging. 12 (2019) 1518–1528, https://doi.org/10.1016/J.JCMG.2018.08.024.
[286] M. Wildgruber, T. Aschenbrenner, H. Wendorff, M. Czubba, A. Glinzer, B. Haller, M. Schiemann, A. Zimmermann, H. Berger, H.-H. Eckstein, R. Meier, W. A. Wohlgemuth, P. Libby, A. Zernecke, The "Intermediate" CD14++CD16+ monocyte subset increases in severe peripheral artery disease in humans, Sci. Rep. 6 (2016) 39483, https://doi.org/10.1038/srep39483.
[287] H. Yamamoto, N. Yoshida, T. Shinke, H. Otake, M. Kuroda, K. Sakaguchi, Y. Hirota, T. Toba, H. Takahashi, D. Terashita, K. Uzu, N. Tahara, Y. Shinkura, K. Kuroda, Y. Nagasawa, Y. Nagano, Y. Tsukiyama, K. Yanaka, T. Emoto, N. Sasaki, T. Yamashita, W. Ogawa, K. Hirata, Impact of CD14++CD16+ monocytes on coronary plaque vulnerability assessed by optical coherence tomography in coronary artery disease patients, Atherosclerosis. 269 (2018) 245–251, https://doi.org/10.1016/J.ATHEROSCLEROSIS.2018.01.010.
[288] S. Yamagishi, K. Fukami, T. Matsui, Evaluation of tissue accumulation levels of advanced glycation end products by skin autofluorescence: A novel marker of vascular complications in high-risk patients for cardiovascular disease, Int. J. Cardiol. 185 (2015) 263–268, https://doi.org/10.1016/J.IJCARD.2015.03.167.
[289] Y. Fujino, G.F. Attizzani, S. Tahara, W. Wang, K. Takagi, T. Naganuma, H. Yabushita, K. Tanaka, T. Sato, Y. Watanabe, S. Mitomo, N. Kurita, H. Ishiguro, S. Nakamura, K. Hozawa, H.G. Bezerra, S. Yamagishi, S. Nakamura, Association of skin autofluorescence with plaque vulnerability evaluated by optical coherence tomography in patients with cardiovascular disease, Atherosclerosis. 274 (2018) 47–53, https://doi.org/10.1016/J.ATHEROSCLEROSIS.2018.03.001.
[290] M.P. Ostrom, A. Gopal, N. Ahmadi, K. Nasir, E. Yang, I. Kakadiaris, F. Flores, S.S. Mao, M.J. Budoff, Mortality incidence and the severity of coronary atherosclerosis assessed by computed tomography angiography, J. Am. Coll. Cardiol. 52 (2008) 1335–1343, https://doi.org/10.1016/j.jacc.2008.07.027.
[291] E.A. Hulten, S. Carbonaro, S.P. Petrillo, J.D. Mitchell, T.C. Villines, Prognostic value of cardiac computed tomography angiography, J. Am. Coll. Cardiol. 57 (2011) 1237–1247, https://doi.org/10.1016/j.jacc.2010.10.011.
[292] J.R. Weir-McCall, P. Blanke, S.L. Sellers, A.A. Ahmadi, D. Andreini, M.J. Budoff, F. Cademartiri, K. Chinnaiyan, J.H. Choi, E.J. Chun, E. Conte, I. Gottlieb, M. Hadamitzky, Y.J. Kim, B.K. Lee, S.-E. Lee, E. Maffei, H. Marques, G. Pontone, G. L. Raff, S. Shin, J.M. Sung, P. Stone, H. Samady, R. Virmani, J. Narula, D.S. Berman, L.J. Shaw, J.J. Bax, F.Y. Lin, J.K. Min, H.-J. Chang, J.A. Leipsic, Impact of Non-obstructive left main disease on the progression of coronary artery disease: a PARADIGM substudy, J. Cardiovasc. Comput. Tomogr. 12 (2018) 231–237, https://doi.org/10.1016/J.JCCT.2018.05.011.
[293] T.M. Sequeira Gross, D. Lindner, F.M. Ojeda, J. Neumann, N. Grewal, T. Kuntze, S. Blankenberg, H. Reichenspurner, D. Westermann, E. Girdauskas, Comparison of microstructural alterations in the proximal aorta between aortic stenosis and regurgitation, J. Thorac. Cardiovasc. Surg. (2020), https://doi.org/10.1016/J.JTCVS.2020.03.002.
[294] G.F. Veraldi, P.F. Nocini, A. Eccher, A. Fenzi, A. Sboarina, L. Mezzetto, Correlation between MDCTA and carotid plaque histological heterogeneity: a pilot study, Eur. J. Vasc. Endovasc. Surg. 56 (2018) 7–14, https://doi.org/10.1016/J.EJVS.2018.04.001.
[295] S. Hassani, R.G. Nogueira, A.R. Al-Bayati, R. Sachdeva, M. McDaniel, D.C. Haussen, Intravascular ultrasound in carotid web, J. Neurointerv. Surg. (2019), https://doi.org/10.1136/NEURINTSURG-2019-015387.
[296] F. Yuan, L. Guo, K. Park, J.R. Woollard, K. Taek-Geun, K. Jiang, T. Melkamu, B. Zang, S.L. Smith, S.C. Fahrenkrug, F.D. Kolodgie, A. Lerman, R. Virmani, L.O. Lerman, D.F. Carlson, Ossabaw pigs with a PCSK9 gain-of-function mutation develop accelerated coronary atherosclerotic lesions: a novel model for preclinical studies, J. Am. Heart Assoc. 7 (2018), https://doi.org/10.1161/JAHA.117.006207.
[297] A.F. Hedayat, K.-H. Park, T.-G. Kwon, J.R. Woollard, K. Jiang, D.F. Carlson, A. Lerman, L.O. Lerman, Peripheral vascular atherosclerosis in a novel PCSK9 gain-of-function mutant Ossabaw miniature pig model, Transl. Res. 192 (2018) 30–45, https://doi.org/10.1016/J.TRSL.2017.10.007.
[298] R.A. Walker, The complexities of breast cancer desmoplasia, (2001).
[299] N.F. Boyd, L.J. Martin, M.J. Yaff, S. Minkin, Mammographic density and breast cancer risk: current understanding and future prospects, (2011) 1–12.
[300] S. Keller, T. Borde, J. Brangsch, L.C. Adams, A. Kader, C. Reimann, P. Gebert, B. Hamm, M. Makowski, Native t1 mapping magnetic resonance imaging as a quantitative biomarker for characterization of the extracellular matrix in a rabbit hepatic cancer model, Biomedicines. 8 (2020) 1–11, https://doi.org/10.3390/biomedicines8100412.
[301] Sheridan Mayo and Marco Endrizzi, X-Ray Phase Contrast Methods, in: Handb. Adv. Nondestruct. Eval., 2019: pp. 1053–1095. DOI: 10.1007/978-3-319-26553-7_28.
[302] M.A. Kimm, M. Willner, E. Drecoll, J. Herzen, P.B. Noël, E.J. Rummeny, F. Pfeiffer, A.A. Fingerle, Grating-based phase-contrast CT (PCCT): Histopathological correlation of human liver cirrhosis and hepatocellular carcinoma specimen, J. Clin. Pathol. 73 (2020) 483–487, https://doi.org/10.1136/jclinpath-2019-206380.
[303] S. Forte, Z. Wang, C. Arboleda, K. Lång, G. Singer, R.A. Kubik-Huch, M. Stampanoni, Can grating interferometry-based mammography discriminate benign from malignant microcalcifications in fresh biopsy samples?, Eur. J. Radiol. 129 (2020) 1–6, https://doi.org/10.1016/j.ejrad.2020.109077.
[304] A.A. Fingerle, M. Dobritz, H. Friess, J. Kleeff, How fibrosis influences imaging and surgical decisions in pancreatic cancer, 3 (2012) 1–16. DOI: 10.3389/fphys.2012.00389.
[305] L.P. Hariri, D.C. Adams, M.B. Applegate, A.J. Miller, B.W. Roop, M. Villiger, B.E. Bouma, M.J. Suter, Distinguishing tumor from associated fibrosis to increase diagnostic biopsy yield with polarization-sensitive optical coherence tomography, Clin. Cancer Res. 25 (2019) 5242–5249, https://doi.org/10.1158/1078-0432.CCR-19-0566.

[306] B. Baumann, Polarization sensitive optical coherence tomography: A review of technology and applications, Appl. Sci. 7 (2017), https://doi.org/10.3390/app7050474.
[307] P.P. Provenzano, D.R. Inman, K.W. Eliceiri, J.G. Knittel, L. Yan, C.T. Rueden, J.G. White, P.J. Keely, Collagen density promotes mammary tumor initiation and progression, BMC Med. 6 (2008) 1–15, https://doi.org/10.1186/1741-7015-6-11.
[308] M.W. Conklin, J.C. Eickhoff, K.M. Riching, C.A. Pehlke, K.W. Eliceiri, P.P. Provenzano, A. Friedl, P.J. Keely, Aligned collagen is a prognostic signature for survival in human breast carcinoma, Am. J. Pathol. 178 (2011) 1221–1232, https://doi.org/10.1016/j.ajpath.2010.11.076.
[309] F. Bochner, L. Fellus-Alyagor, D. Ketter, O. Golani, I. Biton, M. Neeman, Bimodal magnetic resonance and optical imaging of extracellular matrix remodelling by orthotopic ovarian tumours, Br. J. Cancer. 123 (2020) 216–225, https://doi.org/10.1038/s41416-020-0878-7.
[310] J.M. Straub, J. New, C.D. Hamilton, C. Lominska, S.M. Thomas, Radiation-induced fibrosis: mechanisms and implications for therapy, Radiation-Induced Fibros. Mech. Implic. Ther. 141 (2016) 1–16, https://doi.org/10.1007/s00432-015-1974-6.Radiation-induced.
[311] M. Mostyka, J. Jessurun, C. Matrai, Sarcoid-like granulomatosis in a patient with breast cancer mimicking refractory metastatic disease, Int. J. Surg. Pathol. 28 (2020) 668–671, https://doi.org/10.1177/1066896920905887.
[312] C.L. Carter, G.A. Parker, K.G. Hankey, A.M. Farese, T.J. MacVittie, M.A. Kane, MALDI-MSI spatially maps N-glycan alterations to histologically distinct pulmonary pathologies following irradiation, Sci. Rep. 10 (2020) 1–14, https://doi.org/10.1038/s41598-020-68508-y.
[313] F. Chen, M.A. Desai, J.G. Cernigliaro, M.A. Edgar, L.F. Alexander, Perinephric myxoid pseudotumor of fat: a very rare entity that can mimic a renal cyst and retroperitoneal liposarcoma on imaging, Clin. Imaging. 69 (2021) 139–144, https://doi.org/10.1016/j.clinimag.2020.06.041.
[314] B. Leroy-Freschini, V. Lindner, T. Boisramé, M. Demarchi, 18F-FDG PET/CT imaging of peritoneal fibrosis mimicking persistent metastatic ovarian carcinoma, Nucl. Med. Mol. Imaging 54 (2020) (2010) 249–251, https://doi.org/10.1007/s13139-020-00656-5.
[315] A. Hirschmann, V.M. van Praag, R.L. Haas, M.A.J. van de Sande, J.L. Bloem, Can we use MRI to detect clinically silent recurrent soft-tissue sarcoma?, Eur. Radiol. 30 (2020) 4724–4733, https://doi.org/10.1007/s00330-020-06810-z.
[316] I.A. Egoshin, D.V. Pasynkov, A.A. Kolchev, I.V. Kliouchkin, O.O. Pasynkova, Segmentation of breast focal lesions on the ultrasound image, Biomed. Eng. (NY) 54 (2020) 99–103, https://doi.org/10.1007/s10527-020-09982-6.
[317] L. Jiang, J. Wang, X. Liu, Z. Li, C. Xia, L. Xie, Y. Gao, M. Shen, P. Han, Y. Guo, Z. Yang, The combined effects of cardiac geometry, microcirculation, and tissue characteristics on cardiac systolic and diastolic function in subclinical diabetes mellitus-related cardiomyopathy, Int. J. Cardiol. 320 (2020) 112–118, https://doi.org/10.1016/J.IJCARD.2020.07.013.
[318] E.H.M. Paiman, H.J. Eyk, M.M.A. Aalst, M.B. Bizino, R.J. Geest, J.J.M. Westenberg, P.H. Geelhoed-Duijvestijn, A.V. Kharagjitsingh, P.C.N. Rensen, J. W.A. Smit, I.M. Jazet, H.J. Lamb, Effect of Liraglutide on cardiovascular function and myocardial tissue characteristics in Type 2 diabetes patients of south asian descent living in the Netherlands: a double-blind, randomized, placebo-controlled trial, J. Magn. Reson. Imaging. 51 (2020) 1679–1688, https://doi.org/10.1002/jmri.27009.
[319] C. Roy, A. Slimani, C. de Meester, M. Amzulescu, A. Pasquet, D. Vancraeynest, J.-L. Vanoverschelde, A.-C. Pouleur, B.L. Gerber, Age and sex corrected normal reference values of T1, T2 T2* and ECV in healthy subjects at 3T CMR, J. Cardiovasc. Magn. Reson. 19 (2017) 72, https://doi.org/10.1186/s12968-017-0371-5.
[320] E.B. Schelbert, D.R. Messroghli, State of the art: clinical applications of cardiac T1 mapping, Radiology 278 (2016) 658–676, https://doi.org/10.1148/radiol.2016141802.
[321] S. Kucukseymen, U. Neisius, J. Rodriguez, C.W. Tsao, R. Nezafat, Negative synergism of diabetes mellitus and obesity in patients with heart failure with preserved ejection fraction: a cardiovascular magnetic resonance study, Int. J. Cardiovasc. Imaging. 36 (2020) 2027–2038, https://doi.org/10.1007/s10554-020-01915-4.
[322] C. Kropidlowski, M. Meier-Schroers, D. Kuetting, A. Sprinkart, H. Schild, D. Thomas, R. Homsi, CMR based measurement of aortic stiffness, epicardial fat, left ventricular myocardial strain and fibrosis in hypertensive patients, IJC Hear. Vasc. 27 (2020), https://doi.org/10.1016/J.IJCHA.2020.100477 100477.
[323] S. Nakamori, K. Dohi, M. Ishida, Y. Goto, K. Imanaka-Yoshida, T. Omori, I. Goto, N. Kumagai, N. Fujimoto, Y. Ichikawa, K. Kitagawa, N. Yamada, H. Sakuma, M. Ito, Native T1 mapping and extracellular volume mapping for the assessment of diffuse myocardial fibrosis in dilated cardiomyopathy, JACC Cardiovasc. Imaging. 11 (2018) 48–59, https://doi.org/10.1016/J.JCMG.2017.04.006.
[324] M.A. Khan, E.Y. Yang, D.T. Nguyen, F. Nabi, J. Hinojosa, M. Jabel, S.F. Nagueh, E. A. Graviss, D.J. Shah, Examining the relationship and prognostic implication of diabetic status and extracellular matrix expansion by cardiac magnetic resonance, Circ. Cardiovasc. Imaging. 13 (2020), https://doi.org/10.1161/CIRCIMAGING.120.011000.
[325] B. Lam, T.A. Stromp, Z. Hui, M. Vandsburger, Myocardial native-T1 times are elevated as a function of hypertrophy, HbA1c, and heart rate in diabetic adults without diffuse fibrosis, Magn. Reson. Imaging. 61 (2019) 83–89, https://doi.org/10.1016/j.mri.2019.05.029.
[326] A.S. Bojer, M.H. Sørensen, N. Vejlstrup, J.P. Goetze, P. Gæde, P.L. Madsen, Distinct non-ischemic myocardial late gadolinium enhancement lesions in patients with type 2 diabetes, Cardiovasc. Diabetol. 19 (2020) 1–9, https://doi.org/10.1186/s12933-020-01160-y.
[327] G.S. Marchini, I.N. Cestari, V.M.C. Salemi, M.C. Irigoyen, A. Arnold, A. Kakoi, C. Rocon, V.D. Aiello, I.A. Cestari, Early changes in myocyte contractility and cardiac function in streptozotocin-induced type 1 diabetes in rats, PLoS ONE 15 (2020), https://doi.org/10.1371/journal.pone.0237305 e0237305.
[328] F.A. Alomar, A. Al-Rubaish, F. Al-Muhanna, A.K. Al-Ali, J. McMillan, J. Singh, K. R. Bidasee, Adeno-Associated viral transfer of glyoxalase-1 blunts carbonyl and oxidative stresses in hearts of type 1 diabetic rats, Antioxidants. 9 (2020) 592, https://doi.org/10.3390/antiox9070592.
[329] S. Singh, S.K. Venkatesh, R. Loomba, Z. Wang, C. Sirlin, J. Chen, M. Yin, F.H. Miller, R.N. Low, T. Hassanein, E.M. Godfrey, P. Asbach, M.H. Murad, D.J. Lomas, J.A. Talwalkar, R.L. Ehman, Magnetic resonance elastography for staging liver fibrosis in non-alcoholic fatty liver disease: a diagnostic accuracy systematic review and individual participant data pooled analysis, Eur. Radiol. 26 (2016) 1431–1440, https://doi.org/10.1007/s00330-015-3949-z.
[330] G. Andersen, L. Plum-Mörschel, P.D. Hockings, A. Morsing, M.S. Palle, O. Svolgaard, A. Flint, Clinical characteristics of a non-alcoholic fatty liver disease population across the fibrosis spectrum measured by magnetic resonance elastography: analysis of screening data, Adv. Ther. 37 (2020) 4866–4876, https://doi.org/10.1007/s12325-020-01503-x.
[331] H.J. Park, H. Han, E.-Y. Oh, S.R. Kim, K.H. Park, J.-H. Lee, J.-W. Park, Empagliflozin and dulaglutide are effective against obesity-induced airway hyperresponsiveness and fibrosis in a murine model, Sci. Rep. 9 (2019) 15601, https://doi.org/10.1038/s41598-019-51648-1.
[332] Y. Noda, S. Goshima, Y. Tsuji, K. Kajita, Y. Akamine, N. Kawai, H. Kawada, Y. Tanahashi, M. Matsuo, Pancreatic extracellular volume fraction using T1 mapping in patients with impaired glucose intolerance, Abdom. Radiol. 45 (2020) 449–456, https://doi.org/10.1007/s00261-019-02384-7.
[333] A. Smith, V. Iablokov, M. Mazza, S. Guarnerio, V. Denti, M. Ivanova, M. Stella, I. Piga, C. Chinello, B. Heijs, P.A. van Veelen, H. Benediktsson, D.A. Muruve, F. Magni, Detecting proteomic indicators to distinguish diabetic nephropathy from hypertensive nephrosclerosis by integrating matrix-assisted laser desorption/ionization mass spectrometry imaging with high-mass accuracy mass spectrometry, Kidney Blood Press. Res. 45 (2020) 233–248, https://doi.org/10.1159/000505187.
[334] R. Yong, X.M. Chen, S. Shen, S. Vijayaraj, Q. Ma, C.A. Pollock, S. Saad, Plumbagin ameliorates diabetic nephropathy via interruption of pathways that include NOX4 signalling, PLoS ONE 8 (2013) 73428, https://doi.org/10.1371/journal.pone.0073428.
[335] Z.M. Younossi, A.B. Koenig, D. Abdelatif, Y. Fazel, L. Henry, M. Wymer, Global epidemiology of nonalcoholic fatty liver disease—Meta-analytic assessment of prevalence, incidence, and outcomes, Hepatology 64 (2016) 73–84, https://doi.org/10.1002/hep.28431.
[336] H. Hagström, P. Nasr, M. Ekstedt, U. Hammar, P. Stål, R. Hultcrantz, S. Kechagias, Fibrosis stage but not NASH predicts mortality and time to development of severe liver disease in biopsy-proven NAFLD, J. Hepatol. 67 (2017) 1265–1273, https://doi.org/10.1016/j.jhep.2017.07.027.
[337] E.B. Tapper, R. Loomba, Noninvasive imaging biomarker assessment of liver fibrosis by elastography in NAFLD, Nat. Rev. Gastroenterol. Hepatol. 15 (2018) 274–282, https://doi.org/10.1038/nrgastro.2018.10.
[338] P. Bedossa, F. Carrat, Liver biopsy: the best, not the gold standard, J. Hepatol. 50 (2009) 1–3, https://doi.org/10.1016/j.jhep.2008.10.014.
[339] G. Marchesini, C.P. Day, J.F. Dufour, A. Canbay, V. Nobili, V. Ratziu, H. Tilg, M. Roden, A. Gastaldelli, H. Yki-Jarvinen, F. Schick, R. Vettor, G. Fruhbeck, L. Mathus-Vliegen, EASL-EASD-EASO clinical practice guidelines for the management of non-alcoholic fatty liver disease, J. Hepatol. 64 (2016) 1388–1402, https://doi.org/10.1016/j.jhep.2015.11.004.
[340] E.M. Brunt, C.G. Janney, A.M. Di Bisceglie, B.A. Neuschwander-tetri, B.R. Bacon, Nonalcoholic steatohepatitis - a proposal for grading and staging the histological lesions, 94 (1999).
[341] S. Gawrieh, D. Sethunath, O.W. Cummings, D.E. Kleiner, R. Vuppalanchi, N. Chalasani, M. Tuceryan, Automated quantification and architectural pattern detection of hepatic fibrosis in NAFLD, Ann. Diagn. Pathol. 47 (2020), https://doi.org/10.1016/j.anndiagpath.2020.151518 151518.
[342] E. Vilar-Gomez, Z. Lou, N. Kong, R. Vuppalanchi, T.F. Imperiale, N. Chalasani, Cost Effectiveness of different strategies for detecting cirrhosis in patients with nonalcoholic fatty liver disease based on united states health care system, Clin. Gastroenterol. Hepatol. 18 (2020) 2305–2314.e12, https://doi.org/10.1016/j.cgh.2020.04.017.
[343] P.N.T. Wells, H.D. Liang, Medical ultrasound: Imaging of soft tissue strain and elasticity, J. R. Soc. Interface. 8 (2011) 1521–1549, https://doi.org/10.1098/rsif.2011.0054.
[344] P. Ginès, I. Graupera, F. Lammert, P. Angeli, L. Caballeria, A. Krag, I.N. Guha, S. D. Murad, L. Castera, Screening for liver fibrosis in the general population: a call for action, Lancet Gastroenterol. Hepatol. 1 (2016) 256–260, https://doi.org/10.1016/S2468-1253(16)30081-4.
[345] C. Hsu, C. Caussy, K. Imajo, J. Chen, S. Singh, K. Kaulback, M. Da Le, J. Hooker, X. Tu, R. Bettencourt, M. Yin, C.B. Sirlin, R.L. Ehman, A. Nakajima, R. Loomba, Magnetic resonance vs transient elastography analysis of patients with nonalcoholic fatty liver disease: a systematic review and pooled analysis of individual participants, Clin. Gastroenterol. Hepatol. 17 (2019) 630–637.e8, https://doi.org/10.1016/j.cgh.2018.05.059.

[346] EASL-ALEH clinical practice guidelines, Key points of 2015 EASL-ALEH clinical practice guidelines: non invasive tests for evaluation of liver severity and prognosis, J. Hepatol. 23 (2015) 488–492.
[347] Y.N. Zhang, K.J. Fowler, A. Ozturk, C.K. Potu, A.L. Louie, V. Montes, W.C. Henderson, K. Wang, M.P. Andre, A.E. Samir, C.B. Sirlin, Liver fibrosis imaging: a clinical review of ultrasound and magnetic resonance elastography, J. Magn. Reson. Imaging. 51 (2020) 25–42, https://doi.org/10.1002/jmri.26716.
[348] L. Casfera, J. Foucher, P.H. Bernard, F. Carvalho, D. Allaix, W. Merrouche, P. Couzigou, V. De Lédinghen, Pitfalls of liver stiffness measurement: A 5-year prospective study of 13,369 examinations, Hepatology. 51 (2010) 828–835. DOI: 10.1002/hep.23425.
[349] G.L. Zhang, Q.Y. Zhao, C.S. Lin, Z.X. Hu, T. Zhang, Z.L. Gao, F. Schepis, Transient elastography and ultrasonography: Optimal evaluation of liver fibrosis and cirrhosis in patients with chronic hepatitis B concurrent with nonalcoholic fatty liver disease, Biomed Res. Int. 2019 (2019), https://doi.org/10.1155/2019/3951574.
[350] C. Cassinotto, J. Boursier, V. de Lédinghen, J. Lebigot, B. Lapuyade, P. Cales, J.B. Hiriart, S. Michalak, B. Le Bail, V. Cartier, A. Mouries, F. Oberti, I. Fouchard-Hubert, J. Vergniol, C. Aubé, Liver stiffness in nonalcoholic fatty liver disease: a comparison of supersonic shear imaging, FibroScan, and ARFI with liver biopsy, Hepatology. 63 (2016) 1817–1827, https://doi.org/10.1002/hep.28394.
[351] B.K. Budai, A. Tóth, P. Borsos, V.G. Frank, S. Shariati, B. Fejér, A. Folhoffer, F. Szalay, V. Bérczi, P.N. Kaposi, Three-dimensional CT texture analysis of anatomic liver segments can differentiate between low-grade and high-grade fibrosis, BMC Med. Imaging. 20 (2020) 1–11, https://doi.org/10.1186/s12880-020-00508-w.
[352] Wikipedia, Magnetic resonance elastography, (2020).
[353] C.C. Park, P. Nguyen, C. Hernandez, R. Bettencourt, K. Ramirez, L. Fortney, J. Hooker, E. Sy, M. Alquiraish, M.A. Valasek, E. Rizo, L.M. Richards, D.A. Brenner, C.B. Sirlin, R. Loomba, Magnetic Resonance Elastography vs Transient Elastography in Detection of Fibrosis and Noninvasive Measurement of Steatosis in Patients with Biopsy-Proven Nonalcoholic Fatty Liver Disease, Gastroenterology 152 (2017) S70, https://doi.org/10.1016/s0016-5085(17)30587-5.
[354] Liver fibrosis, Ramón Bataller David A. Brenner. 115 (2005) 209–218. DOI: 10.1201/9780429427275-10.
[355] K. Schawkat, A. Ciritsis, S. von Ulmenstein, H. Honcharova-Biletska, C. Jüngst, A. Weber, C. Gubler, J. Mertens, C.S. Reiner, Diagnostic accuracy of texture analysis and machine learning for quantification of liver fibrosis in MRI: correlation with MR elastography and histopathology, Eur. Radiol. 30 (2020) 4675–4685, https://doi.org/10.1007/s00330-020-06831-8.
[356] M. Pavlides, R. Banerjee, J. Sellwood, C.J. Kelly, M.D. Robson, J.C. Booth, J. Collier, S. Neubauer, E. Barnes, Multiparametric magnetic resonance imaging predicts clinical outcomes in patients with chronic liver disease, J. Hepatol. 64 (2016) 308–315, https://doi.org/10.1016/j.jhep.2015.10.009.
[357] M. Pavlides, R. Banerjee, E.M. Tunnicliffe, C. Kelly, J. Collier, L.M. Wang, K.A. Fleming, J.F. Cobbold, M.D. Robson, S. Neubauer, E. Barnes, Multiparametric magnetic resonance imaging for the assessment of non-alcoholic fatty liver disease severity, Liver Int. 37 (2017) 1065–1073, https://doi.org/10.1111/liv.13284.
[358] J.W. Kim, Y.S. Lee, Y.S. Park, B.H. Kim, S.Y. Lee, J.E. Yeon, C.H. Lee, Multiparametric MR index for the diagnosis of non-alcoholic steatohepatitis in patients with non-alcoholic fatty liver disease, Sci. Rep. 10 (2020) 1–9, https://doi.org/10.1038/s41598-020-59601-3.
[359] A. Dennis, S. Mouchti, M. Kelly, J.A. Fallowfield, G. Hirschfield, M. Pavlides, R. Banerjee, A composite biomarker using multiparametric magnetic resonance imaging and blood analytes accurately identifies patients with non-alcoholic steatohepatitis and significant fibrosis, Sci. Rep. 10 (2020) 1–11, https://doi.org/10.1038/s41598-020-71995-8.
[360] R. Banerjee, M. Pavlides, E.M. Tunnicliffe, S.K. Piechnik, N. Sarania, R. Philips, J. D. Collier, J.C. Booth, J.E. Schneider, L.M. Wang, D.W. Delaney, K.A. Fleming, M. D. Robson, E. Barnes, S. Neubauer, Multiparametric magnetic resonance for the non-invasive diagnosis of liver disease, J. Hepatol. 60 (2014) 69–77, https://doi.org/10.1016/j.jhep.2013.09.002.
[361] N. McDonald, P.J. Eddowes, J. Hodson, S.I.K. Semple, N.P. Davies, C.J. Kelly, S. Kin, M. Phillips, A.H. Herlihy, T.J. Kendall, R.M. Brown, D.A.H. Neil, S.G. Hübscher, G.M. Hirschfield, J.A. Fallowfield, Multiparametric magnetic resonance imaging for quantitation of liver disease: a two-centre cross-sectional observational study, Sci. Rep. 8 (2018) 1–10, https://doi.org/10.1038/s41598-018-27560-5.
[362] J.A. Luetkens, S. Klein, F. Traeber, F.C. Schmeel, A.M. Sprinkart, D.L.R. Kuetting, W. Block, K. Hittatiya, F.E. Uschner, R. Schierwagen, J. Gieseke, H.H. Schild, J. Trebicka, G.M. Kukuk, Quantitative liver MRI including extracellular volume fraction for non-invasive quantification of liver fibrosis: a prospective proof-of-concept study, Gut 67 (2018) 592–594, https://doi.org/10.1136/gutjnl-2017-314561.
[363] J.A. Luetkens, S. Klein, F. Träber, W. Block, F.C. Schmeel, A.M. Sprinkart, D.L.R. Kuetting, F.E. Uschner, R. Schierwagen, D. Thomas, J. Trebicka, G.M. Kukuk, Quantification of liver fibrosis: extracellular volume fraction using an MRI bolus-only technique in a rat animal model, Eur. Radiol. Exp. 3 (2019) 22, https://doi.org/10.1186/s41747-019-0100-y.
[364] Z. Ye, Y. Wei, J. Chen, S. Yao, B. Song, Value of intravoxel incoherent motion in detecting and staging liver fibrosis: a meta-analysis, World J. Gastroenterol. 26 (2020) 3304–3317, https://doi.org/10.3748/wjg.v26.i23.3304.
[365] K. Sano, T. Ichikawa, U. Motosugi, H. Sou, A.M. Muhi, M. Matsuda, M. Nakano, M. Sakamoto, T. Nakazawa, M. Asakawa, H. Fujii, T. Kitamura, N. Enomoto, T. Araki, Imaging study of early hepatocellular carcinoma: usefulness of gadoxetic acid-enhanced MR imaging, Radiology 261 (2011) 834–844, https://doi.org/10.1148/radiol.11101840.
[366] A. Nishie, Y. Asayama, K. Ishigami, T. Tajima, D. Kakihara, T. Nakayama, Y. Takayama, D. Okamoto, A. Taketomi, K. Shirabe, N. Fujita, M. Obara, K. Yoshimitsu, H. Honda, MR prediction of liver fibrosis using a liver-specific contrast agent: Superparamagnetic iron oxide versus Gd-EOB-DTPA, J. Magn. Reson. Imaging. 36 (2012) 664–671, https://doi.org/10.1002/jmri.23691.
[367] H.J. Jang, J.H. Min, J.E. Lee, K.S. Shin, K.H. Kim, S.Y. Choi, Assessment of liver fibrosis with gadoxetic acid-enhanced MRI: comparisons with transient elastography, ElastPQ, and serologic fibrosis markers, Abdom. Radiol. 44 (2019) 2769–2780, https://doi.org/10.1007/s00261-019-02041-z.
[368] N. Fujita, A. Nishie, Y. Asayama, K. Ishigami, Y. Ushijima, D. Kakihara, Y. Takayama, T. Yoshizumi, T. Hida, Y. Oda, T. Okuaki, H. Honda, Quantitative evaluation of liver function and pathology with hepatocyte fraction on Gadoxetic acid-enhanced MR imaging, Magn. Reson. Imaging. 73 (2020) 125–129, https://doi.org/10.1016/j.mri.2020.08.018.
[369] S.W. Kim, Y.R. Kim, J.S. Song, J. Kim, T. Kim, Y.H. Lee, K. Yoon, K. Sw, K. Yr, C. Kh, Staging of Liver Fibrosis by Means of Semiautomatic Measurement of Liver Surface Nodularity in MRI, (2020) 624–630.
[370] M. Saif, W.J. Kwanten, J.A. Carr, I.X. Chen, J.M. Posada, A. Srivastava, J. Zhang, Y. Zheng, M. Pinter, S. Chatterjee, S. Softic, C.R. Kahn, K. van Leyen, O.T. Bruns, R.K. Jain, M.G. Bawendi, Non-invasive monitoring of chronic liver disease via near-infrared and shortwave-infrared imaging of endogenous lipofuscin, Nat. Biomed. Eng. 4 (2020) 801–813, https://doi.org/10.1038/s41551-020-0569-y.
[371] G.M. Deborah S. Barkauskas, X. Liang, Y.H. Mohammed, C.A. Thorling, Haolu Wang, M.S. Roberts, Using in vivo multiphoton fluorescence lifetime imaging to unravel disease-specific changes in the liver redox state, Methods Appl. Fluoresc. 8 (2020).
[372] G.C. Ooi, P.L. Khong, N.L. Müller, W.C. Yiu, L.J. Zhou, J.C.M. Ho, B. Lam, S. Nicolaou, K.W.T. Tsang, Severe acute respiratory syndrome: temporal lung changes at thin-section CT in 30 patients, Radiology 230 (2004) 836–844, https://doi.org/10.1148/radiol.2303030853.
[373] E.L. Burnham, W.J. Janssen, D.W.H. Riches, M. Moss, G.P. Downey, The fibroproliferative response in acute respiratory distress syndrome: Mechanisms and clinical significance, Eur. Respir. J. 43 (2014) 276–285, https://doi.org/10.1183/09031936.00196412.
[374] P. Spagnolo, E. Balestro, S. Aliberti, E. Cocconcelli, D. Biondini, G. Della Casa, N. Sverzellati, T.M. Maher, Pulmonary fibrosis secondary to COVID-19: a call to arms?, Lancet Respir. Med. 8 (2020) 750–752, https://doi.org/10.1016/S2213-2600(20)30222-8.
[375] T. Lammers, A.M. Sofias, R. van der Meel, R. Schiffelers, G. Storm, F. Tacke, S. Koschmieder, T.H. Brümmendorf, F. Kiessling, J.M. Metselaar, Dexamethasone nanomedicines for COVID-19, Nat. Nanotechnol. 15 (2020) 622–624, https://doi.org/10.1038/s41565-020-0752-z.
[376] J.P. Salameh, M.M.G. Leeflang, L. Hooft, N. Islam, T.A. McGrath, C.B. van der Pol, R.A. Frank, R. Prager, S.S. Hare, C. Dennie, R. Spijker, J.J. Deeks, J. Dinnes, K. Jenniskens, D.A. Korevaar, J.F. Cohen, A. Van den Bruel, Y. Takwoingi, J. van de Wijgert, J.A.A.G. Damen, J. Wang, M.D.F. McInnes, Thoracic imaging tests for the diagnosis of COVID-19, Cochrane Database Syst. Rev. 2020 (2020), https://doi.org/10.1002/14651858.CD013639.pub2.
[377] M. Marvisi, F. Ferrozzi, L. Balzarini, C. Mancini, S. Ramponi, M. Uccelli, First report on clinical and radiological features of COVID-19 pneumonitis in a Caucasian population: Factors predicting fibrotic evolution, Int. J. Infect. Dis. 99 (2020) 485–488, https://doi.org/10.1016/j.ijid.2020.08.054.
[378] Ground-glass opacification | Radiology Reference Article | Radiopaedia.org, (n.d.). https://radiopaedia.org/articles/ground-glass-opacification-3 (accessed May 29, 2021).
[379] Lobar consolidation | Radiology Reference Article | Radiopaedia.org, (n.d.). https://radiopaedia.org/articles/lobar-consolidation (accessed May 29, 2021).
[380] Y. Pan, H. Guan, S. Zhou, Y. Wang, Q. Li, T. Zhu, Q. Hu, Initial CT findings and temporal changes in patients with the novel coronavirus pneumonia, 30:3306 (2020) 4.
[381] Post COVID-19 pulmonary fibrosis | Radiology Case | Radiopaedia.org, (n.d.). https://radiopaedia.org/cases/post-covid-19-pulmonary-fibrosis (accessed May 29, 2021).
[382] P.M. George, S.L. Barratt, R. Condliffe, S.R. Desai, A. Devaraj, I. Forrest, M.A. Gibbons, N. Hart, R.G. Jenkins, D.F. McAuley, B.V. Patel, E. Thwaite, L.G. Spencer, Respiratory follow-up of patients with COVID-19 pneumonia, Thorax 75 (2020) 1009–1016, https://doi.org/10.1136/thoraxjnl-2020-215314.
[383] W. Zhao, L. He, H. Tang, X. Xie, L. Tang, J. Liu, The relationship between chest imaging findings and the viral load of COVID-19, Front. Med. 7 (2020) 1–8, https://doi.org/10.3389/fmed.2020.558539.
[384] M. Yu, Y. Liu, D. Xu, R. Zhang, L. Lan, H. Xu, Prediction of the development of pulmonary fibrosis using serial thin-section ct and clinical features in patients discharged after treatment for COVID-19 pneumonia, Korean J. Radiol. 21 (2020) 746–755, https://doi.org/10.3348/kjr.2020.0215.
[385] L. Carsana, A. Sonzogni, A. Nasr, R.S. Rossi, A. Pellegrinelli, P. Zerbi, R. Rech, R. Colombo, S. Antinori, M. Corbellino, M. Galli, E. Catena, A. Tosoni, A. Gianatti, M. Nebuloni, Pulmonary post-mortem findings in a series of COVID-19 cases from northern Italy: a two-centre descriptive study, Lancet Infect. Dis. 20 (2020) 1135–1140, https://doi.org/10.1016/S1473-3099(20)30434-5.

[386] A.W. Flikweert, M.J.J.H. Grootenboers, D.C.Y. Yick, A.W.F. du Mée, N.J.M. van der Meer, T.C.D. Rettig, M.K.M. Kant, Late histopathologic characteristics of critically ill COVID-19 patients: different phenotypes without evidence of invasive aspergillosis, a case series, J. Crit. Care. 59 (2020) 149–155, https://doi.org/10.1016/j.jcrc.2020.07.002.
[387] S.E. Rossi, J.J. Erasmus, M. Volpacchio, T. Franquet, T. Castiglioni, H. Page McAdams, "Crazy-paving" pattern at thin-section CT of the lungs: radiologic-pathologic overview, Radiographics. 23 (2003) 1509–1519, https://doi.org/10.1148/rg.236035101.
[388] S. Okamori, H. Lee, Y. Kondo, Y. Akiyama, H. Kabata, Y. Kaneko, M. Ishii, N. Hasegawa, K. Fukunaga, Coronavirus disease 2019-associated rapidly progressive organizing pneumonia with fibrotic feature: Two case reports, Medicine (Baltimore). 99 (2020), https://doi.org/10.1097/MD.0000000000021804 e21804.
[389] H. Shi, X. Han, N. Jiang, Y. Cao, O. Alwalid, J. Gu, Y. Fan, C. Zheng, Radiological findings from 81 patients with COVID-19 pneumonia in Wuhan, China: a descriptive study, Lancet Infect. Dis. 20 (2020) 425–434, https://doi.org/10.1016/S1473-3099(20)30086-4.
[390] Bronchiectasis | Radiology Reference Article | Radiopaedia.org, (n.d.). https://radiopaedia.org/articles/bronchiectasis (accessed May 29, 2021).
[391] H. Zhang, W. Shang, Q. Liu, X. Zhang, M. Zheng, M. Yue, Clinical characteristics of 194 cases of COVID-19 in Huanggang and Taian, China, Infection. 48 (2020) 687–694, https://doi.org/10.1007/s15010-020-01440-5.
[392] I. Carmona, P. Cordero, J. Ampuero, A. Rojas, M. Romero-Gómez, Role of assessing liver fibrosis in management of chronic hepatitis C virus infection, Clin. Microbiol. Infect. 22 (2016) 839–845, https://doi.org/10.1016/j.cmi.2016.09.017.
[393] Wikipedia, Elastography, (2018).
[394] D. Ji, Q. Shao, P. Han, F. Li, B. Li, H. Zang, X. Niu, Z. Li, S. Xin, G. Chen, The frequency and determinants of liver stiffness measurement failure: A retrospective study of "real-life" 38,464 examinations, PLoS ONE 9 (2014) 1–6, https://doi.org/10.1371/journal.pone.0105183.
[395] M. Friedrich-Rust, J. Nierhoff, M. Lupsor, I. Sporea, C. Fierbinteanu-Braticevici, D. Strobel, H. Takahashi, M. Yoneda, T. Suda, S. Zeuzem, E. Herrmann, Performance of Acoustic Radiation Force Impulse imaging for the staging of liver fibrosis: A pooled meta-analysis, J. Viral Hepat. 19 (2012) 212–219, https://doi.org/10.1111/j.1365-2893.2011.01537.x.
[396] J.Y. Jeong, Y.S. Cho, J.H. Sohn, Role of two-dimensional shear wave elastography in chronic liver diseases: A narrative review, World J. Gastroenterol. 24 (2018) 3849–3860, https://doi.org/10.3748/wjg.v24.i34.3849.
[397] G. Ferraioli, C. Tinelli, B. Dal Bello, M. Zicchetti, G. Filice, C. Filice, Accuracy of real-time shear wave elastography for assessing liver fibrosis in chronic hepatitis C: A pilot study, Hepatology 56 (2012) 2125–2133, https://doi.org/10.1002/hep.25936.
[398] R. Villani, F. Cavallone, A.D. Romano, F. Bellanti, G. Serviddio, Two-dimensional shear wave elastography versus transient elastography: A non-invasive comparison for the assessment of liver fibrosis in patients with chronic hepatitis C, Diagnostics. 10 (2020), https://doi.org/10.3390/diagnostics10050313.
[399] Y. Zheng, Y.S. Xu, Z. Liu, H.F. Liu, Y.N. Zhai, X.R. Mao, J.Q. Lei, Whole-liver apparent diffusion coefficient histogram analysis for the diagnosis and staging of liver fibrosis, J. Magn. Reson. Imaging. 51 (2020) 1745–1754, https://doi.org/10.1002/jmri.26987.
[400] K. Ozaki, M. Takeshita, K. Saito, H. Kimura, T. Gabata, A case of focal confluent hepatic fibrosis in the patient with hepatitis C virus-related liver cirrhosis: a mimic of cholangiolocellular carcinoma, Abdom. Radiol. 45 (2020) 2249–2256, https://doi.org/10.1007/s00261-020-02428-3.
[401] K. Patel, G. Sebastiani, Limitations of non-invasive tests for assessment of liver fibrosis, JHEP Reports. 2 (2020), https://doi.org/10.1016/j.jhepr.2020.100067 100067.
[402] M. Baues, A. Dasgupta, J. Ehling, J. Prakash, P. Boor, F. Tacke, F. Kiessling, T. Lammers, Fibrosis imaging: Current concepts and future directions, Adv. Drug Deliv. Rev. 121 (2017) 9–26, https://doi.org/10.1016/j.addr.2017.10.013.
[403] K. Viswanathan, Y.H. Chu, W.C. Faquin, P.M. Sadow, Cytomorphologic features of NTRK-rearranged thyroid carcinoma, Cancer Cytopathol. 128 (2020) 812–827, https://doi.org/10.1002/cncy.22374.
[404] P. Désogère, L.F. Tapias, L.P. Hariri, N.J. Rotile, T.A. Rietz, C.K. Probst, F. Blasi, H. Day, M. Mino-Kenudson, P. Weinreb, S.M. Violette, B.C. Fuchs, A.M. Tager, M. Lanuti, P. Caravan, Type I collagen-Targeted PET probe for pulmonary fibrosis detection and staging in preclinical models, Sci. Transl. Med. 9 (2017) 1–12, https://doi.org/10.1126/scitranslmed.aaf4696.
[405] M. Polasek, Y. Yang, D.T. Schühle, M.A. Yaseen, Y.R. Kim, Y.S. Sung, A.R. Guimaraes, P. Caravan, Molecular MR imaging of fibrosis in a mouse model of pancreatic cancer, Sci. Rep. 7 (2017) 1–10, https://doi.org/10.1038/s41598-017-08838-6.
[406] P. Désogère, S.B. Montesi, P. Caravan, Molecular probes for imaging fibrosis and fibrogenesis, Chem. - A Eur. J. 25 (2019) 1128–1141, https://doi.org/10.1002/chem.201801578.
[407] S.B. Montesi, P. Désogère, B.C. Fuchs, P. Caravan, Molecular imaging of fibrosis : recent advances and future directions, 129 (2019) 24–33.
[408] L.K. Anzola, A.W.J.M. Glaudemans, R.A.J.O. Dierckx, F.A. Martinez, S. Moreno, A. Signore, Somatostatin receptor imaging by SPECT and PET in patients with chronic inflammatory disorders: a systematic review, Eur. J. Nucl. Med. Mol. Imaging. 46 (2019) 2496–2513, https://doi.org/10.1007/s00259-019-04489-z.
[409] X. Zhang, Q. Guo, Y. Shi, W. Xu, S. Yu, Z. Yang, L. Cao, C. Liu, Z. Zhao, J. Xin, 99mTc-3PRGD2 scintigraphy to stage liver fibrosis and evaluate reversal after fibrotic stimulus withdrawn, Nucl. Med. Biol. 49 (2017) 44–49, https://doi.org/10.1016/j.nucmedbio.2017.02.004.
[410] D. Zhang, R. Zhuang, Z. Guo, M. Gao, L. Huang, L. You, P. Zhang, J. Li, X. Su, H. Wu, X. Chen, X. Zhang, Desmin- and vimentin-mediated hepatic stellate cell-targeting radiotracer 99mTc-GlcNAc-PEI for liver fibrosis imaging with SPECT, Theranostics. 8 (2018) 1340–1349, https://doi.org/10.7150/thno.22806.
[411] A. Hatori, J. Yui, L. Xie, K. Kumata, M. Ogawa, M.-R. Zhang, PET imaging of liver fibrosis in rats with 18F-FEDAC, a radiotracer for translocator protein (18 kDa), J. Nucl. Med. 56 (2015).
[412] V. Ambrosini, M. Zompatori, F. De Luca, D. Antonia, V. Allegri, C. Nanni, D. Malvi, E. Tonveronachi, L. Fasano, M. Fabbri, S. Fanti, 68Ga-DOTANOC PET/CT allows somatostatin receptor imaging in idiopathic pulmonary fibrosis: preliminary results, J. Nucl. Med. 51 (2010) 1950–1955, https://doi.org/10.2967/jnumed.110.079962.
[413] B. Pulli, G. Wojtkiewicz, Y. Iwamoto, M. Ali, M.W. Zeller, L. Bure, C. Wang, Y. Choi, R. Masia, A.R. Guimaraes, K.E. Corey, J.W. Chen, Molecular MR imaging of myeloperoxidase distinguishes steatosis from steatohepatitis in nonalcoholic fatty liver disease, Radiology 284 (2017) 390–400, https://doi.org/10.1148/radiol.2017160588.
[414] N.P. Withana, X. Ma, H.M. McGuire, M. Verdoes, W.A. Van Der Linden, L.O. Ofori, R. Zhang, H. Li, L.E. Sanman, K. Wei, S. Yao, P. Wu, F. Li, H. Huang, Z. Xu, P.J. Wolters, G.D. Rosen, H.R. Collard, Z. Zhu, Z. Cheng, M. Bogyo, Non-invasive imaging of idiopathic pulmonary fibrosis using cathepsin protease probes, Sci. Rep. 6 (2016) 1–10, https://doi.org/10.1038/srep19755.
[415] I.T. Ramos, M. Henningsson, M. Nezafat, B. Lavin, S. Lorrio, P. Gebhardt, A. Protti, T.R. Eykyn, M.E. Andia, U. Flögel, A. Phinikaridou, A.M. Shah, R.M. Botnar, Simultaneous assessment of cardiac inflammation and extracellular matrix remodeling after myocardial infarction, Circ. Cardiovasc. Imaging. 11 (2018) 7453, https://doi.org/10.1161/CIRCIMAGING.117.007453.
[416] M. Baues, B.M. Klinkhammer, J. Ehling, F. Gremse, M.A.M.J. van Zandvoort, C. P.M. Reutelingsperger, C. Daniel, K. Amann, J. Bábíčková, F. Kiessling, J. Floege, T. Lammers, P. Boor, A collagen-binding protein enables molecular imaging of kidney fibrosis in vivo, Kidney Int. 97 (2020) 609–614, https://doi.org/10.1016/j.kint.2019.08.029.
[417] L. Zheng, X. Ding, K. Liu, S. Feng, B. Tang, Q. Li, D. Huang, S. Yang, Molecular imaging of fibrosis using a novel collagen-binding peptide labelled with 99mTc on SPECT/CT, Amino Acids 49 (2017) 89–101, https://doi.org/10.1007/s00726-016-2328-7.
[418] H.J. De Haas, E. Arbustini, V. Fuster, C.M. Kramer, J. Narula, Molecular imaging of the cardiac extracellular matrix, Circ. Res. 114 (2014) 903–915, https://doi.org/10.1161/CIRCRESAHA.113.302680.
[419] P. Désogère, L.F. Tapias, L.P. Hariri, N.J. Rotile, T.A. Rietz, C.K. Probst, F. Blasi, H. Day, M. Mino-Kenudson, P. Weinreb, S.M. Violette, B.C. Fuchs, A.M. Tager, M. Lanuti, P. Caravan, Type I collagen-Targeted PET probe for pulmonary fibrosis detection and staging in preclinical models, Sci. Transl. Med. 9 (2017), https://doi.org/10.1126/scitranslmed.aaf4696.
[420] C.T. Farrar, E.M. Gale, R. Kennan, I. Ramsay, R. Masia, G. Arora, K. Looby, L. Wei, J. Kalpathy-Cramer, M.M. Bunzel, C. Zhang, Y. Zhu, T.E. Akiyama, M. Klimas, S. Pinto, H. Diyabalanage, K.K. Tanabe, V. Humblet, B.C. Fuchs, P. Caravan, CM-101: Type I Collagen–targeted MR Imaging Probe for Detection of Liver Fibrosis, Radiology 287 (2018) 581–589, https://doi.org/10.1148/radiol.2017170595.
[421] P. Caravan, Y. Yang, R. Zachariah, A. Schmitt, M. Mino-Kenudson, H.H. Chen, D.E. Sosnovik, G. Dai, B.C. Fuchs, M. Lanuti, Molecular magnetic resonance imaging of pulmonary fibrosis in mice, Am. J. Respir. Cell Mol. Biol. 49 (2013) 1120–1126, https://doi.org/10.1165/rcmb.2013-0039OC.
[422] Q. Sun, M. Baues, B.M. Klinkhammer, J. Ehling, S. Djudjaj, N.I. Drude, C. Daniel, K. Amann, R. Kramann, H. Kim, J. Saez-Rodriguez, R. Weiskirchen, D.C. Onthank, R.M. Botnar, F. Kiessling, J. Floege, T. Lammers, P. Boor, Elastin imaging enables noninvasive staging and treatment monitoring of kidney fibrosis, Sci. Transl. Med. 11 (2019), https://doi.org/10.1126/scitranslmed.aat4865.
[423] F.L. Giesel, C. Kratochwil, T. Lindner, M.M. Marschalek, A. Loktev, W. Lehnert, J. Debus, D. Jäger, P. Flechsig, A. Altmann, W. Mier, U. Haberkorn, 68 Ga-FAPI PET/CT: Biodistribution and preliminary dosimetry estimate of 2 DOTA-containing FAP-targeting agents in patients with various cancers, J. Nucl. Med. 60 (2019) 386–392, https://doi.org/10.2967/jnumed.118.215913.